LABORATORY LOAD TESTS OF SIDE SHEAR FOR AXIALLY LOADED PILES

A Thesis presented to the Faculty of the Graduate School
University of Missouri-Columbia

In Partial Fulfillment
of the Requirements for the Degree

Master of Science

---

by
NATHAN S. ROSE

Dr. J. Erik Loehr, Thesis Supervisor

December 2008

The undersigned, appointed by the dean of the Graduate School, have examined the thesis entitled

LABORATORY LOAD TESTS OF SIDE SHEAR FOR AXIALLY LOADED PILES

presented by Nathan S. Rose,

a candidate for the degree of Masters of Science in Civil Engineering,

and hereby certify that, in their opinion, it is worthy of acceptance.

Professor J. Erik Loehr, P.E.

Professor Brent L. Rosenblad, P.E.

Professor Robert L. Bauer

ACKNOWLEDGEMENTS

I would like to thank my advisor Dr. J. Erik Loehr for advising me throughout my graduate career. He provided guidance and help when asked for, while forcing me to think my own way out of problems when appropriate. The patience he showed throughout the entire project still amazes me. His dedication to helping me graduate is truly appreciated, especially the long nights it took to meet graduation deadlines. Without his input and guidance I would still be working on this project today.

Dr. Brent L. Rosenblad is one of the reasons that I decided to get my master in geotechnical engineering. I would also like to think him for being on my thesis committee, and accommodating the tight schedule for my thesis defense.

I also greatly appreciate Dr. Robert L. Bauer taking time out of his busy schedule to participate on my thesis committee.

Nathan Textor and Jonathan Bailey both proved to valuable colleagues and fiends. Their assistance and friendship helped me get acclimated to the demands of graduate school, and the long hours of a graduate student. Ryan Goetz and Omer Bozok provided assistance to me whenever needed and their help is greatly appreciated. Richard Coffman proved to be an endless source of information for both research and school work. Taylor Day and Wyatt Jenkins worked for me as undergraduate researchers and provided greatly needed assistance. I would also like to thank the College of Engineering's technical staff. This work would not have been possible without Rick Wells, Rich Oberto, and Rex Gish. A special thanks to Michelle Hudson for turning this work when I could not.

Funding for the work in this thesis was provided by Nucor-Yamato Steel, Inc.

TABLE OF CONTENTS

LIST OF FIGURES

Figure Page

LIST OF TABLES

LABORATORY LOAD TESTS OF SIDE SHEAR FOR AXIALLY LOADED PILES

Nathan S. Rose

Dr. J. Erik Loehr, Thesis Supervisor

ABSTRACT

Steel H-piles are small displacement deep foundation elements. Typically, H-piles are driven to/into a hard stratum and the axial capacity of the pile is derived from the end bearing of the pile tip on the hard stratum. However, H-piles can be and are used as friction piles. Presumably, if the side shear capacity of a given H-pile can be increased, the use and applicability of H-piles will also increase. Conventional H-piles have smooth flanges. The objective of the research presented was to evaluate the effect that texturing of pile flanges has on the side shear capacity of an H-pile. The objective was addressed by performing a series of laboratory load tests on full-scale sections of smooth (HP) and textured (HPX) piles to assess differences in load transfer via side shear.

Results from the laboratory testing program suggest that HPX-piles have approximately 10 percent greater side shear capacity than conventional HP-piles, on average. Unit side shear and the side shear parameter β for both smooth and textured piles generally increased with increasing effective stress and increasing over consolidation ratio. HPX-piles were found to exhibit slightly greater settlement at failure than HP-piles, although scatter in the settlement data was significant.

CHAPTER 1: Introduction

1.1 Objective and Methodology

The objective of the work presented in this thesis is to determine what effect, if any, texturing of an H-pile has on axial capacity. Specifically, the effect of texturing on the side shear capacity of an H-pile was examined. Presumably if the side shear capacity of a given H-pile can be increased, then the use and applicability of H-piles will also increase. This includes the effect of texturing on ultimate load, unit side shear, and the side shear parameter, β. The effect of texturing on settlement was also explored.

The methodology used to achieve these objectives was to conduct laboratory load tests on both traditional smooth HP-piles and textured HPX-piles. The load tests were conducted on full scale pile sections in a custom built experimental apparatus which only tests side shear. The basic principle behind the experimental apparatus is similar to conventional field load tests. A pile is placed in the apparatus such that a five foot section of pile is in contact with the soil and both the pile tip and pile top extend through the device. The load test procedure used was similar the ASTMD-1143 Quick Load Test Method for individual Piles. Using this setup, only the side shear acting on the pile is measured. This eliminates the need for data interpretation in order to determine what portion of the capacity comes from end bearing and what portion can be attributed to side shear. The experimental apparatus is capable of producing vertical effective stresses up to about 4000 psf. This allows for investigation of the effects of various effective stresses and over consolidation ratios. The variability usually associated soil properties in field load tests can be closely controlled in the experimental apparatus, greatly reducing one source of variability in the load tests.

The experimental apparatus was used for eight series of load tests for this research. The tests were divided into two groups based on differences in experimental setup. The first group of tests included three test series - one test series for an HP-pile and two test series for an HPX-pile. Each test series included four or five load tests at various effective stress levels. The second group of load tests included five test series - two test series on an HP-pile and three test series on HPX-piles. Each load test was instrumented to measure axial load, pile movement (pile settlement), vertical effective stress, and soil density. Ultimate load, unit side shear, and the side shear parameter, β, were evaluated for each test after collecting and analyzing the data. Statistical analyses were also performed in order to assess the significance of the results. The side shear parameter, β, was back calculated from measured quantities. The settlement at failure for the two types of piles was also examined. Results of all tests and analyses are presented in this thesis.

1.2 Organization of Thesis

A review of pertinent literature is presented in Chapter 2. This begins with general description of H-piles, followed by a summary of current design methods for driven H-pile foundations. The importance and uses of static load tests is discussed as well as some standard test procedures. Various methods for interpretation of static load test results are also discussed. Results of side by side field load tests on HP and HPX piles are also presented.

A description of the experimental apparatus is presented in Chapter 3. The apparatus consists of a chamber assembly, a reaction frame, the piles, a bladder system to apply the desired vertical effective stresses, and an instrumentation system to measure the

applied axial load, pile settlement, bladder pressure, and soil density. Each of these components is described along with the characteristics of the soil used in the testing program. Chapter 3 also contains a summary of the testing procedures from test setup through disassembly of the apparatus.

In Chapter 4, the testing program is described and the experimental results are presented. The description explains how the eight tests are divided among two groups based on the bladder system used. Results for each test, including written summaries of testing conditions and load settlement behavior for each load test are also presented.

Data analysis procedures and results are presented in Chapter 5. The methods used to determine the ultimate load, unit side shear, and side shear parameter, β, are explained. The statistical analyses methods used to evaluate the significance of the results are also described. Results of these analyses for each load test are then presented, and are compared to field and literature values. Finally, a summary of this thesis, conclusions based on the results of this work, and recommendations for future work are presented in Chapter 6.

CHAPTER 2: Literature Review

In this chapter, H-piles are defined and some general characteristics are explained. A summary of several analytic methods related to estimating pile capacity are examined. Next, an overview of static load tests is presented including instrumentation and loading procedures. Various methods for interpretation of static load test results are discussed. Results of side by side field tests on HP and HPX piles are also summarized.

2.1 H-piles

H-piles are special rolled steel sections, similar in shape to wide flange sections, made specifically to be used a driven piles (Coduto, 2001). The primary difference between wide flange sections and H-piles (HP-piles) is that the web is thinner than the flanges in a wide flange section while the web and flanges of an HP-pile have equal thickness. Typically, steel used in HP-piles conforms to ASTM A-572, A-588 or A-690 specifications with yield strengths of 50ksi or greater. HP-piles commonly range in length from 15 to 150 feet, and can carry axial loads of 45 to 225 tons (Bowders, 2007). HP-piles can resist axial and/or lateral loads.

HP-piles are considered small displacement piles, meaning that relatively small soil volumes are displaced during pile driving. The high strength and small displacements caused by driving make HP-piles ideal for difficult driving conditions (Coduto, 2001). In cases when a pile is driven into bedrock, a hardened steel “driving shoe” may be attached to the pile tip. This protects the pile tip and helps to ensure solid contact between the pile and bedrock (Bowders, 2007). HP-piles tend to best suited for end bearing on rock but can be used in other cases (NAVDOCKS, 1962). The axial load capacity of an HP-pile can be determined by three general methods: static load tests,

analytic methods, and dynamic methods. Static load tests and analytic methods will be discussed in more detail in the following sections. The dynamic methods are based on dynamic pile driving formulas and wave propagation (Coduto, 2001) and will not be discussed further.

2.2 Analytic Methods for Estimating Axial Pile Capacity

Analytic methods used to estimate axial pile capacity are based on soil properties obtained from either in-situ or laboratory testing. Laboratory determined effective stress friction angle, ϕ', and cohesion intercept, c', are commonly used. The cone penetration test (CPT) and standard penetration test (SPT) are two of the more common in-situ tests in which the results can be used in various analytic methods. Many analytic methods are empirically developed by comparing static load test results with measured soil properties (Coduto, 2007). Because of the empirical nature of most analytic methods, it is important to use these methods with piles similar to the type used to develop the method.

The capacity of HP-piles, like any deep foundation, is developed from both pile end bearing and pile side shear. End bearing is developed as the pile tip compressively loads soil beneath the pile (Coduto, 2007). Side shear is developed as a result of both friction and adhesion between the pile and the surrounding soil. For design, end bearing and side shear are determined separately, and the sum of the two is taken to be the pile capacity. Both the end bearing and side shear capacities for a pile are dependent on the contact area between the pile and the soil. For HP-piles, the contact area for both end bearing and side shear depends on whether a soil plug develops within the pile flanges. In the case of this research, the experimental apparatus most likely forces a soil plug to form in the pile flanges. The analysis methods presented below focus on estimation of

downward side shear on piles in sand because those are the conditions present in this research.

Side shear analyses are based on the principle of sliding friction and are usually evaluated in terms of effective stress (Coduto, 2001). Side shear analysis can also be performed in terms of total stress. The basic principle behind the determination of side shear is

$$f_s = \sigma'_h \tan\delta \tag{2.1}$$

The unit side shear (f_s) is expressed as a function of the horizontal effective stress (σ'_h) and the soil-foundation interface friction angle (δ). The same relation can be rewritten in terms of vertical effective stress (σ'_v), coefficient of lateral earth pressure at rest (K_o), coefficient of lateral earth pressure (K), soil-foundation interface friction angle (δ), and effective angle of internal friction (ϕ') as

$$f_s = K_o \sigma'_v \left(\frac{K}{K_o}\right)\left(\frac{\delta}{\phi'}\right) \tag{2.2}$$

Once the unit side shear is established the side shear capacity can be determined by multiplying the unit side shear by the pile side shear contact area, using appropriate units.

Difficulties measuring horizontal effective stress and, by association, the coefficient of lateral earth pressure at rest have led to the development of empirical analysis methods. The β-method is one common empirical method that is used. In this method,k unit side shear is computed as

$$f_s = \beta \sigma'_v \tag{2.3}$$

Conceptually, β combines effects due to the coefficient of lateral earth pressure (K), and soil-foundation interface friction angle (δ), into a back calculated, empirical factor. Conceptually β is expressed as

$$\beta = K_o \left(\frac{K}{K_o}\right) \tan\left(\phi' \left(\frac{\delta}{\phi'}\right)\right) \quad (2.4)$$

The β-method was developed by back calculating β values from full scale conventional load tests. These back calculated values were then correlated to soil properties and foundation type (Coduto, 2001). When implementing the β-method in practice it is important to divide the soil into layers, with layer boundaries at the groundwater table and soil strata boundaries.

Several empirical methods have been developed to estimate β values for design. One method for estimating β values proposed by Bhushan (1982) relates β to relative density (D_r) using the relation

$$\beta = 0.18 + 0.65 D_r \quad (2.5)$$

It is important to note that this method was developed for large displacement closed-end steel pipe piles. This method would likely overestimate β values for HP-piles because they are small displacement piles. According to Fellenius (1990) β values in sands range from about 0.3 to 0.6.

The American Petroleum Institute (API) recommends a similar method for determining the unit side shear for steel pipe piles in sand, which will be referred to as the API method. The API method is an effective stress method which relates the unit side shear (f_s) to the coefficient of lateral earth pressure (K), vertical effective stress (σ'_v), and

the soil-foundation interface friction angle (δ) using

$$f_s = K\sigma'_v \tan\delta \quad (2.6)$$

The API method was developed in medium dense to dense siliceous soils, with K values ranging from 0.5 to 1.0 and δ values of 15, 20, 25, and 30 degrees for silt, sandy silt, silty sand, and sand respectively (API, 1981). In the API method Ktanδ is equivalent to the β value used in the β method. The β values presented in Table 2.1 represent typical ranges for cohesionless soils. The values presented for the Bhushan method were determined based on the theoretical maximum and minimum relative density for the sand used in this study.

Table 2.1. Summary of Literature β values from the literature.

Method	β value range
Bhushan	0.18 - 0.83
Fellenius	0.3 - 0.6
API	0.13 - 0.58

2.3 Static Load Tests and Interpretation of Results

Static load tests are the most accurate method for determining ultimate pile capacity (Coduto, 2007). Conventional load test types include axial compression tests, axial tension tests, and lateral load tests. Only axial compression load tests will be discussed in this section. Using load settlement data collected during a load test, the axial capacity of a foundation, in this case HP-pile, can be determined based on various interpretation methods.

The standard test method for testing piles under static axial compressive load is described in ASTM D-1143 Standard Test Method for Piles Under Static Axial Compressive Load. The methods contained in ASTM D-1143 cover testing of vertical or

batter piles individually or groups of vertical piles. In order to conduct a load test, an apparatus that can apply desired loads to the central longitudinal axis of the pile or pile group is needed. The most common method for applying the desired loads is to use a hydraulic jack that reacts against a reaction frame. A typical schematic of this type of setup is shown in Figure 2.1. The reaction frame is secured in place using reaction piles (anchor piles) which are installed on each side of the test foundation (Coduto, 2001).

Typical instrumentation for a static load test includes a load cell, calibrated hydraulic jack, and two or more dial gauges or linear variable differential transformers (LVDT). The dial gauges or LVDTs should have a precision of at least 0.01 inches. The dial gauges are mounted on independent reference beams oriented in a direction that allows placing their supports as far as practicable from the anchor piles (ASTM D-1143). The dial gauges are placed on opposite sides of the pile approximately equidistant from the center along a line perpendicular to the pile center line.

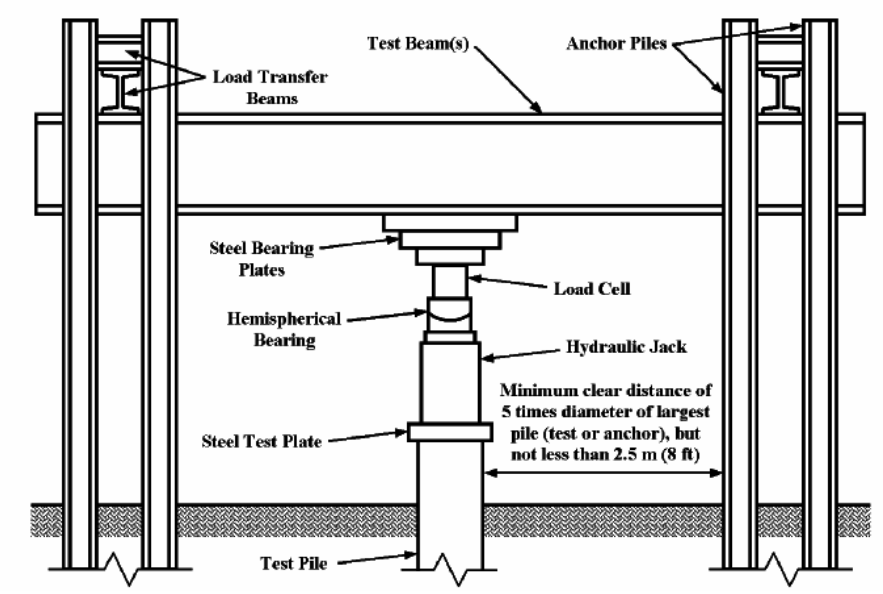

Figure 2.1. Schematic of Hydraulic Jack acting against anchored reaction frame (ASTM D-1143).

There are several loading procedures presented in ASTM D-1143. The most applicable to the research described in this thesis is the Quick Load Test Method for Individual Piles. The basic procedure is to apply axial load in increments of 10 to 15 percent of the design load while maintaining a constant time interval between loading increments. The axial loading is increased in increments until continuous jacking is required to maintain the test load. Once continuous jacking is required to maintain the test load, jacking is ceased and the load is removed from the pile after a specified time interval (e.g. five minures). Readings of time, load, and settlement are recorded immediately before and after the application of each load increment and at intermediate time intervals as specified. Specific details relating to procedures, instrumentation, safety, measurements, and other requirements can be found in ASTM D-1143.

The result of a static load test is a load-settlement curve for the pile tested. However, the "failure" load must be defined. One method proposed by Terzaghi and Peck (1948) suggested the use of a critical load. This critical load (failure load) occurs at a sharp change in the slope of the load settlement plot. One of the most popular and useful interpretation methods is Davisson's Method (Coduto, 2001). Davisson's (1973) Method defines the failure load as the load at which the pile movement exceeds the elastic deformation of the pile (Δ_e) by 0.15 inches plus the pile diameter (D) in inches divided by 120. This relation can be written as

$$\Delta_f = 0.15in + \frac{D}{120} + \Delta_e \qquad (2.7)$$

The elastic deformation of the pile is a function of the applied load (Q), modulus of elasticity for the pile (E), pile cross sectional area (A), and pile length (L)

$$\Delta_e = \frac{QL}{AE} \tag{2.8}$$

An example of Davisson's Method for interpreting static load tests is shown in Figure 2.2. This method is recommended for quick load tests on piles in sands.

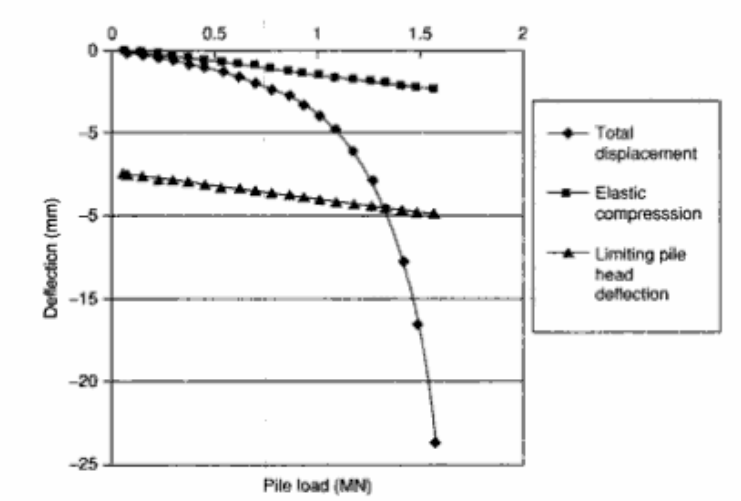

Figure 2.2. Example of Davisson's Method for evaluating pile capacity from a static load test (Gunaratne, 2006).

2.4 Side by Side Field Load Tests

Several side by side field load tests were performed by Hall, Blake and Associates on HP 14x73 and HPX 14x73 piles (Elsayed, 2004; Elsayed, 2005a; Elsayed, 2005b; Elsayed, 2006; Elsayed, 2007b). The tests were performed at five locations: Hickman Arkansas, Berkeley South Carolina, Crawfordsville Indiana, Armorel Arkansas, and Memphis Tennessee. The soil stratigraphy at the Hickman Arkansas site consisted of 8 ft of silt/clay followed by 35 ft of medium dense sand underlain by dense sand. The soil stratigraphy at the Berkeley South Carolina site consisted of 80 to 90 ft of soft to medium clay or loose sand followed by very stiff silt. The soil stratigraphy at the Crawfordsville Indiana site consisted of 20 ft of stiff to very stiff clay underlain by hard clay. No information was provided for the soil stratigraphy at the Armorel Arkansas and Memphis

Tennessee sites. Partial damage to the surface of the HPX pile at the Berkely South Carolina site was observed. The static load tests were performed in accordance with ASTM D-1143 and the results of the load tests were evaluated using the Davisson Method.

The results of the side by side load tests performed by Hall, Blake and Associates are presented in Table 2.2. Overall the HPX-piles produced greater ultimate pile capacities, ranging from approximately 8 to 50 percent greater than measured for convention HP piles at the same location. The relatively large range of ultimate pile capacity increase can be attributed to two main factors: differences in soil stratigraphy from site to site and differences in pile length from site to site. The increase in ultimate pile capacity can be attributed to two main sources: an increase in surface area and the associated increase in frictional resistance and an increase in cross sectional area of the pile resulting in increased bearing resistance (Elsayed, 2007a). An increase in ultimate pile capacity for HPX-piles as compared to HP-piles was not observed at the Armorel Arkansas site. It was suggested (Elsayed, 2007a) that changes in soil stratigraphy could explain the decrease in ultimate pile capacity.

Table 2.2. Results of Static Field Load Tests

Site Locaiton	Ultimate Capacity, tons		Percent Gain in Ultimate Pile Capacity, %
	HP 14x73	HPX 14x73	
Crawfordsville Indiana	325	472	45.2
Berkeley South Carolina	270	291	7.8
Hickman Arkansas	290	358	23.4
Armorel Arkansas	315	285	-9.5
Memphis Tennessee	170	260	52.9

2.5 Summary

In this chapter, background information regarding a variety of topics related to the work presented in this thesis was presented. HP-piles were defined, and their history and classification were explained. Several analytical methods for estimating the unit side shear of driven HP-piles in sands were presented. The quick load test method for individual piles from ASTM D-1143 was presented and the procedures and instrumentation were summarized. Two of the available static load test interpretation methods were described and results of side by side field load tests were also presented.

CHAPTER 3: Experimental Apparatus and Testing Procedure

The experimental apparatus used in this work to evaluate side shear for driven piles is described in this chapter. The apparatus consists of a chamber assembly in which the pile and soil are placed for testing, a reaction frame to apply axial load to the pile, a bladder system to apply the desired vertical effective stresses, and an instrumentation system. Each of these components is described in this chapter, along with the characteristics of the piles and soil used in the testing program. Procedures for assembling the experimental apparatus and testing are also described.

3.1 Chamber Assembly and Reaction Frame

A photograph of the chamber assembly and reaction frame is shown in Figure 3.1. The chamber assembly in which the piles are tested is made up of three main pieces: a cylindrical chamber, a bottom plate, and a top plate. The cylindrical steel chamber is 5 ft tall and 5 ft in diameter with a wall thickness of ¾ inch. The top and bottom plates of the chamber are made from ¾ inch steel plate and are attached to the chamber using ten 1-inch A325 bolts. The top plate is reinforced with C12x20.7 steel sections, which are welded to the top of the top plate. The chamber rests on a bottom assembly constructed from W18x130 steel beams. During testing, the reaction frame is placed on top of the top plate, resting on the C12x20.7 reinforcing sections. The reaction frame is connected to the bottom assembly using eight 1-¼ inch 150 ksi threaded DYWIDAG® bars with anchor plates and nuts. The attached reaction frame is also shown in Figure 3.1.

Figure 3.1. Photograph of the experimental setup showing the bottom assembly, chamber assembly, and Reaction Frame.

The top and bottom plates both have 15-inch square openings in the center of the plates that allows the test pile to extend through both the top and bottom of the chamber. Templates appropriate for the respective pile being tested are then bolted over these openings to help guide the pile during testing, to prevent soil loss around the pile, and to constrain the bladder system at the top of the chamber. The bottom template plate used in this testing has an opening cut to fit a HP14 x76 pile. Strip brushes are attached between the bottom plate and bottom template around the inside perimeter of the opening. The brushes create a seal around the pile that allows the pile to pass through the bottom opening without soil loss while minimizing frictional resistance. A view of the bottom plate with the opening, bottom template plate, and strip brushes is shown in Figure 3.2. The top template plate has an H-shaped opening that allows the pile to pass

through the top plate while effectively sealing the chamber for the bladder system, which is discussed in Section 3.2. A view of the top plate and top template plate with the pile passing through it is shown in Figure 3.3.

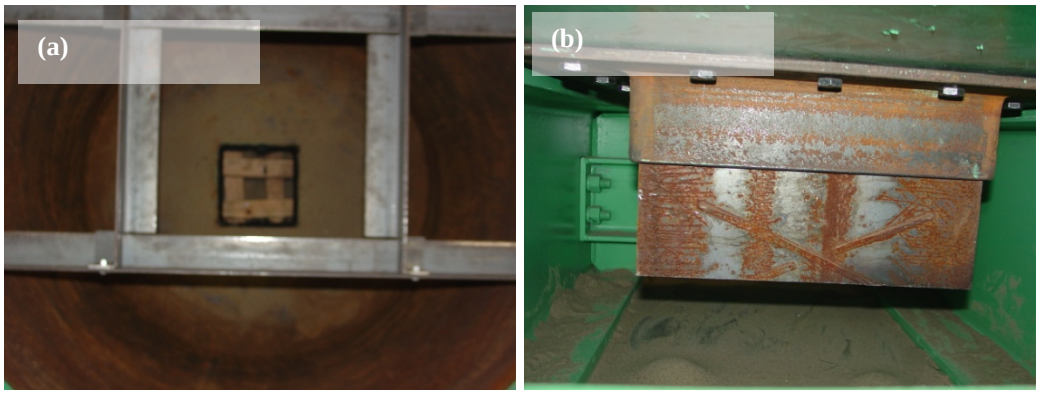

Figure 3.2. Photographs of the bottom plate of the chamber assembly: (a) a view from inside the chamber showing the strip brushes, (b) a view from below the chamber assembly showing the bottom template plate with the pile passing through it.

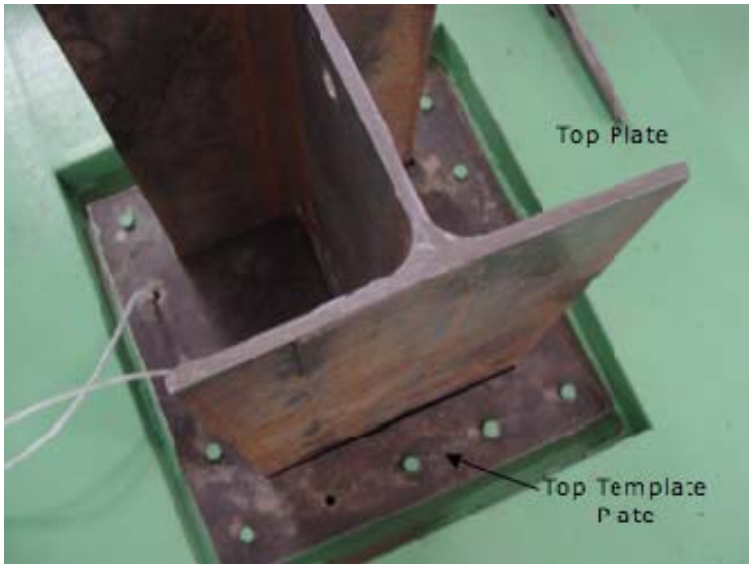

Figure 3.3. Photograph of the top plate and top template plate with the pile passing through it.

The reaction frame consists primarily of a base composed of two W12x152 steel beams and two vertical HP12x74 piles connected by a cross brace formed from two MC12x45 steel members. The height of the cross brace can be adjusted as needed. A load cell is connected to the cross brace using four threaded bars. A hydraulic jack is

connected to the load cell using a single threaded bar. Spacers are placed between the load cell and jack to allow for adjustment to the position of the hydraulic jack. The hydraulic jack has a stroke of approximately 14 inches. A photograph of the reaction frame with the cross brace, hydraulic jack, and load cell is shown in Figure 3.4.

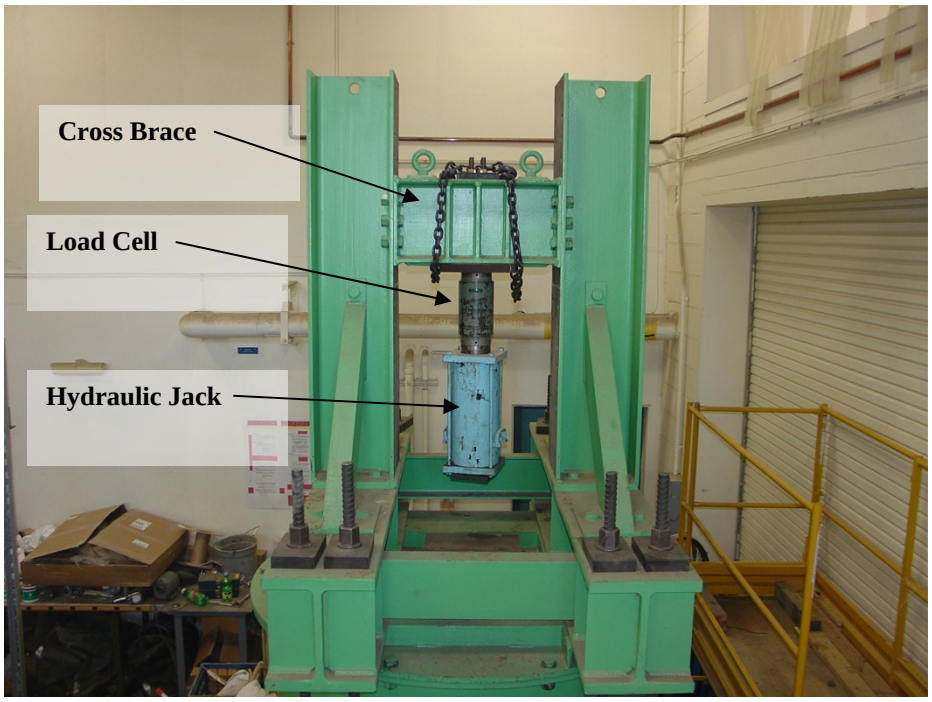

Figure 3.4. Photograph of the load frame with the cross brace, load cell and hydraulic jack.

A four way hydraulic control valve and a manually operated hydraulic regulator control the pressure supplied by the hydraulic pump to the hydraulic jack. The four-way hydraulic control valve is held open during testing and the hydraulic pressure is adjusted using the hydraulic regulator. The hydraulic pump is capable of supplying a maximum pressure of 6000 psi.

3.2 Bladder Systems

The apparatus also includes a bladder system to apply uniform vertical stress to the soil within the chamber, which allows for load tests at vertical effective stresses

greater than the vertical effective stress due to the weight of the soil alone. Development of a bladder system that could reliably hold the pressures desired for testing proved to be the most challenging portion of this project. At the start of the project, a bladder system that could reliably hold 50 psi or more was desired. After several attempts with various system designs it was determined that 30psi was a more realistic maximum target pressure.

The two most critical requirements of the bladder system are: (1) that it be strong enough to hold the desired pressures and (2) for it to be flexible and elastic enough to expand into all available empty space in the chamber so that the pressure was uniformly applied. Several bladder systems were evaluated with mixed results. Commercially available butyl tire tubes were determined to be the best solution. The tubes are connected to a Fairchild pneumatic pressure regulator using ¼ inch NSF Polyethylene Tubing. The valve stems on the tubes were rethreaded in order to fit Swageloc® tube fittings. The polyethylene tubing runs into the chamber through two ½ inch diameter openings in the top template plate. The bladder system is supplied air pressure from the building air supply, which maintains peak pressures between 100 and 110 psi. A Fairchild pneumatic pressure regulator, with a flow capacity of 40 standard cubic feet per minute, an operating range of 2 to 150 psig, and a maximum supply pressure of 500 psig, was used to control the air pressure to the bladder system. The two most successful bladder configurations are described below. The same air pressure supply, pressure regulator, connection tubing, and Swageloc® tube fittings were used for both bladder systems.

3.2.1 Bladder System without Flange Plugs

The first bladder system consisted of four butyl tire tubes. Photographs of the bladder system without flange plugs are shown in Figure 3.5. The four tubes consist of one 16.9/18.4R38 tube, one 11.2/12.4-24 tube, and two 5.50/6.00-16 tubes. The two 5.50/6.00-16 tubes were placed between the pile flanges, one in each flange. The tubes were folded such that they filled the entire flange when pressurized. The 11.2/12.4-24 tube was placed around the pile, inside of the 16.9/18.4R38 tube. The 16.9/18.4R38 tube was placed such that it fit between the inside diameter of the chamber and the outside diameter of the 11.2/12.4-24 tube. The 11.2/12.4-24 and 16.9/18.4R38 tubes were oversized to allow the tubes to expand and fill all available space within the chamber without excessive stress on the tubes.

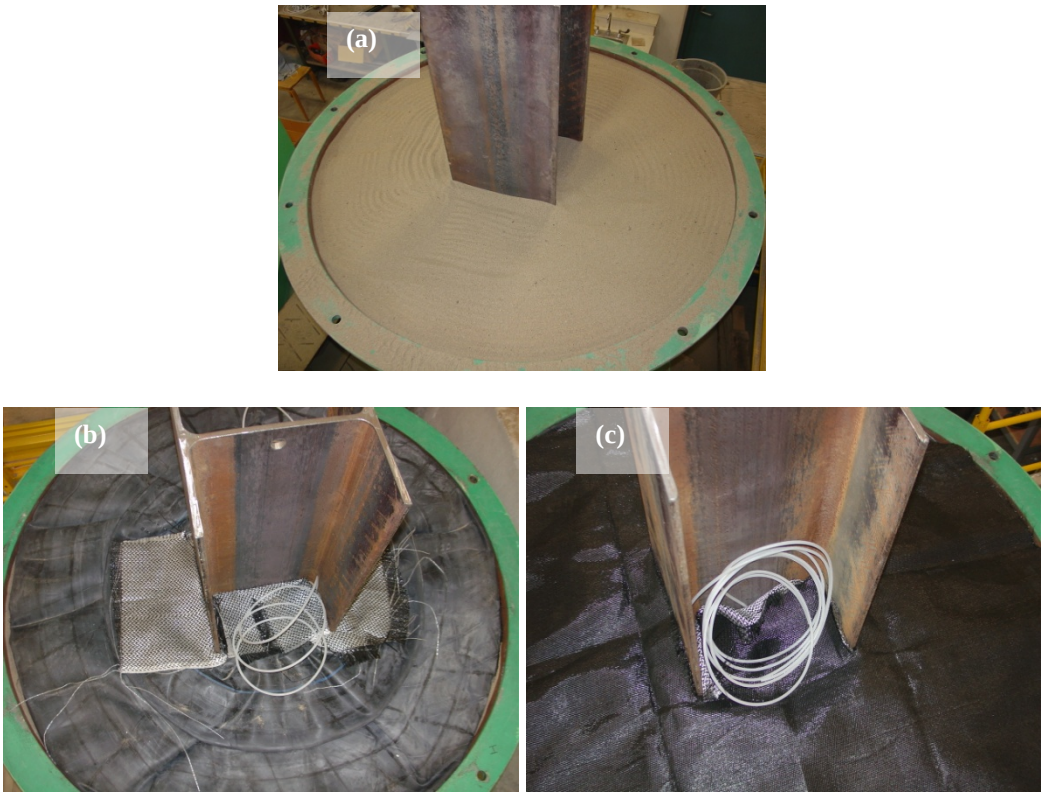

Figure 3.5. Photographs of the bladder system without flange plugs at various stages of installation: (a) a view of the level soil, (b) view of all four butyl tubes in place with geotextile placed between the pile and the tubes, (c) view of the second geotextile in place.

Two geotextiles were used to increase the durability of the bladder system. One geotextile was wrapped around the pile before the tubes were placed into the chamber. Once the tubes were placed, the geotextile w was folded over the tubes partially wrapping the two 5.50/6.00-16 and one 11.2/12.4-24 tubes. This acted as protection for the tubes against the movement of the pile during a load test. The second geotextile was placed between the tubes and the top plate of the chamber. This geotextile had an H shape cut out of the middle so that it fit over the test pile.

The durability of the tubes using this bladder system was a significant issue. While there were problems with all of the tubes in this system, the most common problem occurred with the two small tubes in the flanges. These small tubes would frequently burst at pressures of 20 to 30 psi, which made maintaining bladder pressures in this range challenging. A number of tests were completed using this system. However, this system was abandoned in favor of an alternative system as described in the following section.

3.2.2 Bladder System with Flange Plugs

The second bladder system was similar to the first, except that the two small 5.5/6.00-16 tubes were replaced with polystyrene “flange plugs” that were placed between the flanges. Photographs of the bladder system with flange plugs are shown in Figure 3.6. The two tubes again included one 16.9/18.4R38 tube and one 11.2/12.4-24 tube. The 11.2/12.4-24 tube was placed around the pile and inside the 16.9/18.4R38 tube. Flange plugs were placed between the flanges of the pile to prevent excessive stressing of the smaller tube as it expands into the space between the flanges. The polystyrene inserts were individually cut to fit each flange with approximate dimensions of 12 inch long by 7

inch wide by 6 inch tall. The flange plugs were installed during filling of the chamber such that they were flush with the top of the chamber. Both tubes were oversized in order to allow the tubes to expand and fill all available space within the chamber without excessive stress on the tubes.

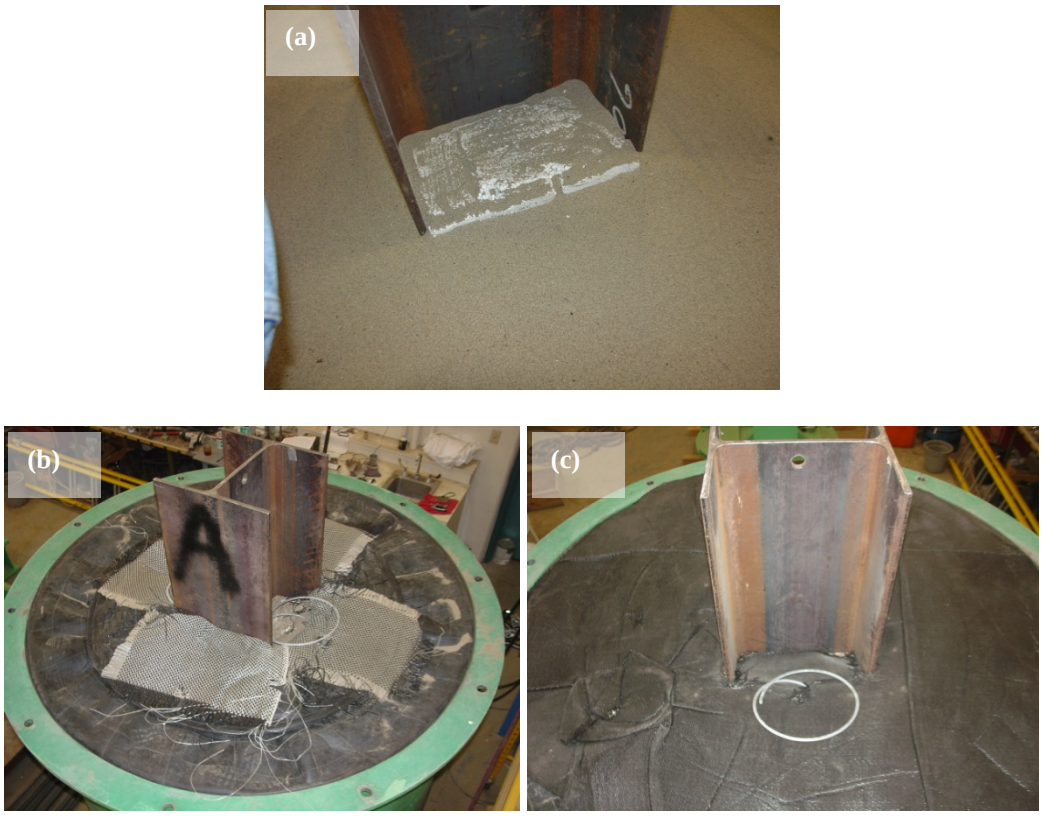

Figure 3.6. Photographs of the bladder system with flange plugs at various stages of installation: (a) view of the leveled soil with the Styrofoam flange plugs in place, (b) view of the two tubes with the geotextile placed between the pile and the tubes, (c) view of the second geotextile in place.

In order to increase the durability of the smaller tube, a used tube of the same size was cut along the outer radius, wrapped around the "new" tube, and glued to it using a cold vulcanizing fluid. As with the first bladder system, a geotextile was placed between the pile and the inner circumference of the smaller tube to protect it as the pile moved during loading. A second geotextile was also placed between the tubes and the top plate

of the chamber. The bladder system with the flange plugs significantly reduced the occurrence of problems with the bladder system.

3.3 Piles

Two types of steel H-piles were tested in this work: conventional "smooth" HP14x76 piles and textured HPX14x76piles. Photographs of an HP and an HPX pile are shown in Figure 3.7. The texturing on the HPX-piles consisted of "X's" that were rolled onto the exterior of the pile flanges during the rolling process. The dimensions of the "X's" were approximately 12 inches wide by 4 inches long and were spaced with one "X" approximately every 6 inches. The "X's" were raised approximately 1/8 inches from the surface of the pile flanges although some variation of the texturing height did exist.

Two specimens of each pile type were prepared for testing. The tested piles ranged in length from 7 ft to 8 ft. The apparatus requires a minimum length of approximately 7 feet and a maximum length of approximately 8 ft for testing as described in Section 3.6. The conventional HP14x76 piles, are referred to as piles A and B; the HPX14x76 piles are referred to as piles C and D. Pile B could not be tested because it did not fit through the bottom template plate due to irregularities in its shape.

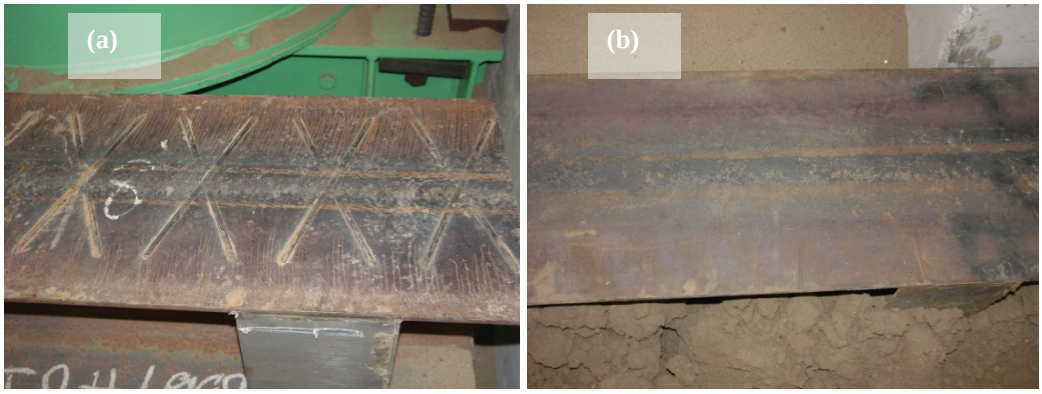

Figure 3.7. Photographs of the two pile types: (a) a conventional smooth HP pile, and (b) a textured HPX pile.

To prevent sand in the chamber from flowing out of the base and to create a "seal" between the pile and the strip brushes attached to the bottom plate of the chamber, "soil catches" were welded in the pile flanges. Photographs of a soil catch attached to an HPX pile are shown in Figure 3.8. The soil catches are made of 3/16-inch sheet metal that was tack welded to the pile to form the catch. The soil catches were attached 6 inches above the base of the pile and extended up the pile 7 inches. This allowed each pile to have a total travel of 7 inches before significant sand loss would occur. The seam between the soil catches and the pile was sealed using a silicone sealant prior to testing.

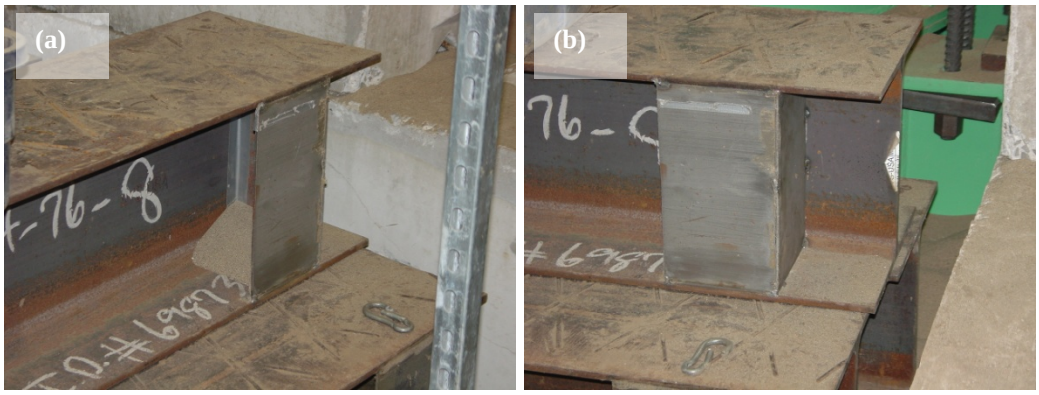

Figure 3.8. Photographs of a sand catch attached to an HPX pile: (a) a top view, and (b), and a bottom view.

3.4 Soil Properties

The soil used to fill the chamber and conduct the load tests was a poorly-graded, fine sand that was dredged from the Missouri River near Jefferson City, Missouri. To characterize the soil a series of index tests was conducted. Results of these tests are summarized in Table 3.1. A plot of the grain size distribution is shown in Figure 3.9. The minimum unit weight of the soil was determined in accordance with ASTM D4254 Method C. The maximum unit weight of the soil was determined in accordance with ASTM D4253, except that a standard proctor mold with a volume of 0.033 cubic feet was

used in place of the recommended mold. The air-dry water content of the soil was measured on multiple dates throughout the project and was consistently about 0.2 percent.

In addition to the index tests, a series of drained direct shear tests were conducted. The results of the direct shear tests indicate the sand has an effective stress friction angle of approximately 32 degrees, as shown in Figure 3.10. The direct shear tests were conducted on air-dry specimens with unit weights that were comparable to the unit weights of the soils placed in the experimental apparatus.

Table 3.1. Summary of results of index tests on test soil

Parameter	*Value*
ASTM Classification	SP
Fines Content (percent passing #200 sieve)	0%
Maximum Unit Weight, γ_{dmax}	108 pcf
Minimum Void Ratio, e_{min}	0.53
Minimum Unit Weight, γ_{dmin}	91pcf
Maximum Void Ratio, e_{max}	0.81
Average Air Dry Water Content, w	0.2%
Angle Of Internal Friction, ϕ	32°
Cohesion Intercept, c	0 psf

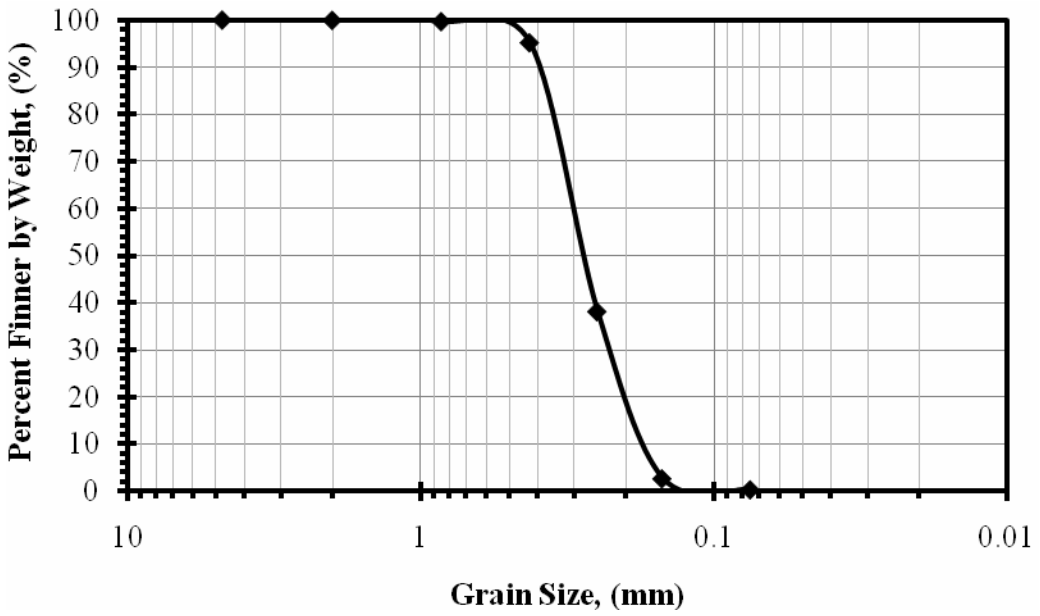

Figure 3.9. Grain Size distribution for test soil.

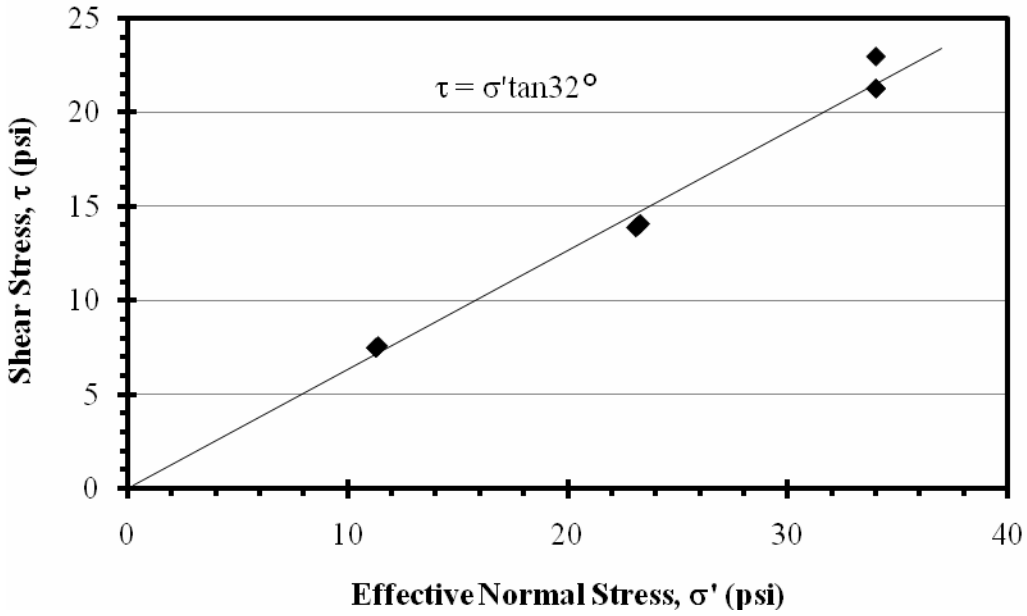

Figure 3.10. Effective stress failure envelope for test soil from direct shear tests

3.5 Instrumentation

Instrumentation was used with the experimental apparatus to measure three data sets: (1) axial load applied to the pile; (2) air pressure in the bladder system; and (3) vertical movement of the pile to establish the load settlement response of the pile. Density tins were also used to determine the final density of the soil in the chamber. Each of these components is described in the following sections.

3.5.1 Load Measurement

The axial load was measured using a load cell. The hydraulic pressure applied to the hydraulic jack was also measured and was used as a secondary check of the accuracy of the load cell. The load cell (Figure 3.4) is a Lobow Associates, Inc. model 3117-106, which has a max capacity of 150kips. The hydraulic pressure was measured using an Omega model PX302-5KGV pressure transducer. It has an operating range of 0 – 5,000 psig and a proof pressure of 10,000 psig.

The secondary check of the load cell was accomplished by plotting the hydraulic pressure as a function of the axial load measured using the load cell as shown in Figure 3.11. The data shown in Figure 3.11 is taken from actual load tests and not a calibration, which was performed separately. The same linear relationship between load and pressure was observed for both the load and reload cycles, indicating consistent load cell readings for all tests. The unload cycle has a different linear relationship indicating an inaccuracy of either the load cell or hydraulic pressure readings during unloading. Because the unload cycle was only used to determine the magnitude of the pile rebound during unloading the change in relationship was not explored further.

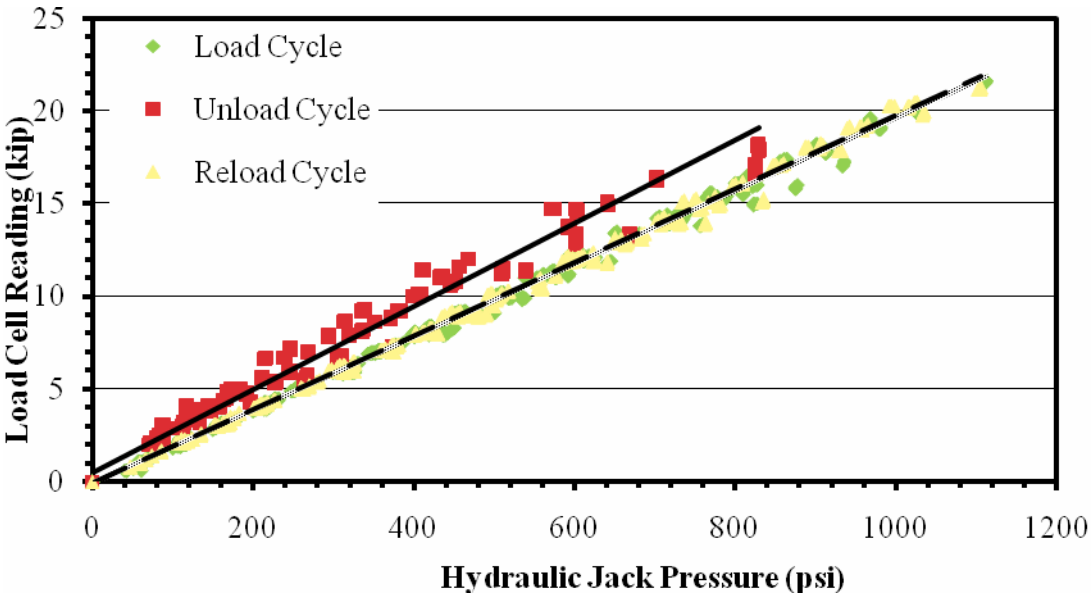

Figure 3.11. Hydraulic Jack Pressure vs Load Cell readings from all load tests.

3.5.2 Bladder Pressure Measurement

The air pressure applied to the bladder system was controlled using a Fairchild pneumatic pressure regulator and measured using a pressure transducer and a digital pressure gauge. The pressure transducer used is an Omega pressure transducer model PX302-100GV with an operating range of 0 to 100 psig and a proof pressure of 200 psig. The digital pressure gauge is an Omega Digital Pressure Gauge model DPG 10000b-100G. It has an operating range of 0 to 100psig. The pressure transducer was attached to the pressure regulator, which was located at the control station away from the apparatus. The digital pressure gauge was located on top of the test chamber next to the load frame.

During testing, the pressure transducer consistently measured higher pressures than the digital pressure gauge. The pressure transducer readings were recalibrated during data reduction based on a calibration between an analog pressure gauge and the pressure transducer. This calibration is shown in Figure 3.12. The corrected pressure

transducer readings were then plotted against the digital pressure gauge readings. The plot in Figure 3.13 shows the nearly one to one relationship between the digital pressure gauge readings and the corrected pressure transducer readings.

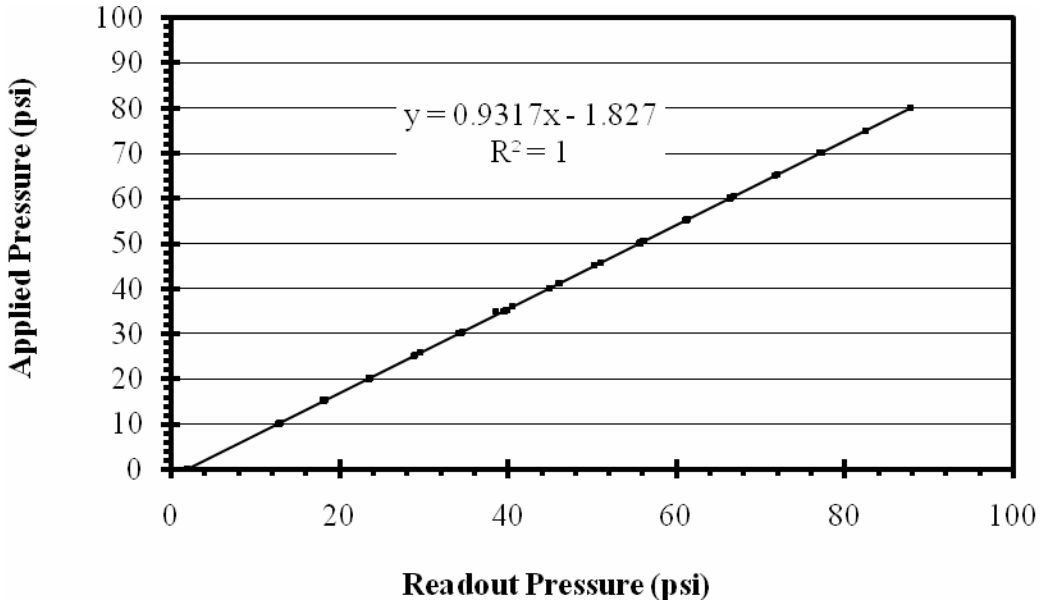

Figure 3.12. Calibration for pressure transducer.

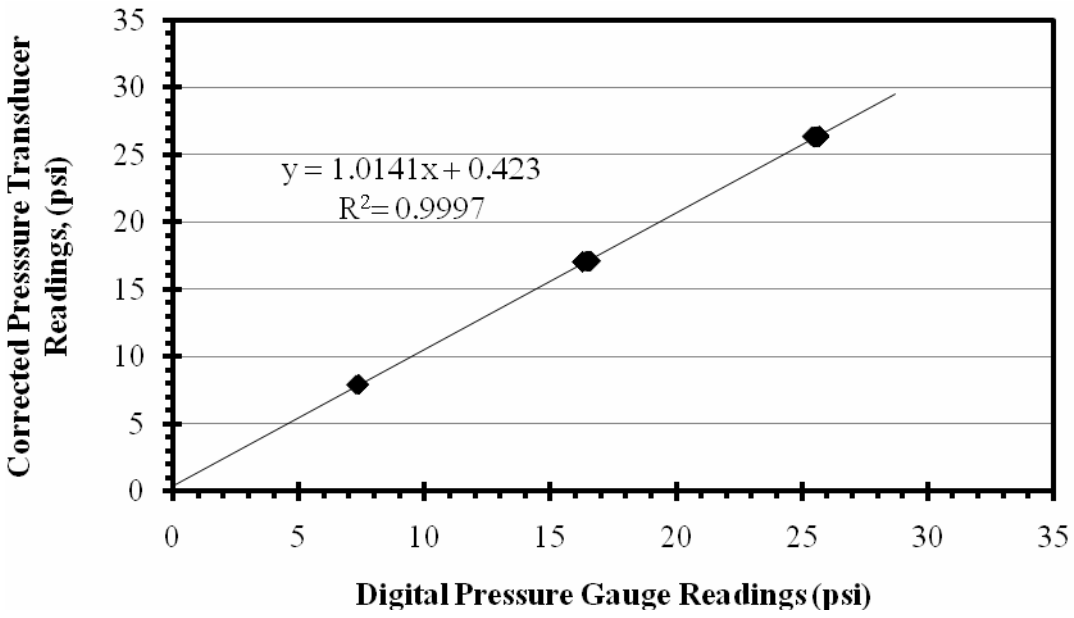

Figure 3.13. Plot showing the nearly one to one relationship between the digital pressure gauge readings and the corrected pressure transducer readings for the air pressure in the bladder system during testing. The data is from all load tests.

3.5.3 Pile Movement Measurement

The vertical movement of the pile was measured using two Starrett four-inch stroke dial gauges. The dial gauges were mounted on opposite corners of the pile top cap using magnetic holders. The vertical movement was measured relative to an independent reference frame. The independent reference frame was constructed of UNISTRUT® in such a way that it was not in contact with the experimental apparatus. A photograph of the independent reference frame and a dial gauge mounted to the pile cap is shown in Figure 3.14.

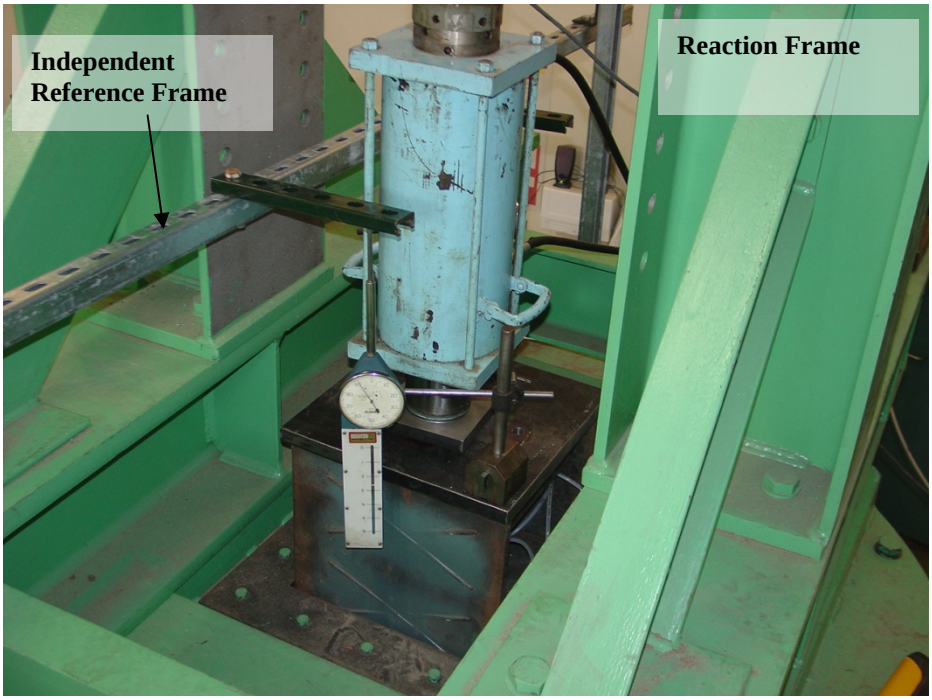

Figure 3.14. Photograph of the independent reference frame and one of the dial gauges mounted to the pile cap.

3.5.4 Soil Density Measurement

The final unit weight of the soil was measured using 12 density tins, which were placed in the soil during filling of the chamber. The density tins were approximately 2 ½ inches in diameter and 1 ¾ inches in height. Placements of the density tins will be discussed further in Section 3.6.1 Experimental Setup. The density tins were removed once testing on a given pile was completed. Care was taken to minimize disturbance of the tins while excavating the soil from the chamber. Tins that were heavily disturbed were not used to determine the final unit weight of the soil. The unit weight of the soil in each tin was determined using the volume of the density tin and the weight of the soil contained in the density tin. The volume of each density tin was determined by measuring the weight of water in the tin and dividing by the unit weight of water. This was done after each test because of deformations to the density tins caused during

excavation. An average of all of the measured unit weights was taken as the final density for a given test. The water content of the sand was measured for each test using the sand from the density tins.

3.6 Testing Procedure

The experimental procedure followed during testing involves three main steps: (1) experimental setup including pile, soil, and bladder system placement; (2) load testing at various vertical effective stresses; and (3) disassembly of the experimental apparatus. Each phase of the testing procedure is described in more detail in this section.

3.6.1 Experimental Setup

The first step in setting up the experimental apparatus was to check and replace any damaged brushes used to create a sand tight seal between the bottom of the chamber and the pile being tested. The test pile was then placed through the opening in the bottom of the chamber such that the brushes aligned with the bottom lip of the sand catch, which maximized pile travel. Wooden blocks placed beneath the tip of the pile were used to keep the pile at the proper height until the chamber was filled with soil. Vertical alignment of the pile was maintained during sand placement using the top template plate and a steel guide frame. Photographs of the guide frame and top template plate holding a pile in position are shown in Figure 3.15.

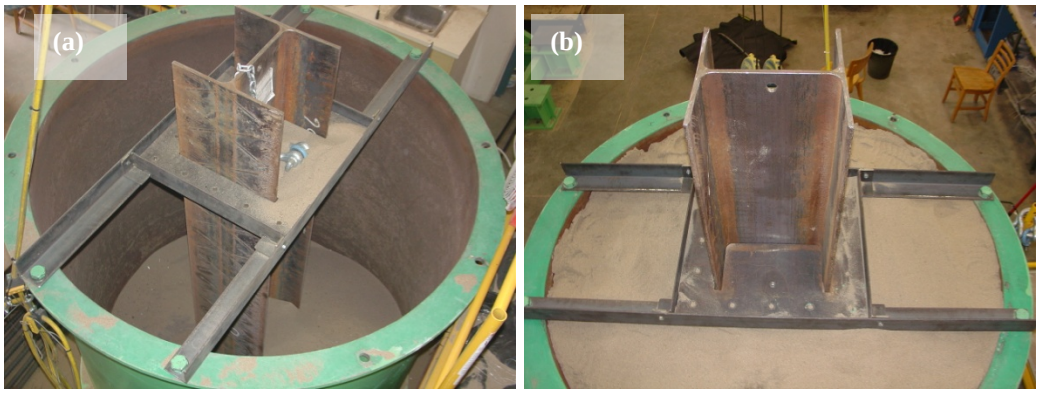

Figure 3.15. Photographs of guide frame and top template plate holding a pile in place: (a) before filling the chamber with soil, (b) after the chamber has been filled with soil.

Once the pile was in place, the chamber was filled with soil using dump bucket and sieve assembly designed to produce uniform soil density. Sand was first placed in the bucket using a skid loader. The sieve assembly was then attached to the base of the bucket prior to placement of the sand into the chamber. The bucket was then lifted above the chamber and dumped from a consistent height to produce a uniform soil "specimen". Photographs of the sand placement technique are shown in Figure 3.16.

Density tins were distributed throughout the chamber in three levels, with four density tins per level during filling. The three levels were roughly one foot from the bottom of the chamber, roughly the middle of the chamber, and roughly one foot from the top of the chamber. The density tins were placed at about the midpoint between the pile and chamber wall, and at roughly north, south, east and west orientations on each level. The guide frame and top template plate were removed once the chamber was filled. The soil surface was then leveled out such that about 1-1/2 inches of free space was left between the top of the soil level and the top of the chamber when the chamber was full. The clear space left between the top of the soil and the top of the chamber was for the bladder system.

When the polystyrene flange plugs were used the flange plugs were installed after the guide frame and top template plate were removed. The flange plugs were installed by excavating soil from between the pile flanges and then placing the flange plugs into the flanges. The flange plugs were placed such that the top of the flange plugs was approximately even with the top of the chamber (Figure 3.6). Once the flange plugs were in place, the open space around them was back filled with sand. The soil surface was then leveled as described previously.

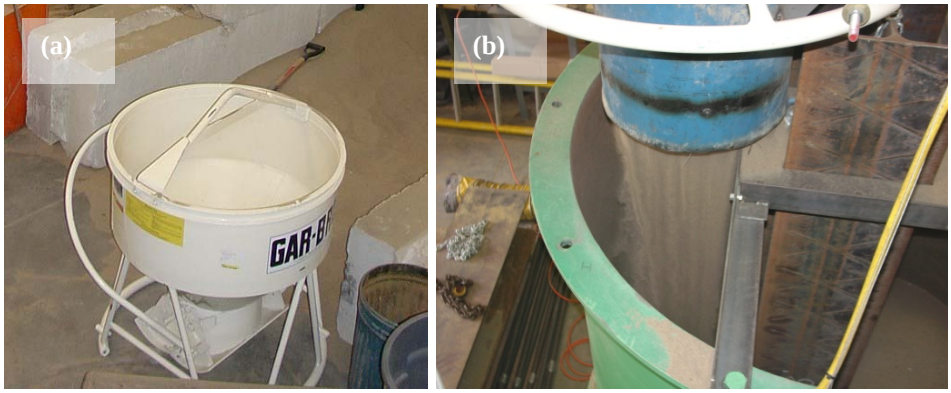

Figure 3.16. Photographs of (a) the dump bucket, and (b) soil being placed into the chamber using the dump bucket and sieve.

The bladder system was then installed as described in Section 3.2. Once the bladder system was installed, the top plate and the top plate template were placed on the chamber using an overhead crane. Polyethylene tubing, which attaches the bladders to the air supply, was run through the openings in the top template plate as it was being lowered into place. The top plate and top plate template were then bolted into place. The loading plate was then placed on top of the pile followed by the reaction frame. Adjustments to the height of the cross brace on the reference frame were made at this point or between individual load tests as needed. The reaction frame was secured to the bottom assembly using the DYWIDAG® bars. Finally, the independent reference frame

and the dial gauges were put into place. The load cell, hydraulic jack, and bladder system were also connected to the digital readout, hydraulic pump, and the air supply respectively at this time.

3.6.2 Pile Load Testing

Once the experimental apparatus was set up, a series of load tests were performed on the pile. Each series of load tests consisted of four or five individual load tests at different bladder pressures. Load tests were performed at various bladder pressures ranging from approximately 10 psi to 30 psi, with the exception of one load test, which was performed at 40 psi. The specific order of the bladder pressures for each test series is discussed in more detail in Chapter 4. Tests were performed on "normally consolidated" sand at increasing effective stresses and on "over-consolidated" sands performed at effective stress less than the maximum that had been applied for each series of tests conducted on an individual pile.

The sand was allowed to settle for at least two hours after each adjustment to the bladder pressure. Adjustment of the bladder pressure caused relatively small settlement of the pile. Settlement of the sand was assumed to cease once pile movement ceased. Typically, pile settlement stopped affecting pile movement after about 30 to 60 minutes. After the second load test in each series, the load frame and top plate were removed and the soil level was checked and adjusted. Typically, the soil did not settle more than approximately one inch. Sand was added to return the sand level to 1-1/2 inches below the top of the chamber. The polystyrene blocks were also readjusted to their original positions while the apparatus was disassembled.

Two different load test procedures were used over the course of testing. The first procedure involved a single monotonic loading while the second procedure involved a "load-unload-reload" cycle. The assembly and preparation for testing were identical for each procedure. The load test procedures outlined below begin after the bladder pressure had been adjusted to the desired level, pile movement due to settlement had ceased, and all instrumentation had been set up.

Monotonic Loading Procedure:

1. Initial readings for air pressure, hydraulic pressure, axial load, the two dial gauges, and initial pile stick up were recorded.
2. A seating load of approximately one kip was applied to the pile and after one minute the air pressure, hydraulic pressure, axial load, and the dial gauge readings were recorded.
3. The load was increased by one kip and air pressure, hydraulic pressure, axial load, and the dial gauge readings were recorded every minute for four minutes. When the load was significantly below the expected failure load, the load was sometimes increased by two or three kips to speed up testing.
4. Step 3 was repeated until failure was reached. Failure was defined during testing as ½ inch of pile movement within one minute.
5. Once failure was reached, the load was removed from the pile and the final pile stick up was measured and recorded.

Load-Unload-Reload Procedure:

1. The initial readings for air pressure, hydraulic pressure, axial load, the two dial gauges, and initial pile stick up were recorded.
2. A seating load of approximately one kip was applied to the pile and, after one minute, the air pressure, hydraulic pressure, axial load, and dial gauge readings were recorded.
3. The load was increased by one kip and air pressure, hydraulic pressure, axial load, and dial gauge readings were recorded every minute for four minutes. When the load was significantly below the expected failure load, the load was sometimes increased by two or three kips to speed up testing.
4. Step 3 was repeated until failure was reached. Failure was defined during testing as 1/2 inch of pile movement within one minute.
5. Once failure was reached, the load on the pile was decreased until pile movement stopped. The air pressure, hydraulic pressure, axial load, and dial gauge readings were recorded every minute for four minutes.
6. The load was then decreased in three equal steps with the final load step being zero load on the pile. At each load step, the air pressure, hydraulic pressure, axial load, and dial gauge readings were recorded every minute for four minutes.
7. Once the last readings at zero load were taken, steps 3 and 4 were repeated until failure was reached.
8. Once failure was reached, the load was removed from the pile and the final pile stick up was measured and recorded.

Once a load test was completed, the bladder pressure was adjusted to the appropriate level for the next load test. The new bladder pressure was maintained for a minimum period of several hours to allow the soil to come to equilibrium under the new bladder pressure. The entire process was then repeated until the pile ran out of stroke. The actual bladder pressures used for each load test are described in Chapter 4, because the order of the bladder pressures in a test series varied from test series to test series.

3.6.3 Apparatus Disassembly

Once the series of load tests on a given pile was completed and the pile ran out of stroke, the experimental assembly was disassembled. This was a relatively simple process that consisted of removing all instrumentation, the independent reference frame, the load frame, the load plate, and the top plate template and top plate. Once the top plate and top plate template were removed, the bladder system was carefully removed. The sand level and the polystyrene insert level were measured and recorded. The pile was then lifted out the chamber using the overhead crane and soil in the chamber was removed using shovels. Care was taken when excavating the sand from the chamber to ensure that the density tins were disturbed as little as possible. When all of the density tins were removed, the sand unit weight and water content were determined as described in section 3.5.4.

3.7 Summary

In this chapter, the experimental apparatus used to load test piles in the laboratory was described. The apparatus includes a chamber assembly, reaction frame, bladder system, piles, soil, and an instrumentation system to measure axial load, bladder pressure, vertical pile movement, and soil density. Each component was described in detail. The

testing procedure, including assembly of the experimental apparatus, load testing procedure, and disassembly of the experimental apparatus, was also described.

CHAPTER 4: Testing Program and Results

This chapter presents the results of eight series of load tests performed on one HP-pile and two HPX-piles. After summarizing the testing program, detailed results for each test are presented. Data presented include written summaries of testing conditions and the accompanying axial load – deflection behavior for each test.

4.1 Testing Program

The eight tests are organized into two groups based on the bladder system that was used during testing. Three series of load tests were conducted using the bladder system without flange plugs. One of these test series was performed on Pile A (HP-pile) and two of these test series were performed on Pile D (HPX-pile). Five series of load tests were conducted using the bladder system with the polystyrene flange plugs. Two of these test series were performed on Pile A (HP-pile), one test series was performed on Pile C (HPX-pile), and two test series were performed on Pile D (HPX-pile).

The tests without flange plugs were the first load tests performed using the experimental setup described in Chapter 3. Because of this, the order and magnitude of the bladder pressures for each individual load test were inconsistent from test series to test series as described in greater detail in Section 4.2. Using the knowledge and experience obtained from tests without flange plugs, the bladder system with flange plugs and the load-unload-reload procedure was developed and used for the tests with flange plugs. In the tests with flange plugs, each test series consisted of five load tests conducted at target average vertical effective stresses of approximately 10 psi, 20 psi, 30 psi, 20 psi, and 10 psi, performed in that order. The tests without flange plugs and the tests with flange plugs used the same experimental setup except for the differences in the

bladder systems. Unless otherwise noted, tests with flange plugs were conducted using the monotonic loading procedure and tests without flange plugs were conducted using the load-unload-reload procedure.

A summary of testing parameters and results for the tests without flange plugs and with flange plugs are shown in Table 4.1 and Table 4.2 respectively. Each test series is identified by the pile tested (A,B,C,D), the group number indicating whether a flange plug was used, and the order in which the pile was tested. Group 1 is used to designate tests performed without the polystyrene flange plugs while Group 2 designates tests performed using the flange plugs. For example, tests series D2-1 was the first test conducted on pile D using the bladder system with flange plugs (Group 2). Any individual load test can be identified using the test number. The test number refers to the test series, target bladder pressure, and whether the sand was tested during virgin compression curve (a), or after rebounding from a greater vertical stress (b). For example, test number D1-2-15b was a test in series D1-2 at a target bladder pressure of 15psi and the sand was at an effective stress less than the maximum effective stress that had been applied to the sand using the bladder system. The difference between the target bladder pressure and the actual bladder pressure is due to the calibration of the pressure transducer readings after testing was completed.

The average vertical effective stress presented in Table 4.1 and Table 4.2 was determined at the midpoint of the sand using the measured bladder pressure and final sand total unit weight, which is also presented. The final sand relative density is presented and was calculated using the final sand total unit weight, a water content of 0.2 percent, a specific gravity of 2.65, and the minimum unit weight and maximum unit

weight reported in Chapter 3. The ultimate load for each load test is also presented in Table 4.1 and Table 4.2. The final sand total unit weight reported in Table 4.1 and Table 4.2 is strictly speaking, a total unit weight. However, because the sand has a water content of 0.2 percent it is also essentially a dry unit weight.

Table 4.1. Summary of testing parameters and results for the tests without flange plugs.

Test Series	Pile Type	Test No.	Bladder Pressure (psi)	Final Sand Total Unit Weight, γ_{final} (pcf)	Final Sand Relative Density, D_r (%)	Average Vertical Effective Stress, σ'_v (psf)	Over Consolidation Ratio, OCR	Ultimate Load, P_{ult} Load Cycle (kips)	Ultimate Load, P_{ult} Reload Cycle (kips)
A1-1	HP	A1-1-10a	7.5	100.1	55.3	1330	1.0	10.1	n/a
		A1-1-20a	16.8			2670	1.0	15.9	n/a
		A1-1-30a	n/a			n/a	1.0	n/a	n/a
		A1-1-10b	7.5			1330	3 †	11.3	n/a
		A1-1-20b	16.9			1680	1.5 †	15.2	n/a
D1-1	HPX	D1-1-10a	7.5	n/a	n/a	1320	1.0	6.0	n/a
		D1-1-20a	16.8			2660	1.0	10.9	n/a
		D1-1-30a	26.1			4000	1.0	19.0	n/a
		D1-1-40a	35.5			5350	1.0	25.0	n/a
D1-2	HPX	D1-2-15a	12.1	97.40	38.9	1980	1.0	7.3	n/a
		D1-2-30a	26.5			4060	1.0	17.0	n/a
		D1-2-10b	7.7			1350	3.0	7.2	n/a
		D1-2-20b	17.0			2690	1.5	9.0	10.9
		D1-2-15b	12.2			2000	2.0	7.2	n/a

Table 4.2. Summary of testing parameters and results for the tests with flange plugs.

Test Series	Pile Type	Test No.	Bladder Pressure (psi)	Final Sand Total Unit Weight, (pcf)	Final Soil Relative Density, D_r (%)	Average Vertical Effective Stress, σ'_v (psf)	Over Consolidation Ratio, OCR	Ultimate Load, P_{ult}	
								Load Cycle (kips)	Reload Cycle (kips)
A2-1	HP	A2-1-10a	8.00	97.39	38.8	1390	1.0	7.3	8.0
		A2-1-20a	16.50			2620	1.0	14.1	14.1
		A2-1-30a	25.60			3930	1.0	19.1	20.5
		A2-1-20b	16.30			2590	1.5	15.5	13.9
		A2-1-10b	7.40			1310	3.0	9.0	n/a
A2-2	HP	A2-2-10a	7.80	97.01	36.4	1360	1.0	6.4	7.1
		A2-2-20a	17.30			2730	1.0	13.4	12.0
		A2-2-30a	26.70			4090	1.0	17.3	18.2
		A2-2-20b	17.30			2730	1.5	14.3	15.3
		A2-2-10b	8.40			1450	2.8	11.0	10.5
C2-1	HPX	C2-1-10a	7.40	97.19	37.6	1310	1.0	8.1	7.3
		C2-1-20a	16.60			2630	1.0	15.9	14.7
		C2-1-30a	26.20			4010	1.0	21.5	21.2
		C2-1-20b	17.20			2720	1.5	17.0	15.1
		C2-1-10b	7.50			1320	3.0	10.0	10.1
D2-1	HPX	D2-1-10a	7.90	97.22	37.8	1380	1.0	4.3	4.1
		D2-1-20a	16.80			2660	1.0	7.0	8.3
		D2-1-30a	26.60			4070	1.0	19.6	20.3
		D2-1-20b	17.10			2700	1.5	16.3	15.2
		D2-1-10b	7.20			1280	3.2	6.1	n/a
D2-2	HPX	D2-2-10a	7.60	97.76	41.1	1340	1.0	8.2	7.3
		D2-2-20a	17.50			2760	1.0	13.4	13.1
		D2-2-30a	27.00			4130	1.0	19.3	20.2
		D2-2-20b	17.20			2720	1.5	15.2	14.0
		D2-2-10b	8.30			1440	2.9	11.1	8.3

Within each group of tests the only variable intentionally modified was the type of pile used, either an HP or an HPX pile. The highlighted load tests are tests in which there was a problem or notable issue during testing. The problems during testing ranged from issues with the bladder system to the pile running out of travel before a test series was complete. These issues will be addressed in Sections 4.2 and 4.3, respectively.

4.2 Results of Tests without Flange Plugs tests

Three series of load tests were conducted on piles without the polystyrene flange plugs. One test series was performed on Pile A, an HP-pile, and two test series were performed on Pile D, an HPX-pile. The monotonic loading procedure was used for all

but two of the tests. The bladder pressure varied from test series to test series and will be discussed in detail for each tests series.

4.2.1 Test Series A1-1

Test series A1-1 was setup and completed in October and November of 2007 on Pile A, an HP-pile. It was tested using the bladder system without flange plugs and the monotonic loading procedure. Four load tests were performed at sequential target bladder pressures of 10 psi, 20 psi, 10 psi, and 20 psi on October 1, October 2, November 4, and November 6, respectively. The average vertical effective stresses for these tests was 1330 psf, 2670 psf, 1330 psf and 2680 psf. Several attempts at a load test with a target bladder pressure of 30 psi were made but were unsuccessful because the bladder system without the flange plugs could not hold the pressure. These attempts are included in Table 4. as test number A1-1-30a even though a load test was not performed because the average vertical effective stress was increased from load test A1-1-20a. This increase in bladder pressure affected the final sand unit weight and final sand relative density. The final sand total unit weight was 100.1 pcf and the final sand relative density was 55.3 percent.

Axial load-settlement plots for each of the four load tests run in test series A1-1 are shown in Figure 4.. The ultimate load for each test is shown in Table 4.. The two tests at 1330 psf failed at similar axial loads. Test A1-1-10a failed at 10.1 kips and test A1-1-10b failed at 11.3 kips, an increase for the test after rebounding from a higher vertical effective stress. Tests A1-1-20a ad A1-1-20b were tested at approximately the same effective stress and failed at 15.9 and 15.2 kips, respectively. The four tests show an increase in ultimate load with an increase in effective stress.

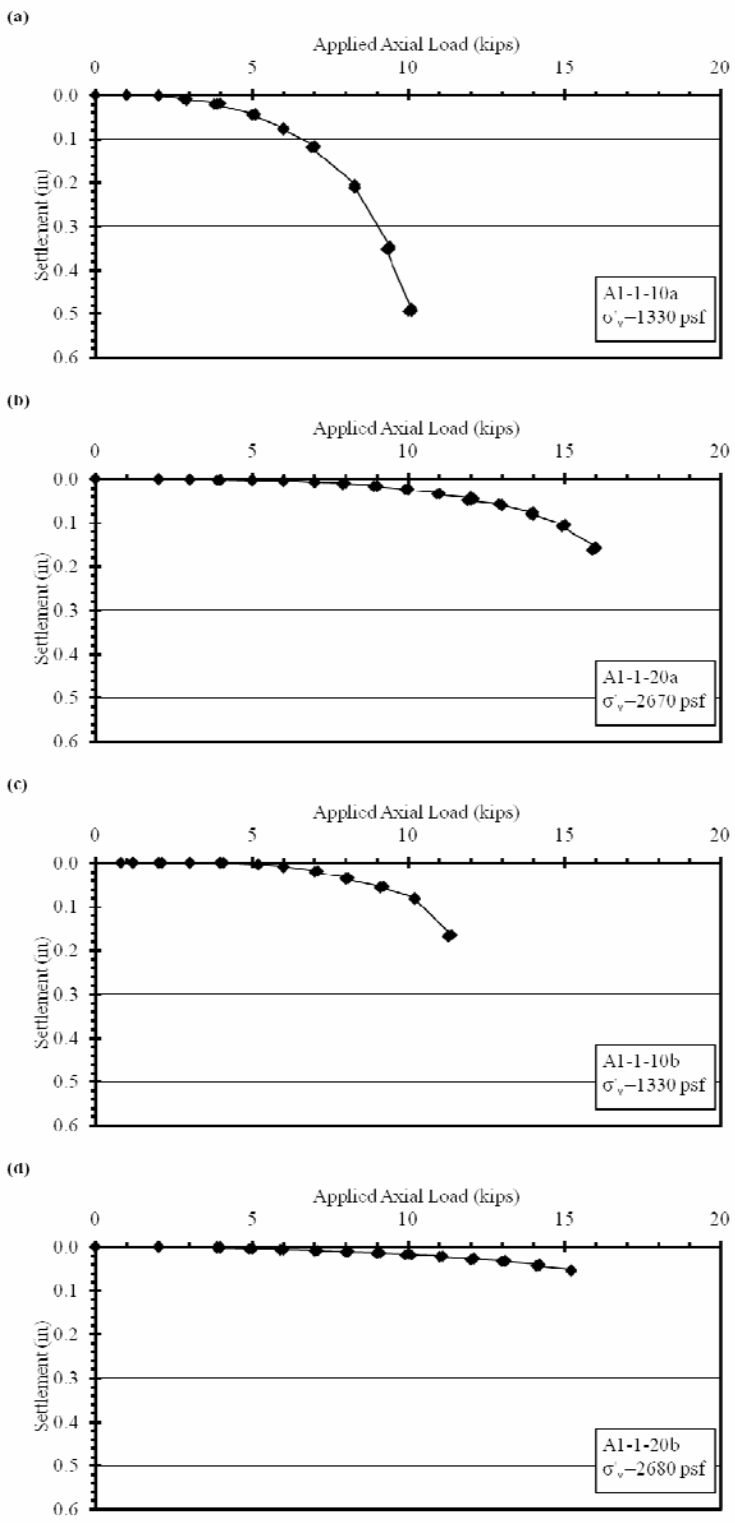

Figure 4.1. Axial load vs pile settlement plots for Test Series A1-1: (a) Test A1-1-10a, (b) Test A1-1-20a, (c) Test A1-1-10b, (d) Test A1-1-20b.

In test A1-1-10a, the pile settled approximately 0.5 inches before plunging failure was observed. Load tests A1-1-20a, and A1-1-10b settled less than 0.2 inches and test A1-1-20b settled less than 0.1 inches before failure. The load settlement curves for the last three tests show a sudden failure with relatively small movements prior to plunging when compared to the first test. The sudden failure is shown clearly in Figure 4.d.

4.2.2 Test Series D1-1

Test series D1-1 was setup and completed in July of 2007 on Pile D, an HPX-pile. It was tested using the bladder system without flange plugs and the monotonic loading procedure. Four load tests were performed at sequential target bladder pressures of 10 psi, 20 psi, 30 psi, and 40 psi on July 26, 27, 30, and 31, respectively. These target bladder pressures resulted in tests that were performed at average vertical effective stresses of 1320 psf, 2660 psf, 4000 psf and 5350 psf. This was the only test series in which a load test was run at an effective stress greater than 4000 psf. When the load was removed from the pile following load test D1-1-40a, one of the bladders burst. This prevented more load tests from being performed in test series D1-1. The final sand total unit weight and final sand relative density were not measured for this test series.

Axial load-settlement plots for each of the four load tests completed in test series D1-1 are shown in Figure 4.. The ultimate loads are presented in Table 4., and increase steadily with the increasing vertical effective stress. In test D1-1-10a, the pile settled approximately 0.4 inches before plunging failure was observed. Load tests D1-1-20a, D1-1-30a, and D1-1-40a settled approximately 0.2 inches prior to plunging. The sudden failures observed in the test series A1-1 load settlement curves are not seen in the load settlement curves of test series D1-1 presented in Figure 4..

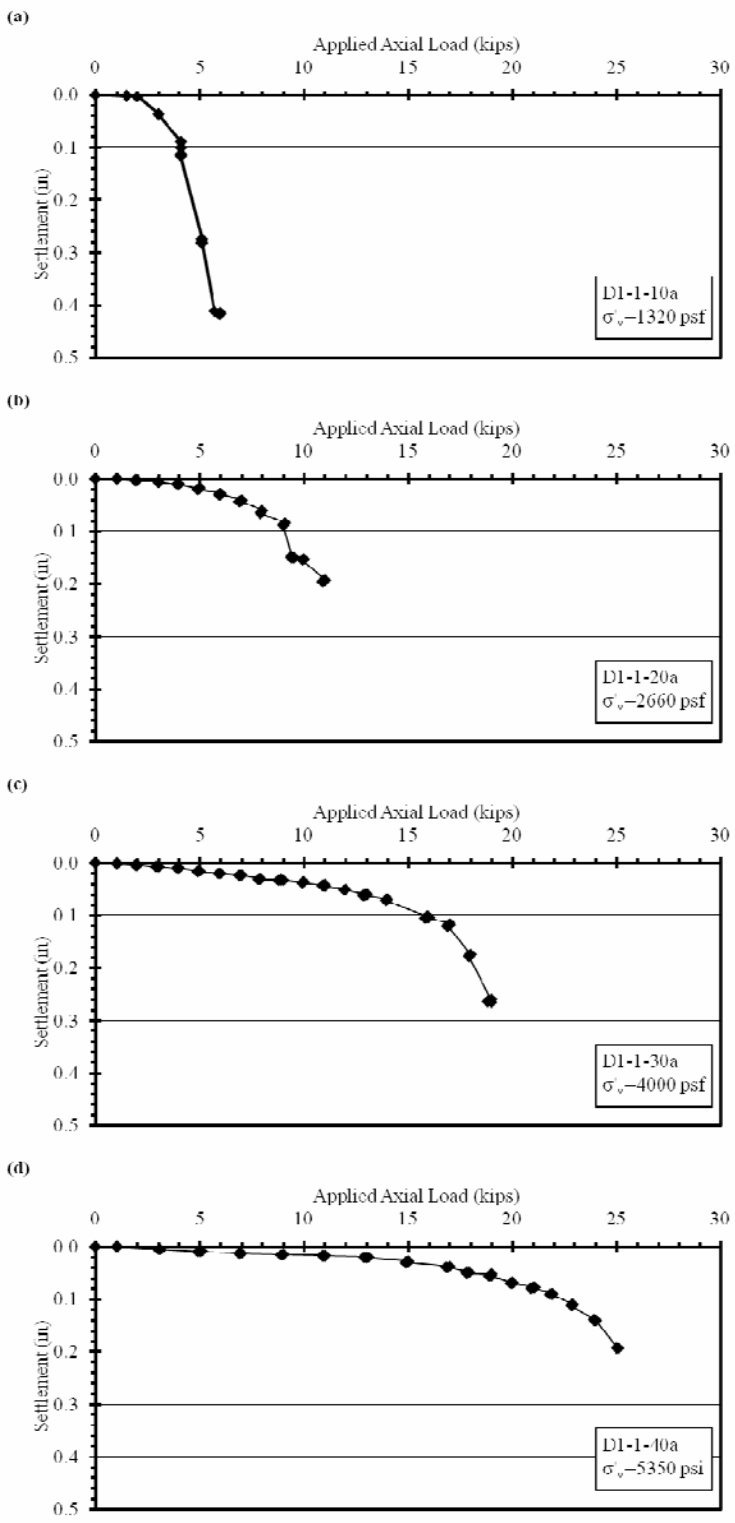

Figure 4.2. Axial load vs pile settlement plots for Test Series D1-1: (a) Test D1-1-10a, (b) Test D1-1-20a, (c) Test D1-1-30a, (d) Test D1-1-40a.

4.2.3 Test Series D1-2

Test series D1-2 was setup and completed in December of 2007 on Pile D, an HPX-pile. It was tested using the bladder system without flange plugs for all load tests. The monotonic loading procedure was used on all load tests except for test D1-1-20b in which the load-unload-reload procedure was used. Five load tests were performed at sequential target bladder pressures of 15 psi, 30 psi, 10 psi, 20 psi, and 15 psi on December 8, 10, 14, 17, and 18, respectively. The average vertical effective stresses were 1980 psf, 4060 psf, 1350 psf, 2690 psf, and 2000 psf. The final sand total unit weight was 97.4 pcf, and the final sand relative density was 38.9 percent.

Axial load-settlement plots for each of the five load tests completed in test series D1-2 are shown in Figure 4.3. The ultimate loads from each test are presented in Table 4.. In all of the test series D1-1 tests, the pile settled approximately 0.2 inches before plunging failure was observed. The sudden failures observed in test series A1-1 were again observed and can be seen in all five load settlement curves presented in Figure 4.3.

In Figure 4.3d, the load settlement curves for the load-unload-reload sequence used in the load-unload-reload procedure are shown. The initial loading curve follows the trend of the other four load tests in this series. The unload curve shows such little rebound of the pile that it is indistinguishable from the reload curve. The settlement of the pile before failure on the reload curve was approximately 0.8 inches at an ultimate load of approximately 12.4 kips. If some interpretation is done the ultimate load is approximately 10 or 11 kips, approximately the equal to the initial load sequence. If the data is interpreted, the settlement at failure for the reload cycle was approximately 0.1 to 0.3 inches, similar to the pile settlement for the initial loading.

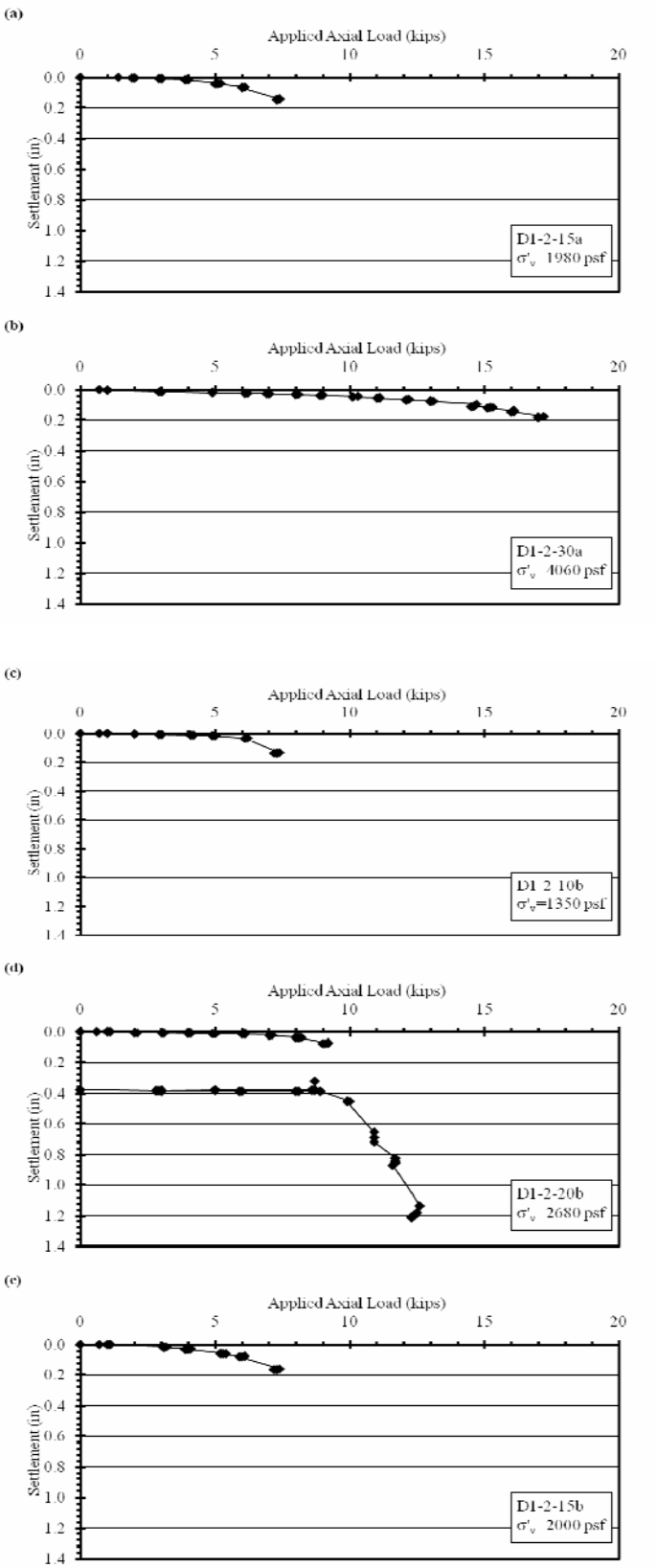

Figure 4.3. Axial load vs pile settlement plots for Test Series D1-2: (a) Test D1-2-15a, (b) Test D1-2-30a, (c) Test D1-2-10b, (d) Test D1-2-20b, (e) Test D1-2-15b.

4.3 Results of Tests with Flange Plugs

Five series of load tests were conducted on piles with the polystyrene flange plugs: two test series on Pile A (HP-pile), one test series on Pile C (HPX-pile), and two test series on Pile D (HPX-pile). The bladder system with the flange plugs and load-unload-reload procedure were used for all of these load tests. The target bladder pressure sequence for the tests with flange plugs was 10 psi, 20 psi, 30 psi, 20 psi, and 10 psi for each test series. These bladder pressures equates to average vertical effective stresses of approximately 1350 psf, 2600 psf, 4000 psf, 2600 psf, and 1350 psf respectively. The actual vertical effective stresses for each test series will be described in subsequent sections.

4.3.1 Test Series A2-1

Test series A2-1 was setup and completed in February and March of 2008 on Pile A, an HP-pile. All load tests in this series were tested using the bladder system with flange plugs and the load-unload-reload procedure. Five load tests were performed at sequential average vertical effective stresses of 1390 psf, 2620 psf, 3930 psf, 2590 psf, and 1310 psf on February 27, and March 15, 20, 25, and 26, respectively. During test A2-1-10b, the pile ran out of travel on the initial load sequence and there was significant sand loss. The reload sequence could, therefore, not be performed for this test.

After the initial filling of the chamber, the sand level was approximately 1.5 inches below the top of the chamber and the flange plugs were approximately even with the top of the chamber. The sand level was checked after the first load test, test A2-1-10a, and the sand level was approximately 2 inches below the top of the chamber and the flange plugs were approximately 1 inch below the top of the chamber. The sand level

was raised to approximately 1.5 inches below the top of the chamber and the flange plugs were returned to be even with the top of the chamber. The sand level after testing was completed was approximately 1.5 to 2 inches below the top of the chamber, and the flange plugs were approximately 4 to 6 inches below the top of the chamber. The difference in sand level and the flange plug level was mostly caused by the pile running out of travel and the associated sand loss. The final sand total unit weight was 97.4 pcf, and the final sand relative density was 38.3 percent.

Axial load-settlement plots for each of the five load tests completed in test series A2-1 are shown in Figure 4.4. The ultimate loads are presented in Table 4.2. During the initial loading sequence, all piles tested in series A2-1 experienced approximately 0.2 inches of settlement before plunging failure was observed, except for test A2-1-10a, the first test. During the reload sequences, the piles experienced less than 0.1 inches of settlement before failure in all but test A2-2-30a. Sudden failures were observed in all but the initial load sequence for test A2-1-10a and the reload sequence for test A2-1-30a. This is similar to tests without flange plugs. The unload curves for each load test show such little rebound of the pile that is generally indistinguishable from the reload curve.

During test A2-1-10b, the pile ran out of stroke during the initial load sequence and produced an ultimate load that was higher than the ultimate load for test A2-1-10a. This suggests that the pile ran out of stroke near the ultimate capacity of the pile. For this reason, the ultimate load for this test was used in data analysis. However, the reload sequence could not be completed for test A2-1-10b. In general, the initial load sequence and the reload sequence produced ultimate loads within approximately one kip of each other. While some fluctuation between the ultimate loads from the load and reload cycles

is expected, the difference also depends on the size of the last load step of the sequence. This is particularly evident in load test A2-1-30a shown in Figure 4.4c. The initial loading sequence produced a sudden failure but the reload sequence did not because the last load step in the reload sequence is near the ultimate capacity of the pile, as evidenced by the large jump in settlement during the last load step. This can also be seen to a lesser extent in Figure 4.4d.

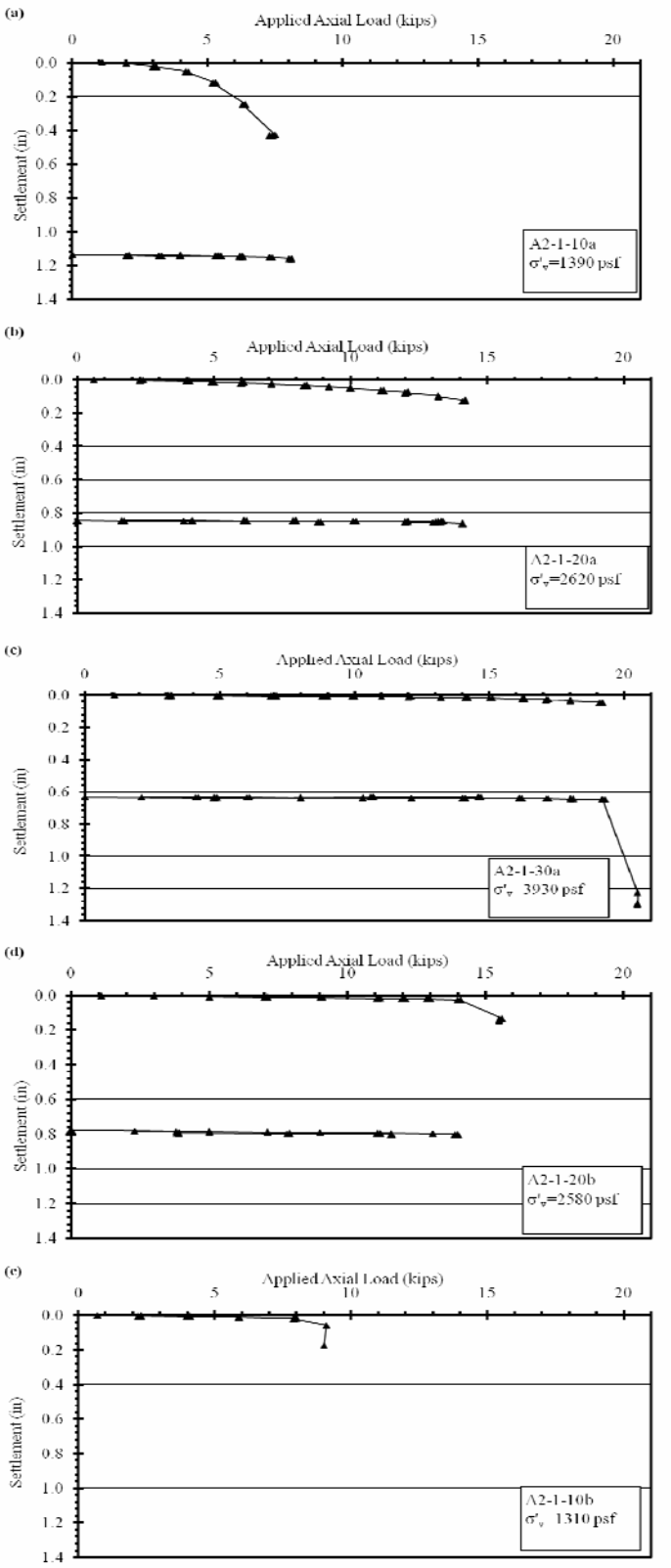

Figure 4.4. Axial load vs pile settlement plots for Test Series A2-1: (a) Test A2-1-10a, (b) Test A2-1-20a, (c) Test A2-1-30a, (d) Test A2-1-20b, (e) Test A2-1-10b.

4.3.2 Test Series A2-2

Test series A2-2 was setup and completed in June of 2008 on Pile A, an HP-pile. All load tests in this series were tested using the bladder system with the flange plugs and the load-unload-reload procedure. Five load tests were performed at sequential average vertical effective stresses of 1360 psf, 2730 psf, 4090 psf, 2730 psf, and 1450 psf. The first three load tests were performed on June 4 and the last two load tests were performed on June 5.

After the chamber was filled, the sand level was approximately 1.5 to 2 inches below the top of the chamber initially and the flange plugs were approximately even with the top of the chamber. The sand level was checked after the first load test, test A2-2-10a, and was approximately 2 to 3 inches below the top of the chamber and the flange plugs were approximately 1.25 inches below the top of the chamber. The sand level was raised to approximately 1.5 inches below the top of the chamber and the flange plugs were returned to be approximately even with the top of the chamber. The sand level after testing was completed was approximately 2 inches below the top of the chamber, and the flange plugs were approximately 4 inches below the top of the chamber. The pile did not run out of stroke during this test series and there was very little sand loss. The settlement of the flange plugs in this test series was caused primarily by the downward movement of the pile and the sand catch and not sand loss. The setup of the sand catch and pile likely caused the sand in the flanges to move downward with the pile as it settles, similar to when the flanges of a pile plug in the field. The final total unit weight of the sand was 97.0 pcf, and the final sand relative density was 36.4 percent.

Axial load-settlement plots for each of the five load tests completed in test series A2-2 are shown in Figure 4.5. Ultimate loads for these tests are presented in Table 4.2. During the initial loading, pile settlement in most tests from series A2-2 was approximately 0.2 to 0.3 inches before plunging failure was observed. The exception was test A2-2-10a, the first test, which experienced approximately 0.4 inches of settlement. During the reload sequence the pile experienced less than 0.1 inches of settlement before failure in all but test A2-2-20b. Sudden failures were again observed and can be seen in Figure 4.5 except for in the initial load sequence for test A2-2-10a and the reload sequence for test A2-2-20b. The unload curve for each load test shows little rebound of the pile during the unloading sequence. There was no significant difference in the ultimate loads observed during the load and the reload sequences.

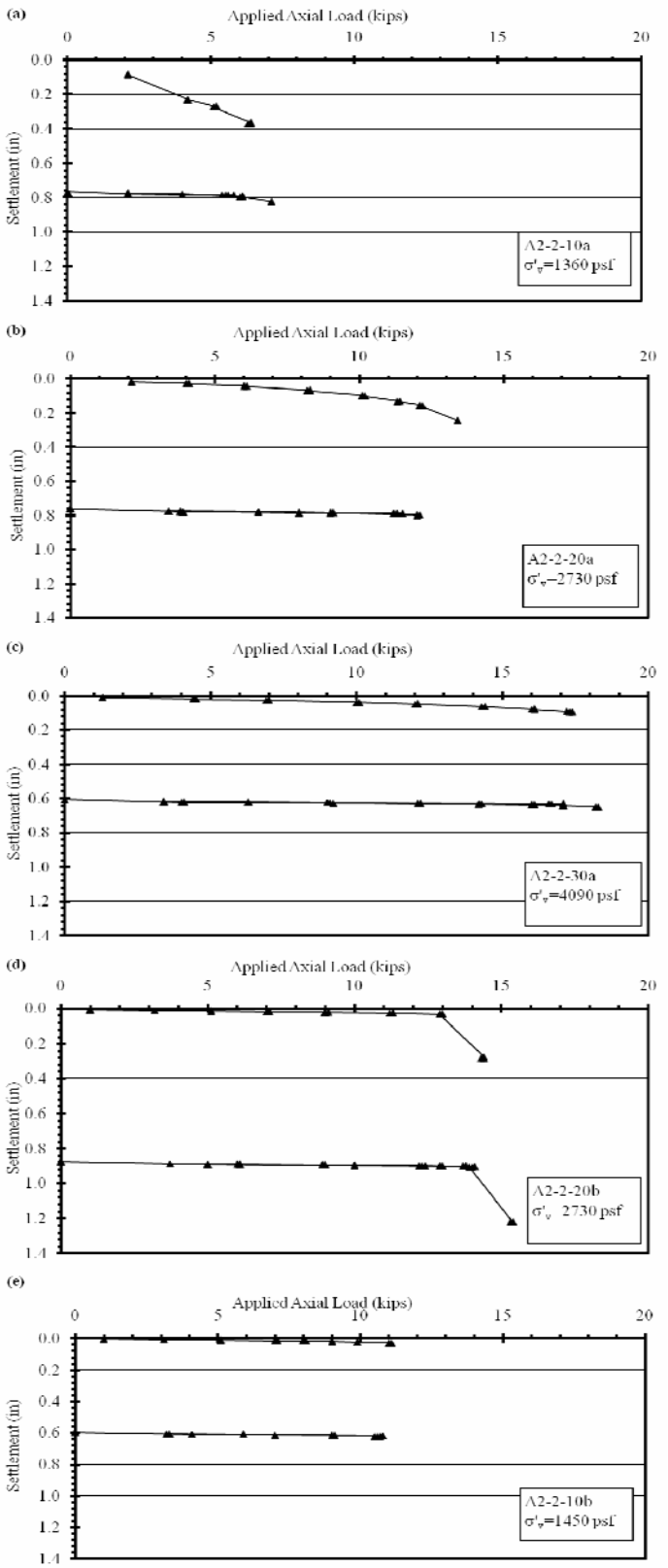

Figure 4.5. Axial load vs settlement plots for Test Series A2-2: (a) Test A2-2-10a, (b) Test A2-2-20a, (c) Test A2-2-30a, (d) Test A2-2-20b, (e) Test A2-2-10b.

4.3.3 Test Series C2-1

Test series C2-1 was setup and completed in April of 2008 on Pile C, an HPX-pile. The load tests in this series were tested using the bladder system with flange plugs and the load-unload-reload procedure. In this test series, five load tests were performed at sequential average vertical effective stresses of 1310 psf, 2630 psf, 4010 psf, 2720 psf, and 1320 psf. The load tests were run on April 12, 18, 21, 22, and 25. An additional load test was attempted on April 17 at approximately 2600 psf but was aborted because of inconsistencies with the dial gauges. While the dial gauges were being adjusted one of the bladders burst. The bladder system was repaired and the test was repeated the next day. This attempted load test was not included in the data analyses because it was stopped before failure was reached and the test was repeated the next day at the same average vertical effective stress. The repeated load test is test C2-1-20a.

After the chamber was filled, the sand level was initially approximately 1.25 to 1.5 inches below the top of the chamber and the flange plugs were approximately even with the top of the chamber. The sand level was checked and adjusted after the failed load test on April 17. The sand level was approximately 1.5 to 2.75 inches below the top of the chamber and the flange plugs were approximately 1.25 to 1.5 inches below the top of the chamber. The sand level was raised to approximately 1.5 inches below the top of the chamber and the flange plugs were returned to approximately even with the top of the chamber. The sand level after testing was completed was approximately 1.5 to 2.5 inches below the top of the chamber, and the flange plugs were approximately 4 to 5 inches below the top of the chamber. The relatively large flange plug settlement was caused by the pile and sand catch movement and sand loss. The setup of the sand catch likely causes

the sand in the flanges to move downward with the pile as it settles, similar to when soil plugs the flanges of a pile in the field. It is the author's opinion that the pile flanges did plug with soil during testing because the apparatus forced this type of failure. While the pile did not completely run out of stroke during this test series, there was notable sand loss at the failure of the reload sequence of test C2-1-10b. The final sand total unit weight was 97.2 pcf, and the final sand relative density was 37.6 percent.

Axial load-settlement plots for each of the five load tests run in test series C2-1 are shown in Figure 4.6. The corresponding ultimate loads are presented in Table 4.2. The initial loading sequence of test C2-1-10a resulted in approximately 0.6 inches of pile settlement and the initial loading sequence of test C2-1-20b resulted in approximately 0.4 inches of settlement. However, approximately 0.3 inches of settlement in test C2-1-20b resulted from the last load step. The initial loading sequence of the other tests in series C2-1 experienced approximately 0.2 inches of settlement before plunging failure was observed.

During the reload sequence the pile experienced less than 0.1 inches of settlement before failure in all but test D2-2-10a, which experienced approximately 0.2 inches of settlement prior to plunging. Sudden failures were observed and can be seen in Figure 4.6 in all but the initial load sequence for test C2-1-20b. The unload curve for each load test again show little rebound of the pile during the unload sequence. The reload sequence in test C2-1-20b had to be reattempted because the hydraulic jack ran out of travel before failure was reached. The reload and the reload-reload sequence can be seen in Figure 4.6d. Both the first and second reload sequences resulted in the same ultimate pile capacity, suggesting that the initial reload sequence was just below failure when the

hydraulic jack ran out of stroke. In general, the initial load sequence and the reload sequence produced ultimate loads within approximately one kip of each other.

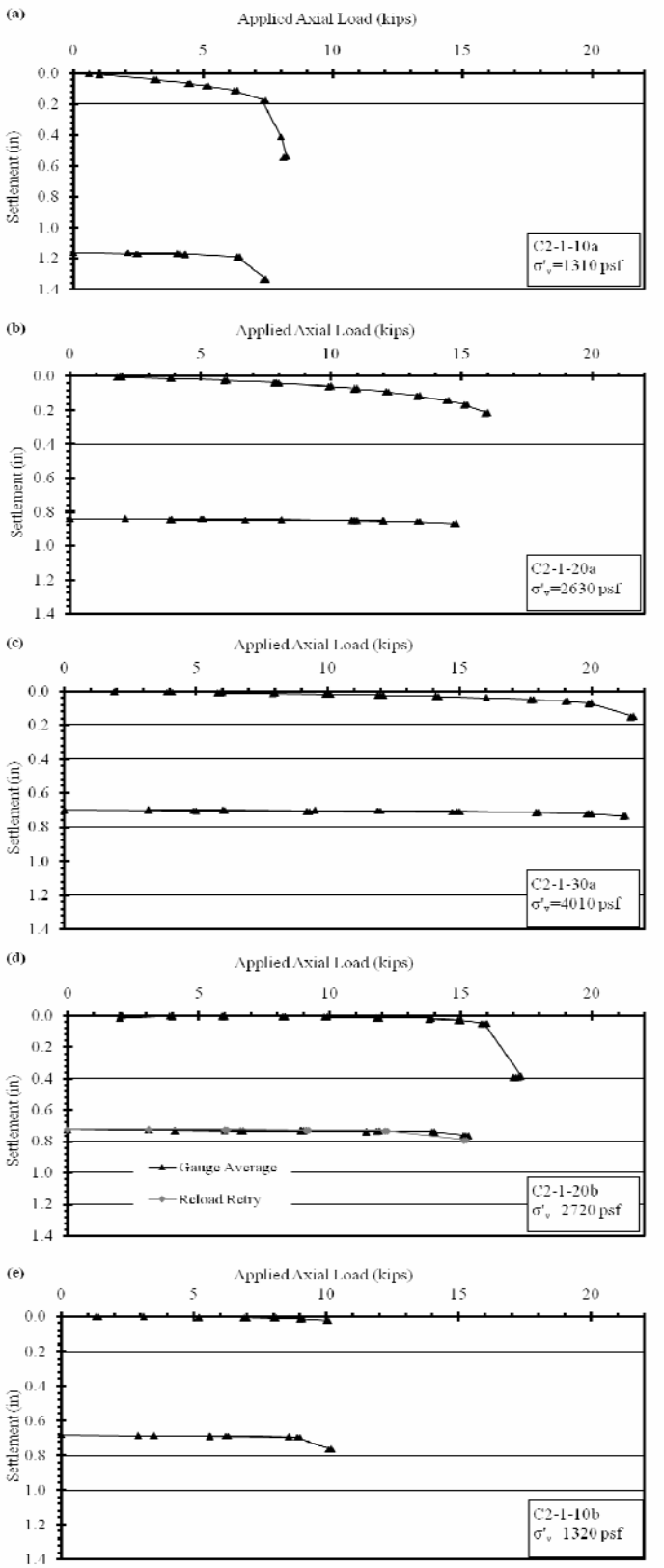

Figure 4.6. Axial load vs Settlement plots for Test Series C2-1: (a) Test C2-1-10a, (b) Test C2-1-20a, (c) Test C2-1-30a, (d) Test C2-1-20b, (e) Test C2-1-10b.

4.3.4 Test Series D2-1

Test series D2-1 was setup and completed in May of 2008 on Pile D, an HPX-pile. The load tests in this series were tested using the bladder system with flange plugs and the load-unload-reload procedure. In this test series, five load tests were performed at sequential average vertical effective stresses of 1380 psf, 2660 psf, 4070 psf, 2700 psf, and 1280 psf. The first two load tests were performed on May 20 and the last three load tests were performed on May 21. There were several problems during this test series. A load test that was not included in the results was attempted on May 19 at an effective stress of approximately 1370 psf but a plunging failure was observed at approximately 4.9 kips, well below the ultimate load of previous load tests conducted at similar vertical effective stresses. The bladder system was inspected but no problems were found. Tests D2-1-10a and D2-1-20a were then tested and lower than expected ultimate loads resulted again. A test was attempted at an average effective vertical stress of approximately 4000 psf but the bladder system failed. After the bladder system was repaired, tests D2-1-30a, D2-1-20b, and D2-1-10b did not experience the same problem as tests D2-1-10a and D2-1-20a. However, the pile began to run out of stroke on the reload sequence of test D2-1-20b and there was significant sand loss. The pile ran out of stroke and failed prematurely on the load sequence of D2-1-10b. The validity of these test results is discussed in subsequent paragraphs.

After the chamber was filled, the sand level was approximately 1.5 inches below the top of the chamber and the flange plugs were approximately even with the top of the chamber. The sand level was checked and adjusted after the failed load test at an effective stress of approximately 4000 psf. The sand level and the flange plugs were

approximately 2 to 3 inches below the top of the chamber. The sand level was raised to approximately 1.5 inches below the top of the chamber and the flange plugs were returned to approximately even with the top of the chamber. After testing was completed the sand level was approximately 1.5 inches below the top of the chamber and the flange plugs were approximately 12 inches below the top of the chamber. The difference in the flange plug settlement was caused by both the pile movement and the significant sand loss during the last two load tests. In this test series, the sand loss was the dominate source of the settlement of the flange plugs and the sand near the pile. The final sand total unit weight was 97.2 pcf, and the final sand relative density was 37.8 percent.

Axial load-settlement plots for each of the five load tests completed in test series D2-1 are shown in Figure 4.7. The ultimate loads are presented in Table 4.2. All of the initial loading sequences resulted in approximately 0.1 to 0.2 inches of pile settlement but the initial loading sequence for test D2-1-20b resulted in approximately 0.4 inches of settlement. The difference in settlement resulted from the last load step. The reload sequences for tests D2-1-10a and D2-1-20b experienced less than 0.1 inches of settlement before failure. Tests D2-1-20a and D2-1-20b experienced settlements of 0.5 and 0.4 inches, respectively. In the three cases where relatively large settlements were observed, approximately 0.3 inches of settlement can be attributed to the last load step as seen in Figure 4.7b and Figure 4.7d. The unload curve for each load test again shows little rebound of the pile during the unload sequence.

In general, the initial load sequence and the reload sequence produced ultimate loads within approximately one kip of each other. The ultimate loads for test D2-1-10a, D2-1-20a, and D2-1-10b were all below the ultimate loads for other load tests at similar

effective stresses. The lower than expected ultimate loads in tests D2-1-10a and D2-1-20a are believed to result from bladder system issues. The lower than expected ultimate load in test D2-1-10b was the result of the pile running out of travel and the associated sand loss. For this reason, these three tests are not included in the data analysis presented in Chapter 5. The reload sequence in test D2-1-20b was not excluded from the data analysis even though there was sand loss because the resulting ultimate load was within approximately one kip of the ultimate load of the initial loading sequence, which did not experience sand loss.

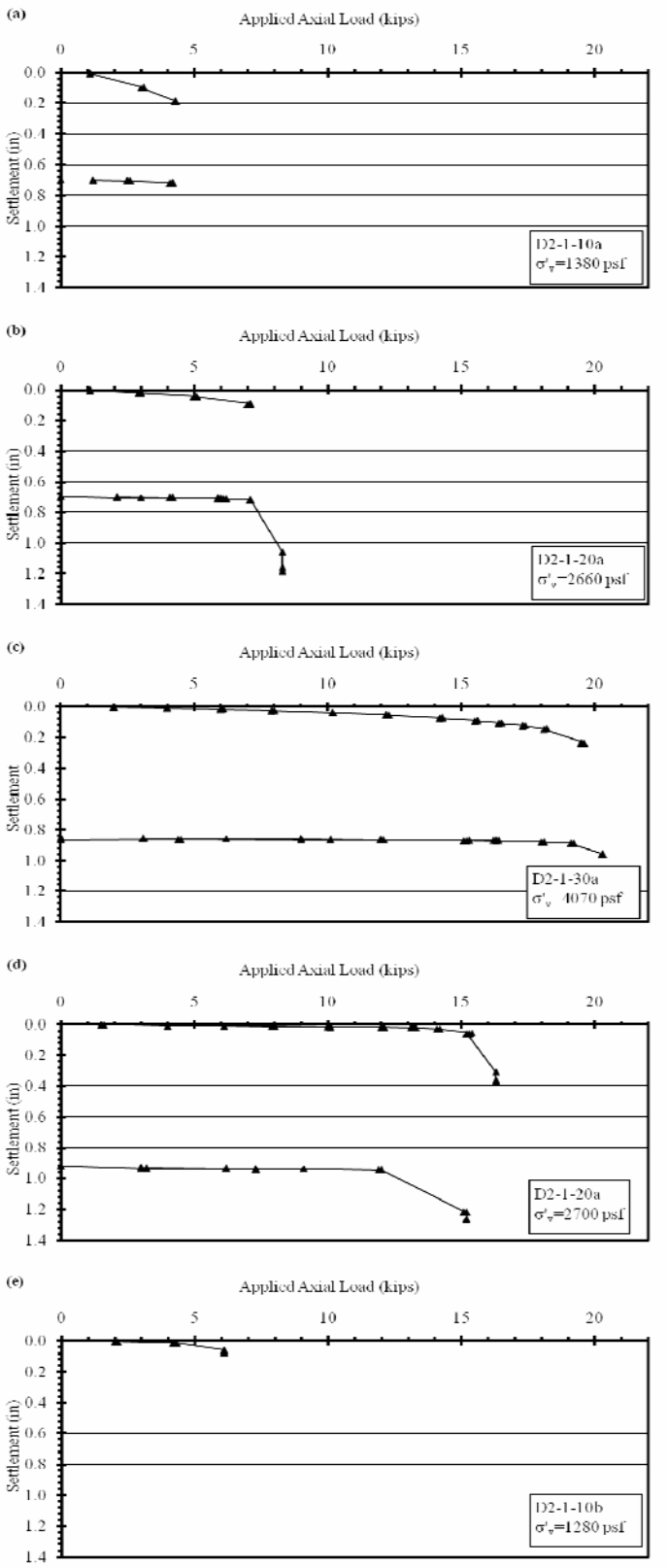

Figure 4.7. Axial foad vs settlement plots for Test Series D2-1: (a) Test D2-1-10a, (b) Test D2-1-20a, (c) Test D2-1-30a, (d) Test D2-1-20b, (e) Test D2-1-10b.

4.3.4 Test Series D2-2

Test series D2-2 was setup and completed in June of 2008 on Pile D, an HPX-pile. All load tests in this series were tested using the bladder system with flange plugs and the load-unload-reload procedure. In this test series, five load tests were performed at sequential average vertical effective stresses of 1340 psf, 2760 psf, 4130 psf, 2720 psf, and 1440 psf. The first load test was performed on June 9, the next two load tests were performed on June 10, and the last two load tests were performed on June 11.

After the chamber was filled, the sand level was initially approximately 1.75 to 2 inches below the top of the chamber and the flange plugs were approximately even with the top of the chamber. The sand level was checked and adjusted after the first load test, test D2-2-10a. The sand level was approximately 2.5 inches below the top of the chamber and the flange plugs were approximately 1 to 2 inches below the top of the chamber. The sand level was raised to approximately 1.75 to 2 inches below the top of the chamber and the flange plugs were returned to approximately even with the top of the chamber. The sand level after testing was completed was approximately 2 to 2.5 inches below the top of the chamber, and the flange plugs were approximately 5 inches below the top of the chamber. There was very little sand loss during this test series. The final sand total unit weight was 97.8 pcf, and the final sand relative density was 41.1 percent.

Axial load-settlement plots for each of the five load tests in test series D2-2 are shown in Figure 4.8. The corresponding ultimate loads are presented in Table 4.2. The settlement due to the initial loading sequence in test D2-2-10a was approximately 0.8 inches. Settlement due to the initial loading sequence for the other tests was approximately 0.2 inches except for test D2-2-30a, which had settlement of

approximately 0.4 inches before plunging failure. The settlement due to the reload sequence was less than approximately 0.1 for each test except for test D2-2-30a, which had settlement of approximately 0.4 inches. However, almost all of this settlement was experienced on the last load step. In general, the initial load sequence and the reload sequence produced ultimate loads within approximately one kip of each other.

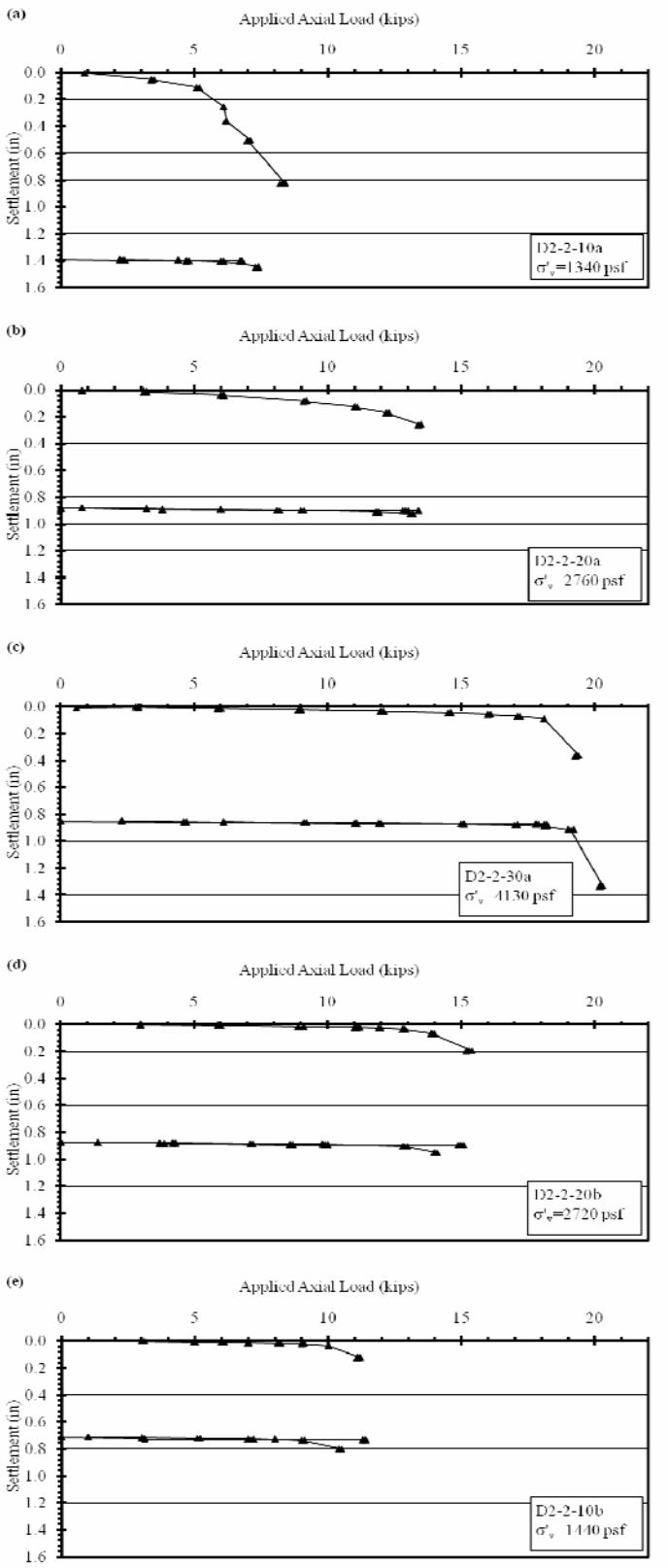

Figure 4.8. Axial load vs settlement plots for Test Series D2-2: (a) Test D2-2-10a, (b) Test D2-2-20a, (c) Test D2-2-30a, (d) Test D2-2-20b, (e) Test D2-2-10b.

4.4 Summary

The testing program and its results were presented. The testing program was divided into 2 groups of tests, those performed without polystyrene flange plugs and those performed with the plugs. Load tests performed without flange plugs included three series of load tests: one series of tests on HP-piles and two series of tests on HPX-piles tests. Tests without flange plugs were conducted using the bladder system without flange plugs and the monotonic loading procedure with two noted exceptions. Tests with flange plugs included five series of load tests: two series of tests on HP-piles tests, and three series of tests on HPX-piles. The bladder system with flange plugs and the load-unload-reload procedure were used for all tests with flange plugs. Results presented for each test series included details regarding the testing conditions and axial load–pile settlement plots for each test.

CHAPTER 5: Analysis

The data presented in Chapter 4 was analyzed in order to determine trends in the axial load capacity for HP and HPX piles. Analyses were performed to examine the effect of vertical effective stress on the ultimate unit side shear and the side shear parameter, β. The effect of over consolidation ratio on the side shear parameter β was examined. Settlement at failure was also examined for each load test. Statistical analyses were performed to evaluate the significance of differences between the two types of piles. Results of these analyses are presented in this chapter.

5.1 Analysis Procedure

The basic procedure for the analyses presented in this chapter involved first establishing an ultimate capacity for each load test. The ultimate pile capacity for each load test was then used to determine the ultimate unit side shear and side shear parameter β. Each analysis is described in more detail in this section.

5.1.1 Ultimate Pile Capacity and Unit Side Shear

For the analyses presented here, the ultimate capacity of each tested pile was taken as the maximum load achieved during the initial load cycle of each test. This approach was taken because the maximum load was generally achieved at relatively low settlements and because failure was generally abrupt. Other methods, such as Davisson's Method, could therefore not be reasonably applied. The settlement at failure was determined at the ultimate load.

Once the ultimate pile capacity was established for each test, the ultimate unit side shear (f_s) for for each test was determined. By analyzing the pile capacities in terms of unit side shear, the effects of embedment depth and pile soil interface area are accounted

for. This allows for a more direct comparison between piles. The unit side shear capacity was determined for two possible pile failure modes. One mode considered that the flanges of the pile plugged during failure the second mode considered that the flanges of the pile did not plug during failure. If the flanges of the pile plug, the pile and the soil within the flanges move or settle as one. If the flanges of the pile do not plug, the soil in the flanges does not move or settle as the pile settles. When the pile flanges plug during failure, the pile soil interface is smaller than when the pile flanges do not plug. For a given pile, the pile circumference is larger in cases when the pile does not plug. The pile circumference for each pile for cases when the pile flanges plug and do not plug is presented in Table 5.1. The experimental apparatus most likely forces the pile flanges to plug during failure, but both failure modes were examined anyway.

Table 5.1. Pile Circumferences used to determine the pile soil interface contact area, A_s.

Pile	Pile Type	Pile Circumference	
		No Plugging of Pile Flanges	Plugging of Pile Flanges
		In	in
Pile A	HP	83	57.5
Pile B	HP	83	57.5
Pile C	HPX	82.5	57
Pile D	HPX	82.5	57

The side shear parameter, β, was found by dividing the ultimate pile capacity (P_{ult}) by the side shear contact area (A_s) as shown

$$f_s = \frac{P_{ult}}{A_s} \tag{5.1}$$

The side shear contact area was determined by multiplying the depth of pile embedment by the pile circumference. A constant depth of pile embedment equal to 4.95

feet was used for all tests for three reasons. First, the soil depth in the chamber was kept relatively constant for each test series. The maximum deviation from the assumed value was 0.16 feet. Second, the few load tests in which the soil depth was significantly less than 4.95 feet at the pile soil interface were the last load tests in a series in which there was considerable sand loss caused by the pile running out of travel. These tests were generally not included in these analyses anyway because the results are not reliable. Third, the sensitivity of the analysis to changes in the depth of pile embedment is relatively small; a 5 percent (3 inch) error in embedment depth results in a 5 percent error in the unit side shear capacity.

5.1.2 Determination Side Shear Parameter β

The beta method is one of the most popular analytical methods used to determine the unit side shear capacity of a deep foundation. The side shear parameter, β collectively accounts for the effects of soil friction angle (ϕ), the pile-soil interface friction angle (δ), and the earth pressure coefficients (K and K_o). By combining these factors together in β, determination of the unit side shear (f_s) becomes a simple calculation involving only β and vertical effective stress (σ'_v). The side shear parameter β was back calculated for each individual load test as where f_s is the measured unit side shear and σ'_v the average vertical effective stress provided in Tables 4.1 and 4.2.

$$\beta = \frac{f_s}{\sigma'_v} \tag{5.2}$$

5.1.3 Statistical Analysis

Simple statistical analyses were performed to determine the significance of differences between smooth HP piles and textured HPX piles. Once the data was reduced

and graphed and once basic linear trends had been established, the standard deviation of the data about the linear trends, i.e. the conditional standard deviation, was computed. Two methods were used to estimate the conditional standard deviation about these linear trends. The first method consisted of establishing the least squares best fit linear trend for the data set and then computing the deviation (Δy) in measured values ($y_{measured}$) from values predicted by the linear trend (y_{trend})

$$\Delta y = y_{measured} - y_{trend} \tag{5.3}$$

The standard deviation of the difference (Δy) was then computed as

$$\sigma = \sqrt{\frac{\sum(y-\Delta y)^2}{n-1}} \tag{5.4}$$

Where y is the mean of the Δy values and n is the sample size. This is the n-1 method of determining standard deviation.

A second method for estimating the conditional standard deviation was also used because of the relatively small sample sizes. This method is based on the assumption that the expected range of values in unit of standard deviations, is related to the sample size for normally distributed data. This relation between sample size and expected range was developed by Snedecore and Cochran (1956) and is shown in Figure 5.1. In this method, the range of Δy was computed and the expected range established from Figure 5.1 based on the sample size. The standard deviation was then computed as

$$\sigma = \frac{Range\ of\ \Delta y}{Expected\ Range} \tag{5.5}$$

Differences in the standard deviations estimated using both of these are discussed subsequently. The conditional standard deviations about the trends presented in the figures in this chapter were determined using the expected range method.

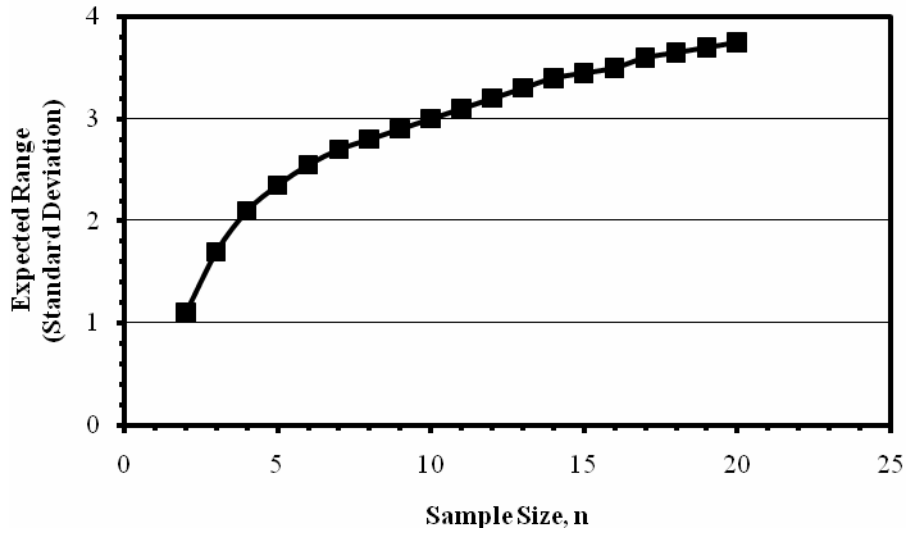

Figure 5.1. Expected range of normal sample in standard deviation units (Snedecor and Cochran 1956).

5.2 Results of Data Analysis

Results of the analysis described in Section 5.1 are presented in this section. Comparisons between results for the smooth HP piles and the textured HPX piles are made and trends noted. Comparisons between results for tests performed with and without the flange plugs are also made.

5.2.1 Summary Data

A summary of the results and analysis parameters (P_{ult}, f_s, β) for the tests without flange plugs are presented in Table 5.2. The table contains the raw data used to determine the analysis parameters as well as the analysis parameters themselves. Load test A1-1-30a in Table 5.2 was not performed because of bladder system issues, but is included to indicate that the soil was subjected to increased effective vertical stresses.

The over consolidation ratios for tests A1-1-10b and A1-1-20b were determined using an assumed average vertical effective stress of 4000psf for test A1-1-30a. The final soil unit weight was not measured for test series D1-1. The ultimate pile capacity, unit side shear, and side shear parameter β are also presented.

Table 5.2. Summary of the tests without flange plugs load test results and analysis.

Test Series	Pile Type	Test No.	Bladder Pressure (psi)	Final Soil Total Unit Weight, γ_{final} (pcf)	Final Soil Relative Density, D_r (%)	Average Vertical Effective Stress, σ'_v (psf)	Over Consolidation Ratio, OCR	Ultimate Pile Capacity, P_{ult} (kips)	Unit Side Shear Capacity, f_s		β	
									Plug (psf)	No Plug (psf)	Plug	No Plug
A1-1	HP	A1-1-10a	7.5	100.1	55.3	1330	1.0	10.1	425.1	294.5	0.32	0.22
		A1-1-20a	16.8			1670	1.0	15.9	669.2	463.6	0.40	0.28
		A1-1-30a	n/a			4000 *	1.0	n/a	n/a	n/a	n/a	n/a
		A1-1-10b	7.5			1330	3.0	11.3	475.6	329.5	0.36	0.25
		A1-1-20c	16.9			2680	1.5	15.2	639.8	443.2	0.24	0.17
D1-1	HPX	D1-1-10a	7.5	n/a	n/a	1320	1.0	6.0	254.8	176.0	0.19	0.13
		D1-1-20a	16.8			2660	1.0	10.9	462.8	319.8	0.17	0.12
		D1-1-30a	26.1			4000	1.0	19.0	806.8	557.4	0.20	0.14
		D1-1-40a	35.5			5350	1.0	25.0	1061.5	733.4	0.20	0.14
D1-2	HPX	D1-2-15a	12.1	97.40	38.9	1980	1.0	7.3	310.0	214.2	0.16	0.11
		D1-2-30a	26.5			4060	1.0	17.0	721.9	498.7	0.18	0.12
		D1-2-10b	7.7			1350	3.0	7.2	305.7	211.2	0.23	0.16
		D1-2-20b	17.0			2690	1.5	9.0	382.2	264.0	0.14	0.10
		D1-2-15c	12.2			2000	2.0	7.2	305.7	211.2	0.15	0.11

*** - assumed value**

A summary of the results and analysis parameters for the tests with flange plugs is presented in Table 5.3. The table contains the raw data used to determine the analysis parameters as well as the analysis parameters. The ultimate pile capacities presented were determined from the initial load cycle. The ultimate pile capacity, unit side shear capacity, and side shear parameter β are also presented in Table 5..

The three highlighted load tests (D2-1-10a, D2-1-20a, and D2-1-10b) presented in Table 5.3 were not included in the data analysis. Tests D1-1-10a and D1-1-20a were not included because of issues with the bladder system that resulted in lower than expected ultimate loads for the given average effective stresses. The issue with the bladder system was noted during testing and was confirmed during data analysis. Load test D1-1-10b was not included because the pile ran out of travel during testing and experienced

significant sand loss. The failure also occurred at a lower than expected ultimate pile capacity.

Table 5.3. Summary of the tests with flange plugs load test results and analysis.

Test Series	Pile Type	Test No.	Bladder Pressure (psi)	Final Soil Total Unit Weight, γ_{final} (pcf)	Final Soil Relative Density, D_r (%)	Average Vertical Effective Stress, σ'_v (psf)	Over Consolidation Ratio, OCR	Ultimate Pile Capacity, P_{ult} (kips)	Unit Side Shear Capacity, *fs*		β	
									Plug (psf)	No Plug (psf)	Plug	No Plug
A2-1	HP	A2-1-10a	8.0	97.39	38.8	1390	1.0	7.3	307.3	212.9	0.22	0.15
		A2-1-20a	16.5			2620	1.0	14.1	593.5	411.1	0.23	0.16
		A2-1-30a	25.6			3930	1.0	19.1	803.9	556.9	0.20	0.14
		A2-1-20b	16.3			2590	1.5	15.5	652.4	452.0	0.25	0.17
		A2-1-10b	7.4			1310	3.0	9.0	378.8	262.4	0.29	0.20
A2-2	HP	A2-2-10a	7.8	97.01	36.4	1370	1.0	6.4	269.4	186.6	0.20	0.14
		A2-2-20a	17.3			2730	1.0	13.4	564.0	390.7	0.21	0.14
		A2-2-30a	26.7			4090	1.0	17.3	728.2	504.5	0.18	0.12
		A2-2-20b	17.3			2730	1.5	14.3	601.9	417.0	0.22	0.15
		A2-2-10b	8.4			1450	2.8	11.0	463.0	320.8	0.32	0.22
C2-1	HPX	C2-1-10a	7.4	97.19	37.6	1310	1.0	8.1	343.9	237.6	0.26	0.18
		C2-1-20a	16.6			2630	1.0	15.9	675.1	466.5	0.26	0.18
		C2-1-30a	26.2			4010	1.0	21.5	912.9	630.8	0.23	0.16
		C2-1-20b	17.2			2720	1.5	17.0	721.9	498.7	0.27	0.18
		C2-1-10b	7.5			1320	3.0	10.0	424.6	293.4	0.32	0.22
D2-1	HPX	D2-1-10a	7.9	97.22	37.8	1380	1.0	4.3	182.6	126.2	0.13	0.09
		D2-1-20a	16.8			2660	1.0	7.0	297.2	205.4	0.11	0.08
		D2-1-30a	26.6			4070	1.0	19.6	832.3	575.0	0.20	0.14
		D2-1-20b	17.1			2700	1.5	16.3	692.1	478.2	0.26	0.18
		D2-1-10b	7.2			1280	3.2	6.1	259.0	179.0	0.20	0.14
D2-2	HPX	D2-2-10a	7.6	97.76	41.1	1340	1.0	8.2	348.2	240.6	0.26	0.18
		D2-2-20a	17.5			2760	1.0	13.4	569.0	393.1	0.21	0.14
		D2-2-30a	27.0			4130	1.0	19.3	819.5	566.2	0.20	0.14
		D2-2-20b	17.2			2720	1.5	15.2	645.4	445.9	0.24	0.16
		D2-2-10b	8.3			1430	2.9	11.1	471.3	325.6	0.33	0.23

5.2.2 Unit Side Shear

It is useful to examine the load tests in terms of unit side shear. It is necessary to examine the unit side shear of each load test in two ways, one way is to assume the soil plugs between the pile flanges during failure and the other is to assume the soil does not plug between the pile flanges during failure. The experimental setup most likely forced the pile flanges to plug during failure, but both possibilities were examined.

The results of the unit side shear analysis assuming the pile flanges plug for the tests without flange plugs are plotted in Figure 5.2 The trends the trends in unit side shear for the HP and HPX piles have an approximately 25 percent difference in slope.

The HP piles produced greater unit side shear at a given effective stress than the HPX tests. The conditional standard deviation in unit side shear for the HP piles is approximately one third of the conditional standard deviation for the HPX piles. The two methods for determining the conditional standard deviation about a trend produced similar results as seen in Table 5.4.

Table 5.4. Summary of conditional standard deviations about a trend for ultimate load vs effective stress and unit side shear vs effective stress analyses.

	Pile Type	Conditional Standard Deviation, σ					
		Ultimate Load vs Vertical Effective Stress		Unit Side Shear vs Vertical Effective Stress (Assumes Plugging of Flange)		Unit Side Shear vs Vertical Effective Stress (Assumes No Plugging of Flange)	
		n-1 Method (kip)	Expected Range Method (kip)	n-1 Method (psf)	Expected Range Method (psf)	n-1 Method (psf)	Expected Range Method (psf)
Tests without Flange Plugs	HP	0.58	0.47	24.3	24.1	16.9	19.2
	HPX	1.45	1.55	61.5	66.6	42.5	46.0
Tests with Flange Plugs	HP	1.51	1.48	63.7	62.3	44.1	43.2
	HPX	1.34	1.18	56.8	50.1	39.2	34.7

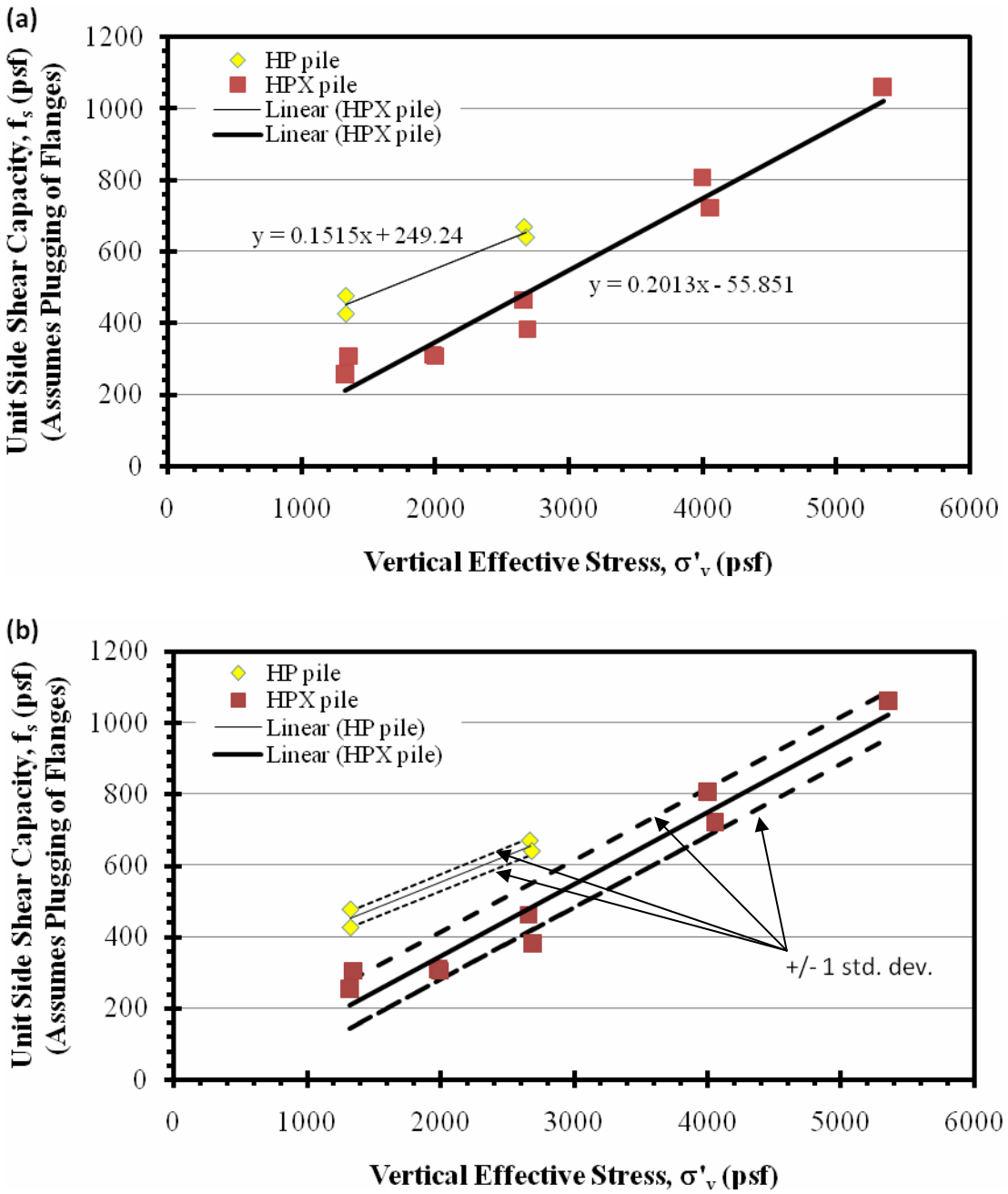

Figure 5.2. Unit side shear capacity vs vertical effective stress for tests without flange plugs assuming the pile flanges plug during failure: (a) linear trends and (b) linear trends showing conditional standard deviation about the trend determined using the expected range method.

Results of the unit side shear analysis assuming the pile flanges do not plug for the tests without flange plugs are plotted in Figure 5.3. The general trends are similar for both assumed failure conditions, however the unit side shear at a given effective stress is higher when the pile flanges are assumed to plug. The slope of the trends when the pile flanges are assumed to plug is approximately 0.1 psf per psf. The HP and HPX linear trends for both assumed failure conditions again showed non-zero ultimate pile capacities at zero effective stress. This is most likely the result of non linearity in the failure envelope at low effective stresses.

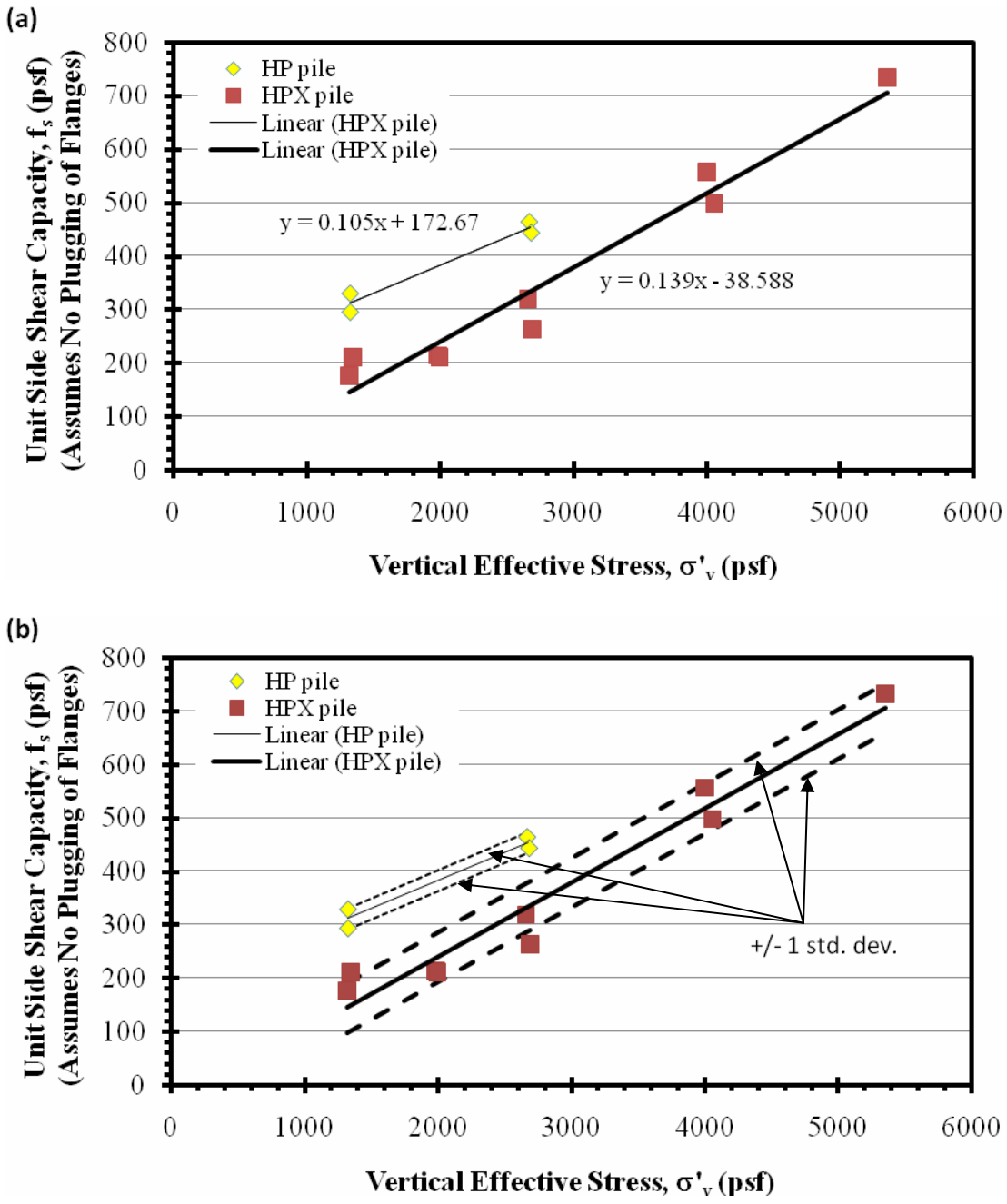

Figure 5.3. Unit side shear capacity vs vertical effective stress for tests without flange plugs assuming the pile flanges do not plug during failure: (a) linear trends and (b) linear trends showing conditional standard deviation about the trend determined using the expected range method.

Results of the unit side shear analysis assuming the pile flanges plug for the tests with flange plugs are plotted in Figure 5.4. The linear trends for the HP and the HPX piles are approximately parallel with a slope of approximately 0.16 psf per psf. The HPX piles, on average, produced higher unit side shear at a given effective stress than the HP piles as evidenced by the best fit trend lines in Figure 5.4. The difference in unit side shear for the two pile types is approximately 30 to 80 psf. The conditional standard deviations for both the HP and HPX tests were approximately 60 psf. The linear trends for the HP and HPX piles were approximately one standard deviation apart from each other. The two methods for determine the conditional standard deviation produced similar results, as shown in Table 5.4.

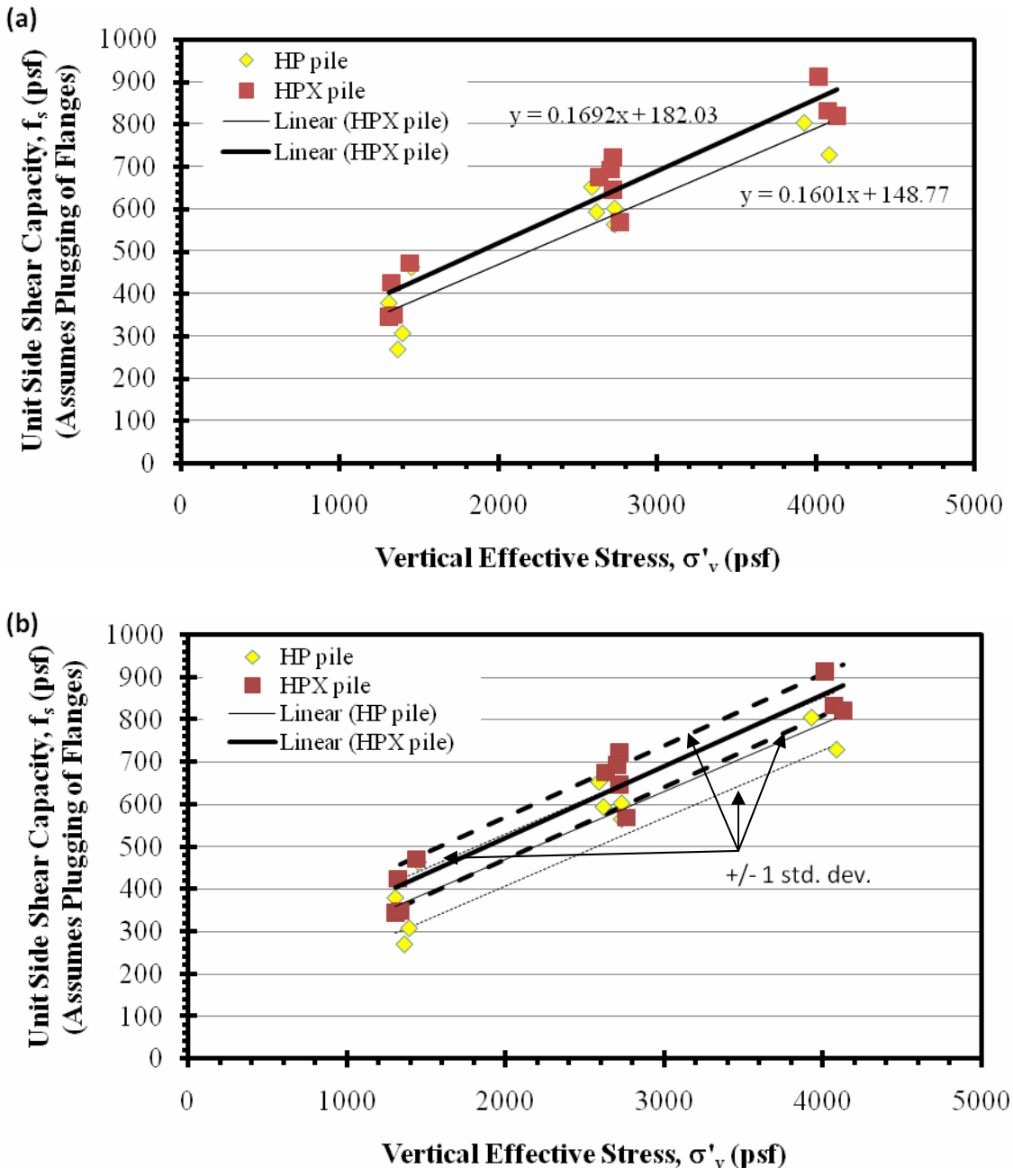

Figure 5.4. Unit side shear capacity vs vertical effective stress for tests with flange plugs assuming the pile flanges plug during failure: (a) linear trends and (b) linear trends showing conditional standard deviation about the trend determined using the expected range method.

Results of the unit side shear analyses assuming the pile flanges do not plug for the tests with flange plugs are plotted in Figure 5.5. The general trends are similar for both assumed failure conditions. The unit side shear at a given effective stress is greater when the pile flanges are assumed to not plug. The slope of the trends when the pile flanges are assumed to not plug is approximately 0.11 psf per psf. The linear trends for both the HP and HPX piles showed approximately 150 psf unit sides shear capacity at zero effective stress. This is most likely the result of non linearity in the failure envelope at low effective stresses.

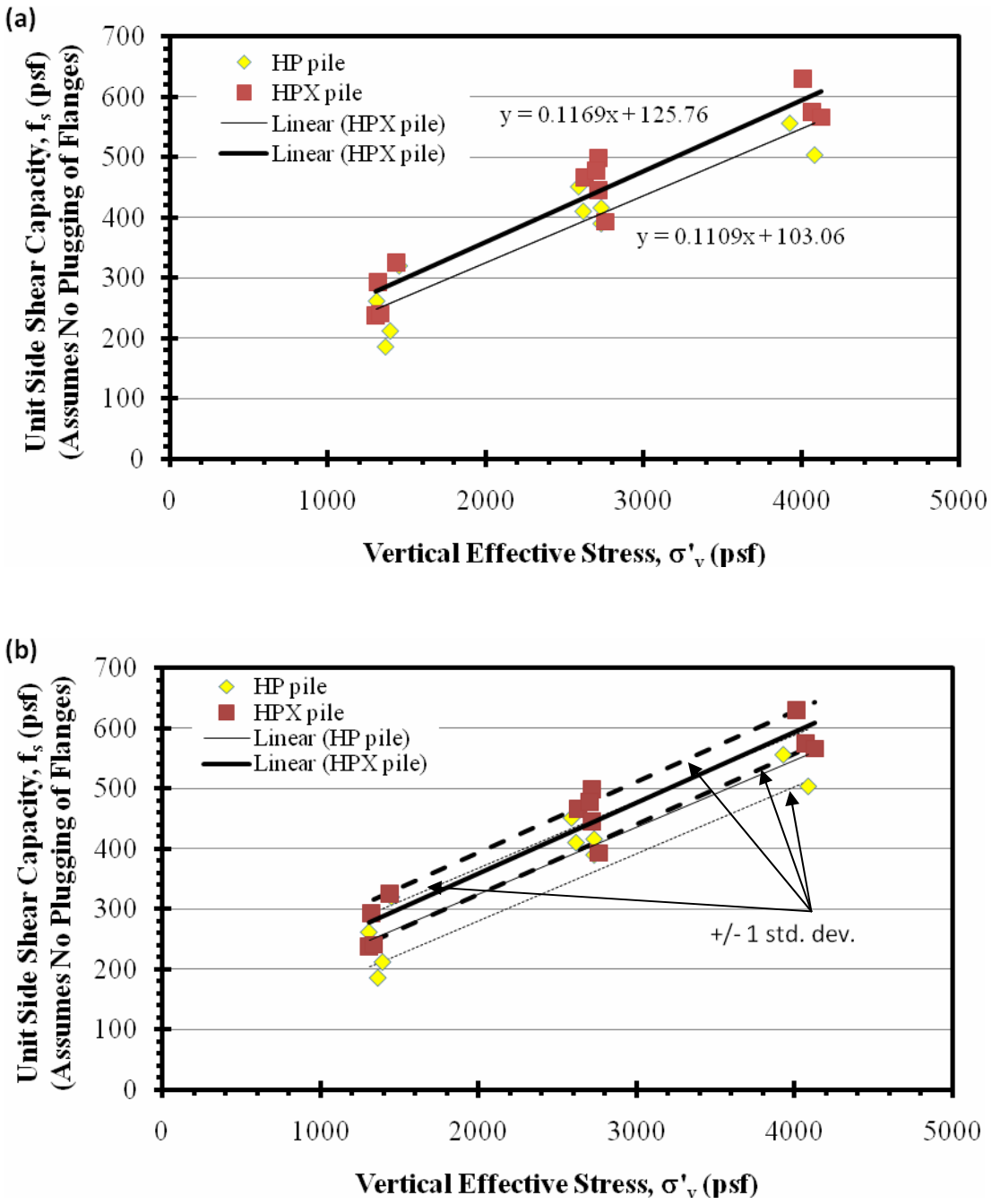

Figure 5.5. Unit side shear capacity vs vertical effective stress for tests with flange plugs assuming the pile flanges do not plug during failure: (a) linear trends and (b) linear trends showing conditional standard deviation about the trend determined using the expected range method.

When comparing results from tests without flange plugs to tests with flange plugs in terms of unit side shear there are several similarities and one notable difference. The linear trends for all of the tests without flange plugs and the tests with flange plugs are, practically speaking, parallel. The conditional standard deviations in unit side shear for the HPX piles tested without flange plugs and the HP and HPX tests with flange plugs are similar. The HPX tests without flange plugs and the HPX tests with flange plugs also resulted in relatively similar slopes for the linear trends. The most notable difference is that the HP piles have a higher unit side shear at a given effective stress than the HPX piles for the tests performed without flange plugs. However, the unit side shear values at a given vertical effective stress for the HP piles tested without flange plugs are similar to the unit side shears at a given vertical effective stress for the HP piles tested with flange plugs. The HPX piles tested without flange plugs produced lower unit side shear at a given effective stress than the HPX piles tested with flange plugs. This suggests that there was an issue with the tests conducted on the HPX piles that did not have flange plugs.

5.2.3 Side Shear Parameter β

Another useful way to examine the load tests is in terms of side shear parameter β. As stated in Section 5.1.2, β accounts for the effects of soil friction angle, pile-soil interface friction, and earth pressure coefficients, which allows for a simple relation between unit side shear and effective overburden stress. β values were back calculated using the known values of ultimate unit side shear and vertical effective stress. It is necessary to examine the side shear parameter β in terms of both assumed failure conditions, i.e. assuming the pile flanges plug during failure and assumes the pile flanges

do not plug during failure. As previously stated, the experimental setup most likely forced the pile flanges to plug during failure, but both possibilities were examined. The effect of the vertical effective stress and the over consolidation ratio on the side shear parameter β was examined.

Results of analyses of the side shear parameter β as a function of effective stress for the tests without flange plugs assuming soil plugs form are plotted in Figure 5.6. For the tests on HPX piles, β is relatively constant at 0.17 regardless of the vertical effective stress. The conditional standard deviation is approximately 0.03. The HP piles however show a decreasing β values with increasing effective stress. The HP piles also produced significantly higher β values than the HPX tests for tests performed without the flange plugs. The standard deviation for the HP tests is about half the standard deviation of the HPX tests.

Results of analyses for the side shear parameter β as a function of effective stress for the tests without flange plugs assuming soil plugs do not form are plotted in Figure 5.7. Again, the HPX tests had relatively constant β values of approximately 0.12 regardless of the vertical effective stress. The HP tests showed a decreasing β values with increasing effective stress and the β values are greater than for the HPX test values.

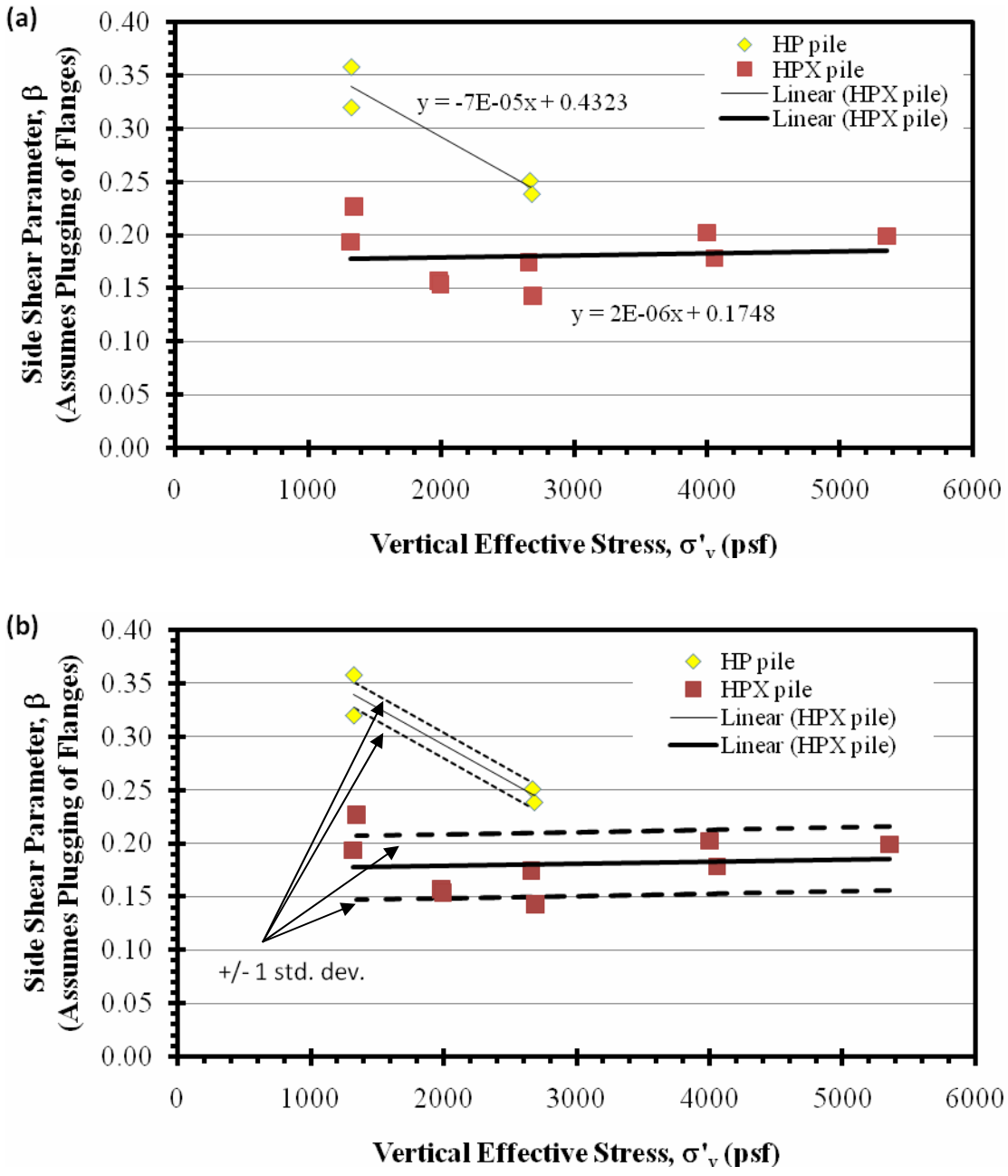

Figure 5.6. Side shear parameter β vs vertical effective stress for tests without flange plugs assuming the pile flanges plug during failure: (a) linear trends and (b) linear trends showing conditional standard deviation about the trend determined using the expected range method.

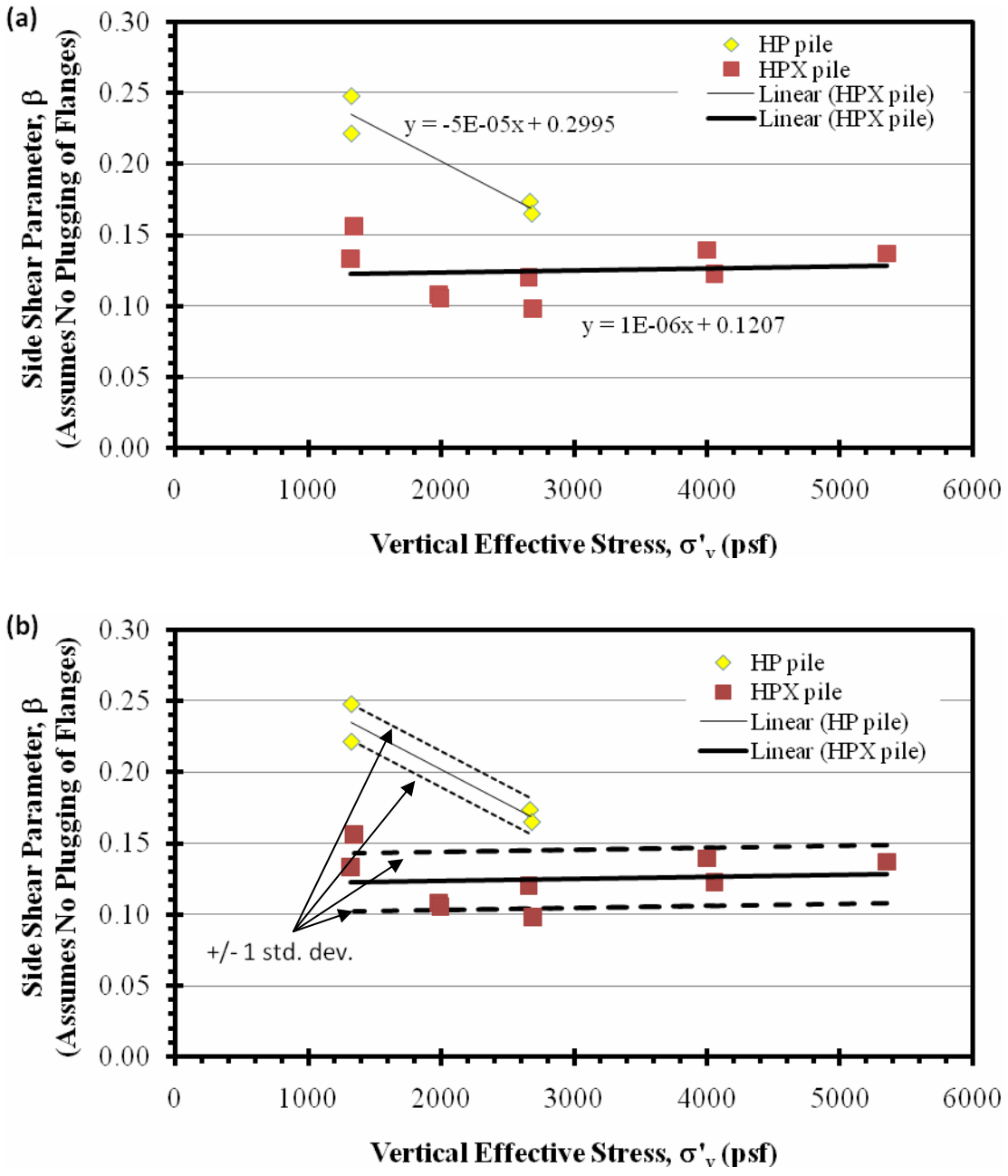

Figure 5.7. Side shear parameter β vs vertical effective stress for tests without flange plugs assuming the pile flanges do not plug during failure: (a) linear trends and (b) linear trends showing conditional standard deviation about the trend determined using the expected range method.

Results of analyses for the side shear parameter β as a function of effective stress for the tests with flange plugs assuming soil plugs do form are plotted in Figure 5.8. The β values for the HPX tests are approximately 0.05 larger than for the HP tests. For both the HP and HPX piles, the β values decrease from approximately 0.3 at 1000 psf to approximately 0.2 at 4000 psf, with the HP β values being a little less than the HPX values. The linear trends are essentially parallel. The conditional standard deviation for the HP piles is approximately twice the conditional standard deviation for the HPX tests. The standard deviation values can be seen in Table 5.5. In this case the linear trend for the HPX piles and plus and minus one standard deviation about that trend are within one conditional standard deviation of the linear trend of the HP piles. This can be seen in Figure 5.8b.

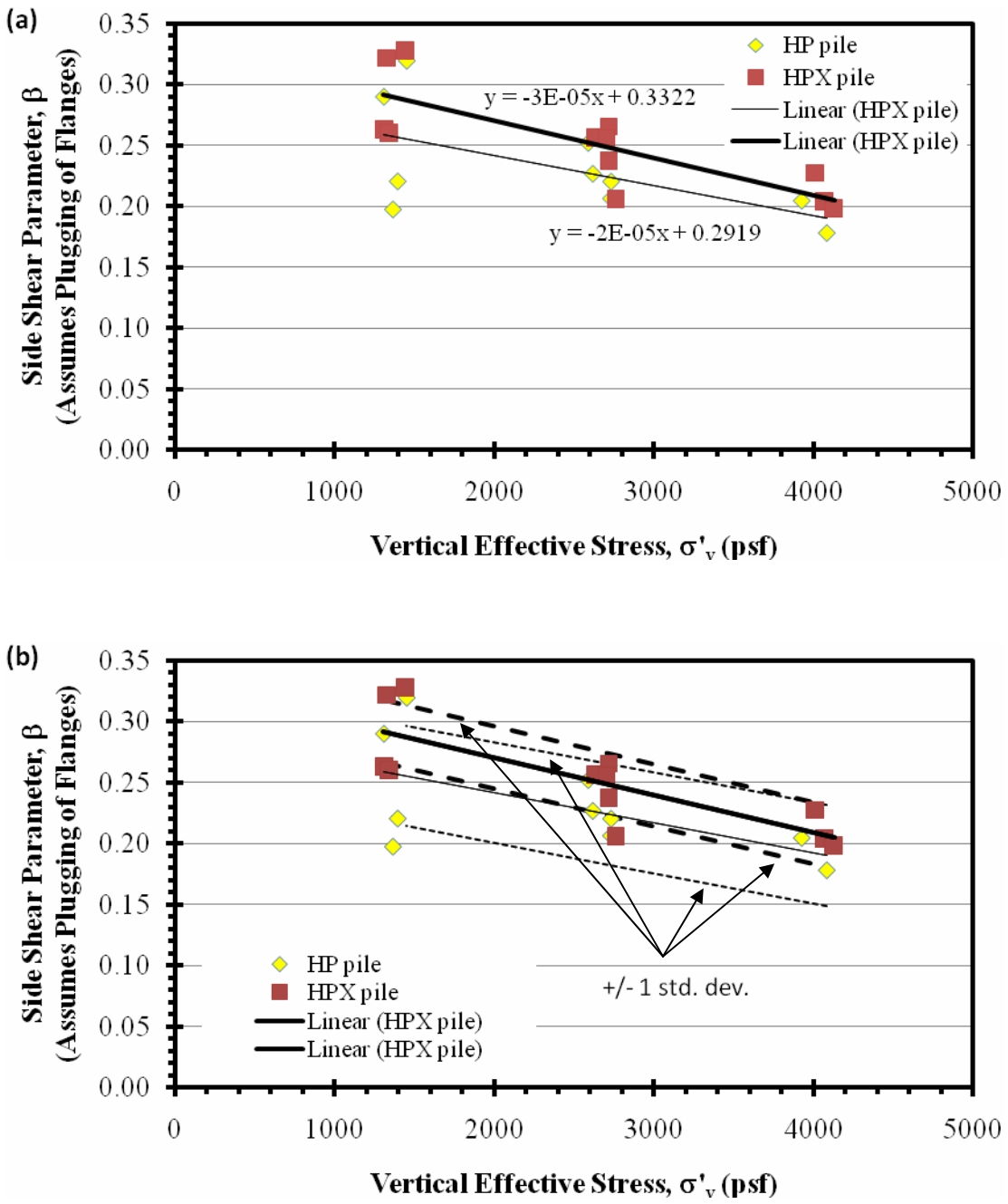

Figure 5.8. Side shear parameter β vs vertical effective stress for tests with flange plugs assuming the pile flanges plug during failure: (a) linear trends and (b) linear trends showing conditional standard deviation about the trend determined using the expected range method.

Table 5.5. Summary of conditional standard deviations for side shear parameter β vs vertical effective stress and side shear parameter β vs over consolidation ratio analyses.

	Pile Type	Conditional Standard Deviation, σ							
		Side Shear Parameter β vs Vertical Effective Stress				Side Shear Parameter β vs Over Consolidaiton Ratio			
		(Assumes Plugging of Flange)		(Assumes No Plugging of Flange)		(Assumes Plugging of Flange)		(Assumes No Plugging of Flange)	
		n-1 Method (psf)	Expected Range Method (psf)	n-1 Method (psf)	Expected Range Method (psf)	n-1 Method	Expected Range Method	n-1 Method	Expected Range Method
Tests without Flange Plugs	HP	0.0162	0.0120	0.0113	0.0126	0.0436	0.0333	0.0298	0.0482
	HPX	0.0270	0.0300	0.0187	0.0206	0.0259	0.0159	0.0256	0.0230
Tests with Flange Plugs	HP	0.0352	0.0412	0.0245	0.0287	0.0175	0.0160	0.0121	0.0112
	HPX	0.2490	0.0257	0.0173	0.0180	0.0225	0.0203	0.0155	0.0140

Results of the analyses for the side shear parameter β as a function of effective stress for the tests without flange plugs assuming soil plugs do not form are plotted in Figure 5.9. The same general trends noted when the pile flanges were assumed to plug is present, however the magnitude of the β values are reduced. The conditional standard deviation of the HP tests again is approximately twice the conditional standard deviation for the HPX piles, and the linear trend for HPX piles plus and minus one conditional standard deviation is within one conditional standard deviation of the HP piles. This can be seen in Figure 5.9b.

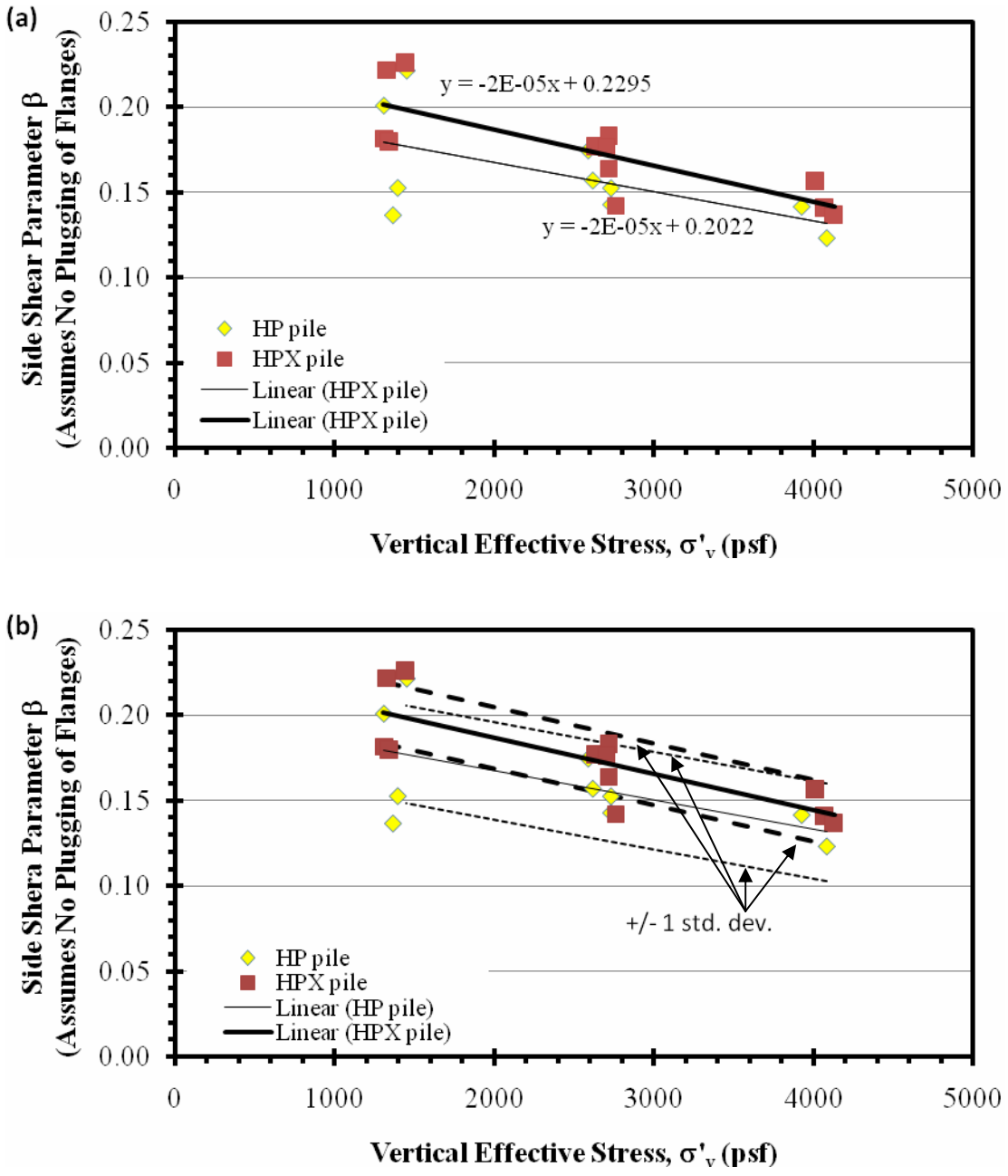

Figure 5.9. Side shear parameter β vs vertical effective stress for tests with flange plugs assuming the pile flanges do not plug during failure: (a) linear trends and (b) linear trends showing conditional standard deviation about the trend determined using the expected range method.

Comparisons between the tests performed without flange plugs and the tests performed with flange plugs for the side shear parameter β as a function of effective stress do not lead to many general trends observed between the two groups. The HP tests without flange plugs produced the highest β values at a given effective stress. The HPX tests with flange plugs is the only grouping where the β values were constant and did not decrease with increasing effective stress. The HPX tests with flange plugs also produced the lowest β values at a given effective stress. This is not unexpected when the issues with these tests are considered. The linear trends of the tests with flange plugs are within one standard deviation of one another, suggesting that differences in β values for the two tests are not significant. The issues which have been raised about the HPX tests performed without flange plugs in Section 5.2.2 are still valid.

Results of the analyses of the side shear parameter β as a function of over consolidation ratio for the tests without flange plugs assuming soil plugs do form are shown in Figure 5.10. The linear trends for both the HP and HPX piles, while not quite parallel, both show an increase in the β values with increasing over consolidation ratio. The β values for the HP piles are again higher than the HPX piles for a given over consolidation ratio. Similar results for the tests performed without flange plugs assuming the pile flanges do not plug are shown in Figure 5.11. The magnitude of the β values decreases when the pile flanges are assumed not to plug but the general trends which have been noted are still evident.

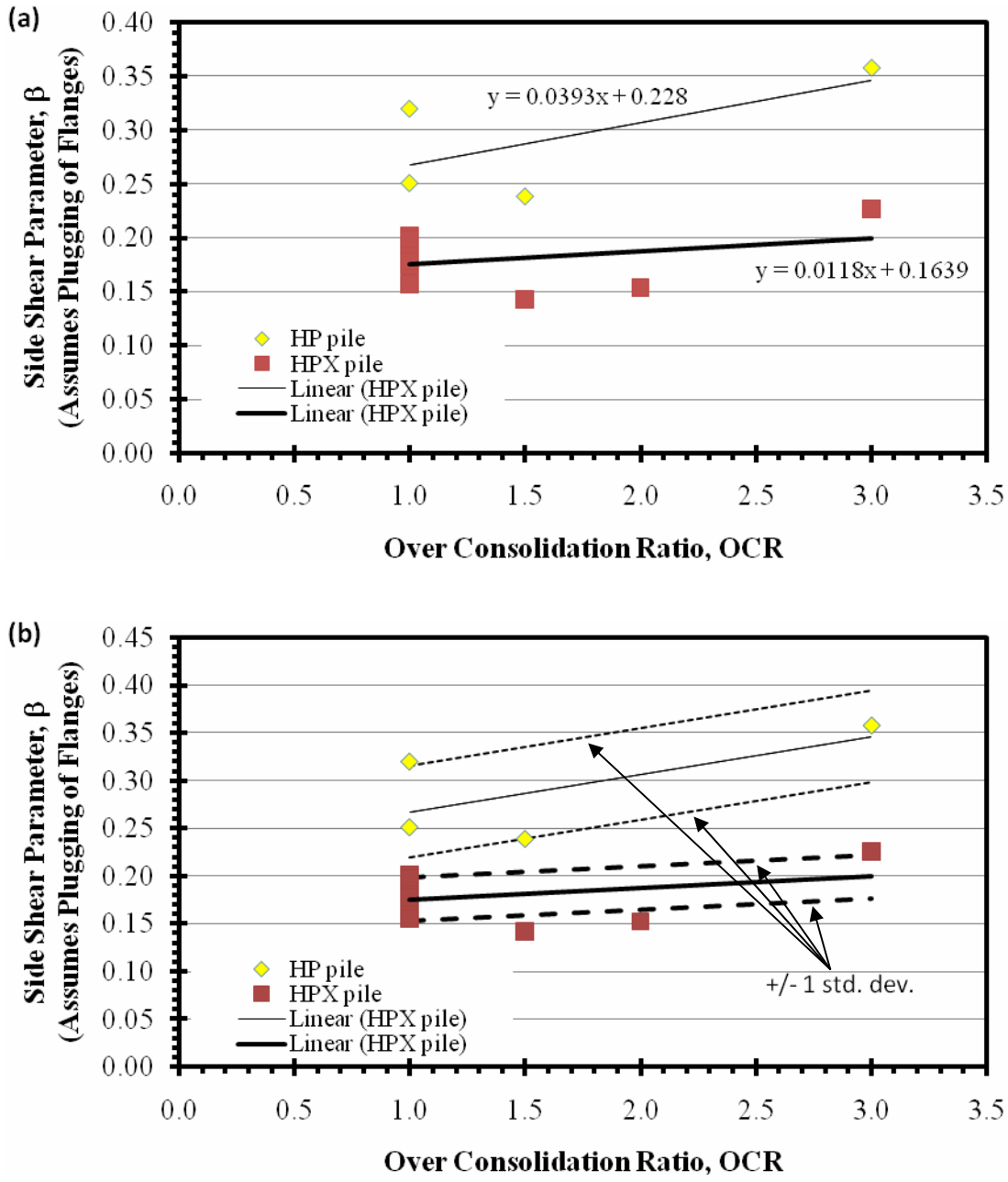

Figure 5.10. Side shear parameter β vs over consolidation ratio for tests without flange plugs assuming the pile flanges plug during failure: (a) linear trends and (b) linear trends showing conditional standard deviation about the trend determined using the expected range method.

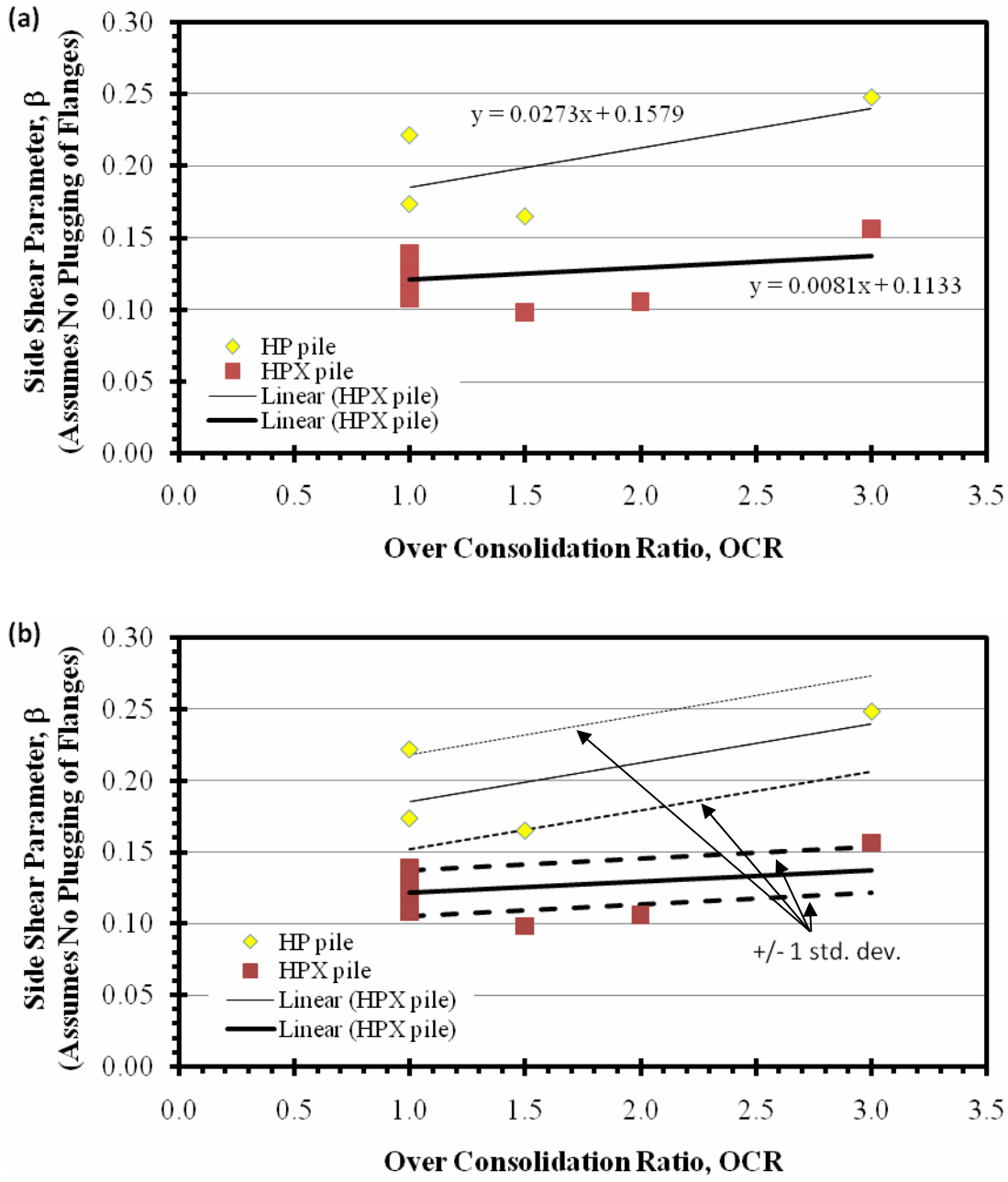

Figure 5.11. Side shear parameter β vs over consolidation ratio for tests without flange plugs assuming the pile flanges do not plug during failure: (a) linear trends and (b) linear trends showing conditional standard deviation about the trend determined using the expected range method.

The conditional standard deviation for the HP piles in this plot is approximately twice that for the HPX piles. Analyses for tests without flange plugs are the only analyses in which the method used to determine the standard deviation had a significant effect on the conditional standard deviation. The expected range method resulted in approximately a 30 percent and 50 percent decrease standard deviation in comparison to the n-1 method for the HP piles.

Results for the analyses for the side shear parameter β as a function of over consolidation ratio are plotted in Figure 5.12 for the tests with flange plugs assuming soil plugs do form. The linear trends shown are essentially parallel with slopes of approximately 0.05. The β values for the HPX piles are larger than the β values for the HP piles at a given effective stress. However, the linear trends for both are within approximately one standard deviation of each other as shown in Figure 5.12b. Similar results for the tests with flange plugs s assuming the pile flanges do not plug are shown in Figure 5.13. The same general trends can be observed with the only difference being the magnitude of the β values and the slope of the two parallel linear trends.

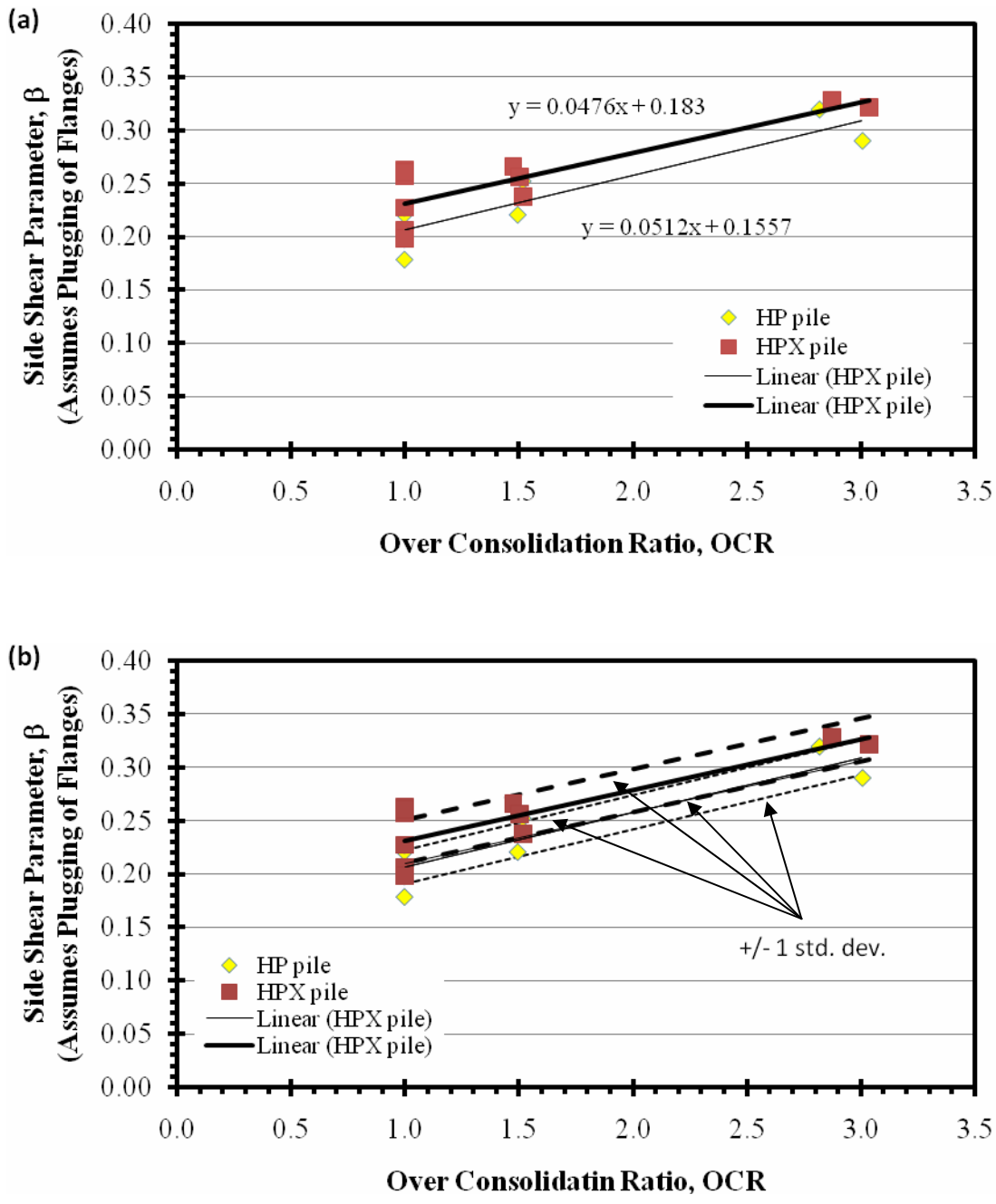

Figure 5.12. Side shear parameter β vs over consolidation ratio for tests with flange plugs assuming the pile flanges plug during failure: (a) linear trends and (b) linear trends showing conditional standard deviation about the trend determined using the expected range method.

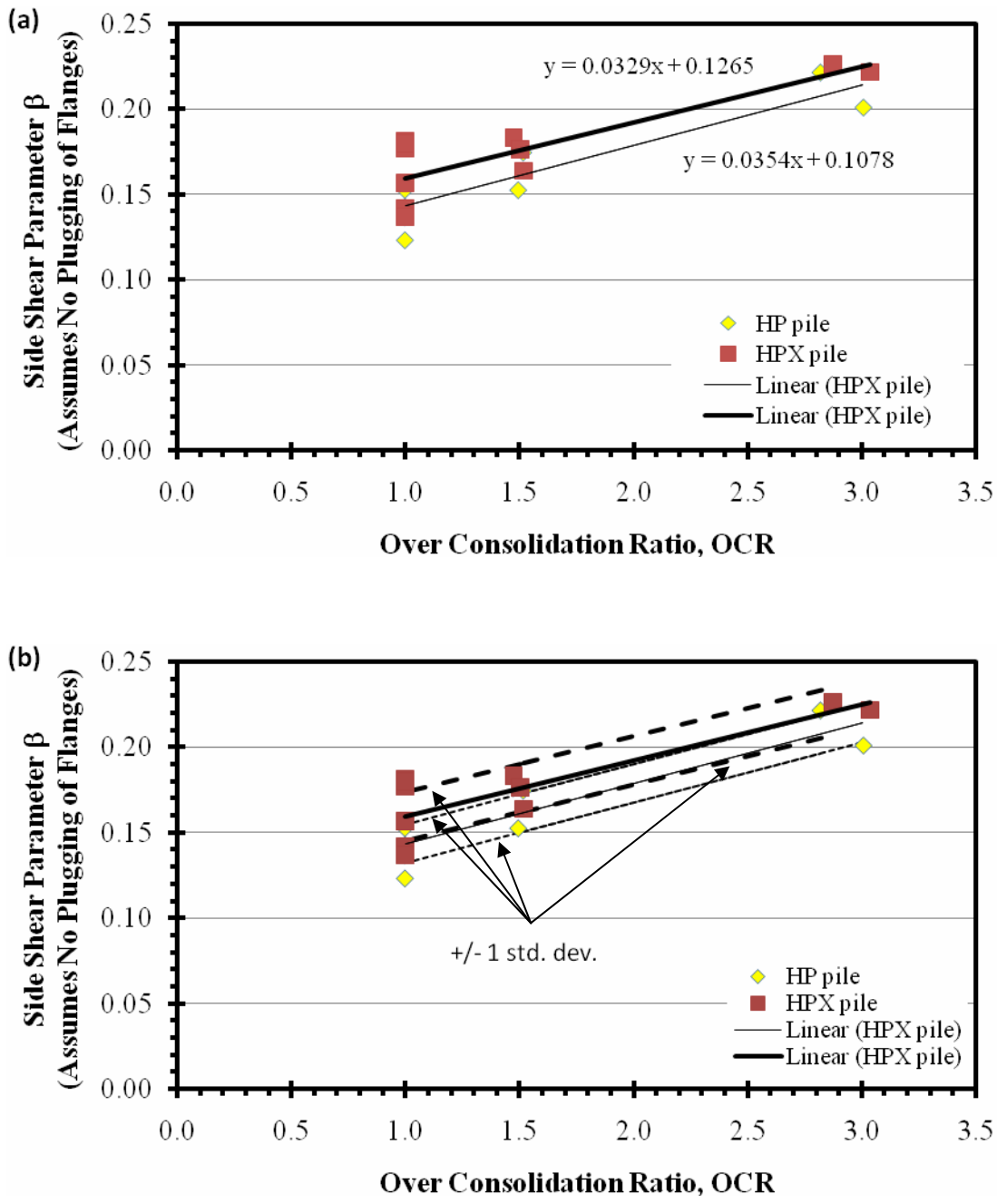

Figure 5.13. Side shear parameter β vs over consolidation ratio for tests with flange plugs assuming the pile flanges do not plug during failure: (a) linear trends and (b) linear trends showing conditional standard deviation about the trend determined using the expected range method.

A general trend can be noted by comparing results of tests without flange plugs to tests with flange plugs tests in terms of the side shear parameter β as a function of the over consolidation ratio. For all tests, the β values increased with increasing over consolidation ratio. However, the tests without flange plugs and the tests with flange plugs did not produce the same magnitude of β values. Tests performed on HPX piles without flange plugs produced the lowest β values at a given effective stress. The fact that the HPX piles tested without flange plugs resulted in the lowest β values reinforces the idea that there were issues with those tests. The slope of the linear trends was not similar between the tests without flange plugs and the tests with flange plugs. This also reinforces the idea that there was an issue with the tests performed without flange plugs. In the author's opinion, the tests performed with flange plugs are more representative.

5.3 Settlement

The total pile settlement at failure was also examined. Because of the close relation between vertical effective stress, ultimate load, unit side shear, and, to a lesser extent, the side shear parameter β, only the settlement analyses conducted using the unit side shear are presented. The total pile settlement as a function of unit side shear analyses are presented because the unit side shear allows for a more direct comparison between tests. The effect of over consolidation ratio on total pile settlement was also examined. It is important to remember that the settlement at failure depends a great deal on the last loading increment of the load test. As such, the trends presented below are subject to effects of the last load increment. The settlement analyses presented in this section assume that soil plugs form in the pile flanges. The trends and relationships noted are qualitatively similar if soil plugs are assumed to not form.

Results of analyses of pile settlement as a function of unit side shear are presented in Figure 5.14 for the tests performed without flange plugs assuming soil plugs do form. There is considerable scatter in the data. The linear trends for both data sets are plotted, but it is difficult to draw any conclusions regarding settlement for the HP-pile because of the small sample size. The linear trend of settlement of the HPX pile relatively constant at approximately 0.2 inches, but again there is considerable scatter. The conditional standard deviation about the trends is approximately 0.1 inches for both pile types. This is another indicator of the considerable scatter because the conditional standard deviation represents as much as 50 percent of the total settlement. The conditional standard deviation ignoring any trend is approximately 0.2 inches for the HP-pile and approximately 0.1 inches for the HPX pile. The standard deviations for the settlement analyses are presented in Table 5.6.

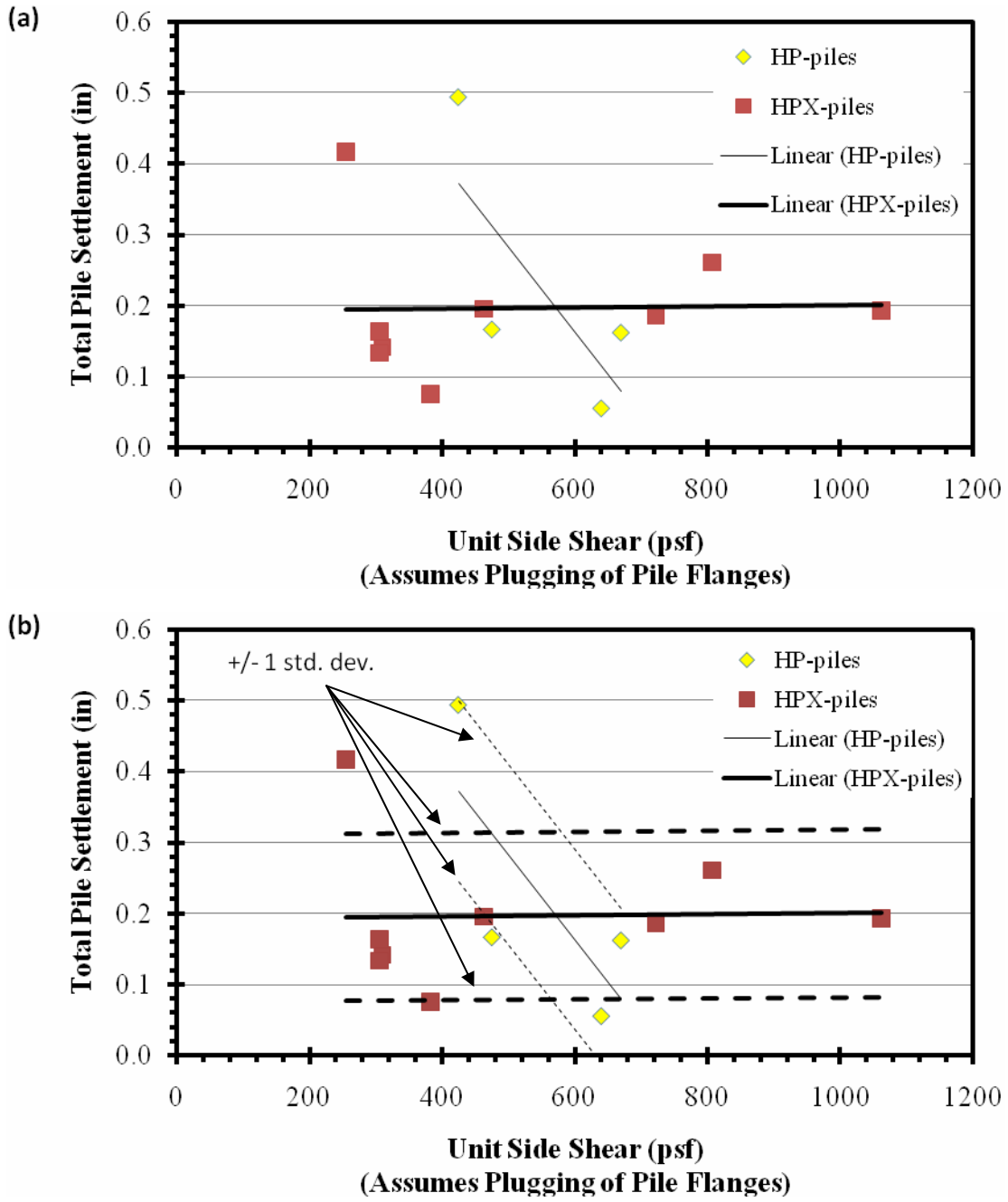

Figure 5.14. Total pile settlement vs unit side shear for tests without flange plugs assuming the pile flanges do not plug during failure: (a) linear trends and (b) linear trends showing conditional standard deviation about the trend determined using the expected range method.

Results of analyses of pile settlement as a function of unit side shear for the tests performed with flange plugs assuming soil plugs do form are presented in Figure 5.15. There is again considerable scatter in the data. However, there is a general and constant trend that can be observed for both pile types. The HPX-piles tend to experience more settlement at failure than the HP-piles when considered in aggregate. Because of the large scatter and resulting large standard deviations, this is more of a qualitative observation than quantitative observation. The standard deviations about the trends are approximately 0.1 and 0.2 inches for the HP and HPX-piles respectively. Again, this represents 50 percent or more of the total pile settlement at failure. For both the HP and HPX-piles, the total settlement decreased as the unit side shear increased. It should be noted that the effect of the bladder pressure sequencing on this trend is unknown. The first load test was always performed at a target bladder pressure of 10 psi (an average vertical effective stress of approximately 1400 psf) so it is possible that the trend is a result of the testing procedure.

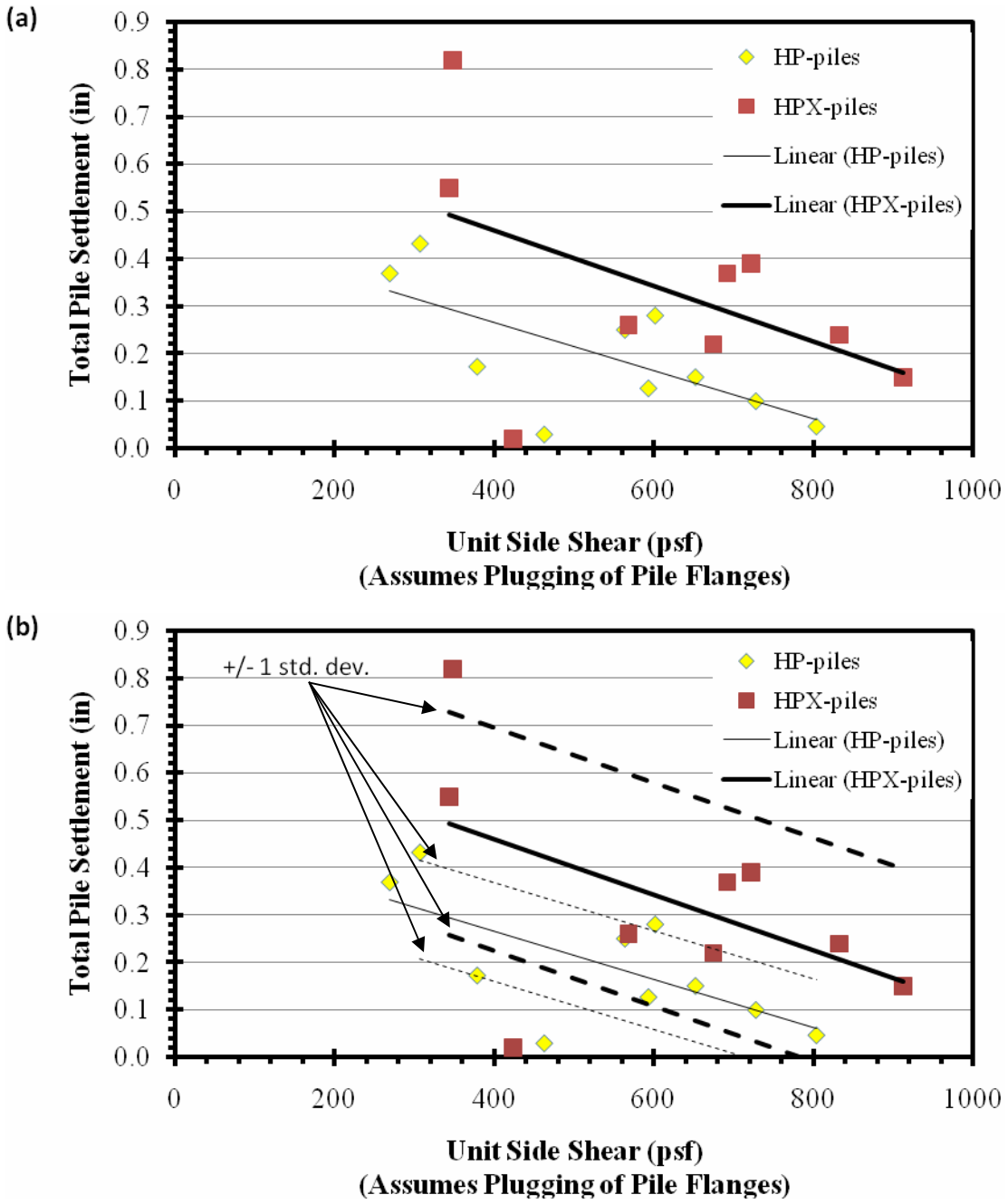

Figure 5.15. Total pile Settlement vs unit side shear for tests with flange plugs assuming plugging of the pile flanges: (a) linear trends and (b) linear trends conditional standard deviation about the trend determined using the expected range method.

Results of analyses of pile settlement as a function of over consolidation ratio for the tests without flange plugs assuming soil plugs do form are presented in Figure 5.16. The general trend for both the HP and HPX-piles is decreasing settlement at failure with increasing over consolidation ratio. The two linear trends are approximately parallel. The HP-pile does show slightly more settlement at failure for a given over consolidation ratio, but when scatter and standard deviation are taken into account the difference in the linear trends is of little practical significance.

Results of the analyses of pile settlement as a function of over consolidation ratio for the tests performed with flange plugs assuming soil plugs do form are presented in Figure 5.17. Again, the general trend of decreased settlement at failure with increasing over consolidation ratio can be observed. It should be noted that the effect of the over consolidation sequencing on this trend is unknown. The first load test was always performed at an over consolidation ratio of 1 and the last at an over consolidation ratio of 3 so it is possible that the trend is a result of the testing procedure. The HPX-piles experienced greater settlement at failure for normally consolidated soils, but at approximately an OCR of 3 the trends intersect and the settlement at failure is approximately equal. Because of the small number of tests on over consolidated soils, it is difficult to draw conclusions about the differences in settlement between the two types of pile in over consolidated soil. The scatter and standard deviation about the trends is again as much as 50 percent of the total settlement.

The standard deviations for the settlements analyses performed on both tests without flange plugs and tests with flange plugs are presented in Table 5.6. The standard deviations determined by method 1 and method 2 are again similar to one another. The

standard deviation of the total pile settlements was also determined regardless of any trends. These standard deviations are also presented in Table 5.6. These standard deviations are similar to the standard deviation about the trends, a further indication of the large amount of scatter, and of the quantitative nature of the noted trends.

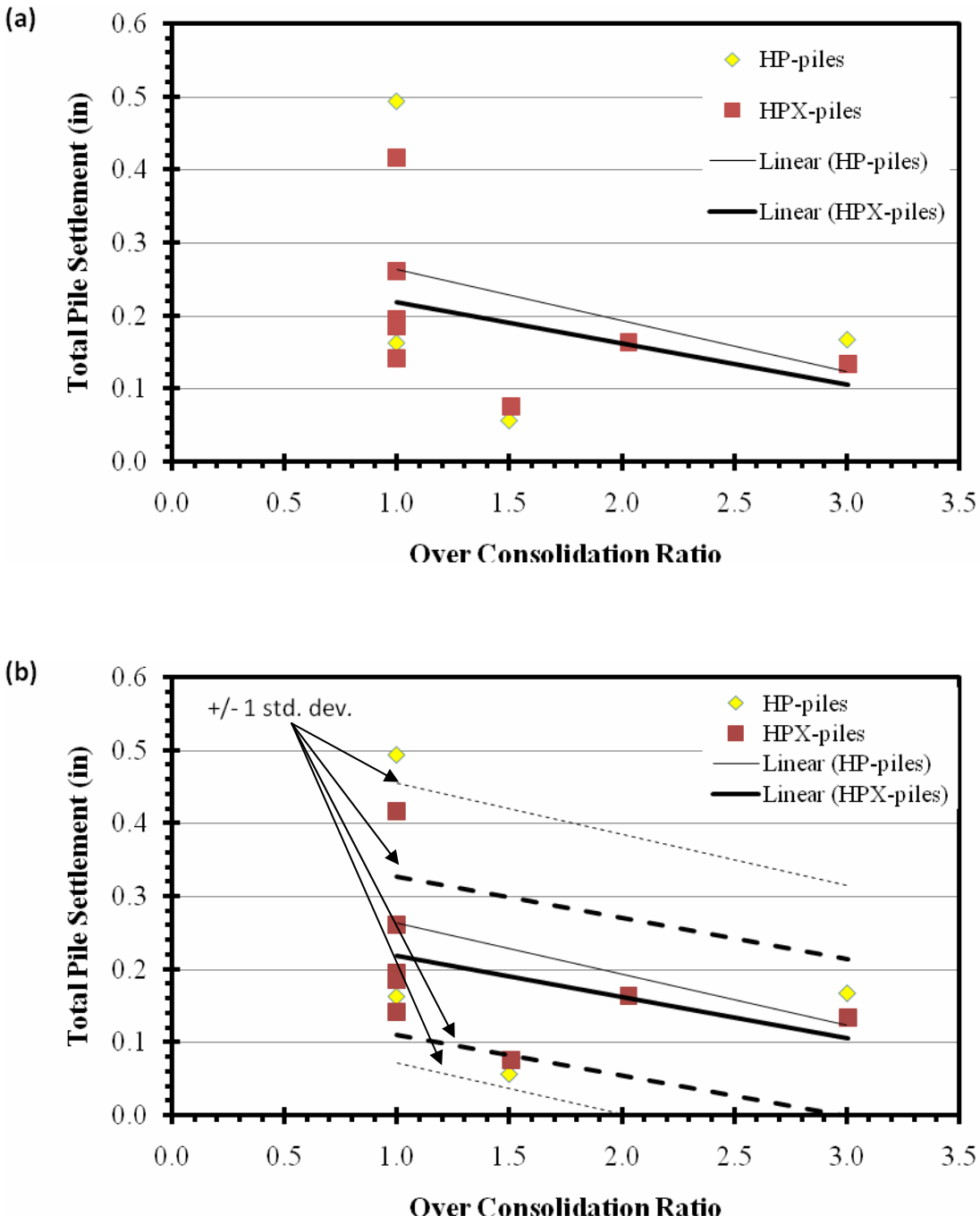

Figure 5.16. Total pile settlement vs over consolidation ratio for tests without flange plugs load tests: (a) linear trends and (b) linear trends conditional standard deviation about the trend determined using the expected range method.

Table 5.6. Summary of conditional standard deviations related to pile settlement.

	Pile Type	Conditional Standard Deviation, σ				Standard Deviation, σ	
		Pile Settlement vs Unit Side Shear (Assumes Plugging of		Settlement vs Over Consolidation Ratio		Settlement*	
		Method 1	Method 2	Method 1	Method 2	Method 1	Method 2
Tests without Flange Plugs	HP	0.124	0.127	0.178	0.192	0.190	0.209
	HPX	0.097	0.118	0.089	0.108	0.097	0.118
Tests with Flange Plugs	HP	0.099	0.104	0.125	0.104	0.134	0.129
	HPX	0.202	0.236	0.181	0.219	0.214	0.250

* - The standard deviation was determined for all settlement values, not considering a trend.

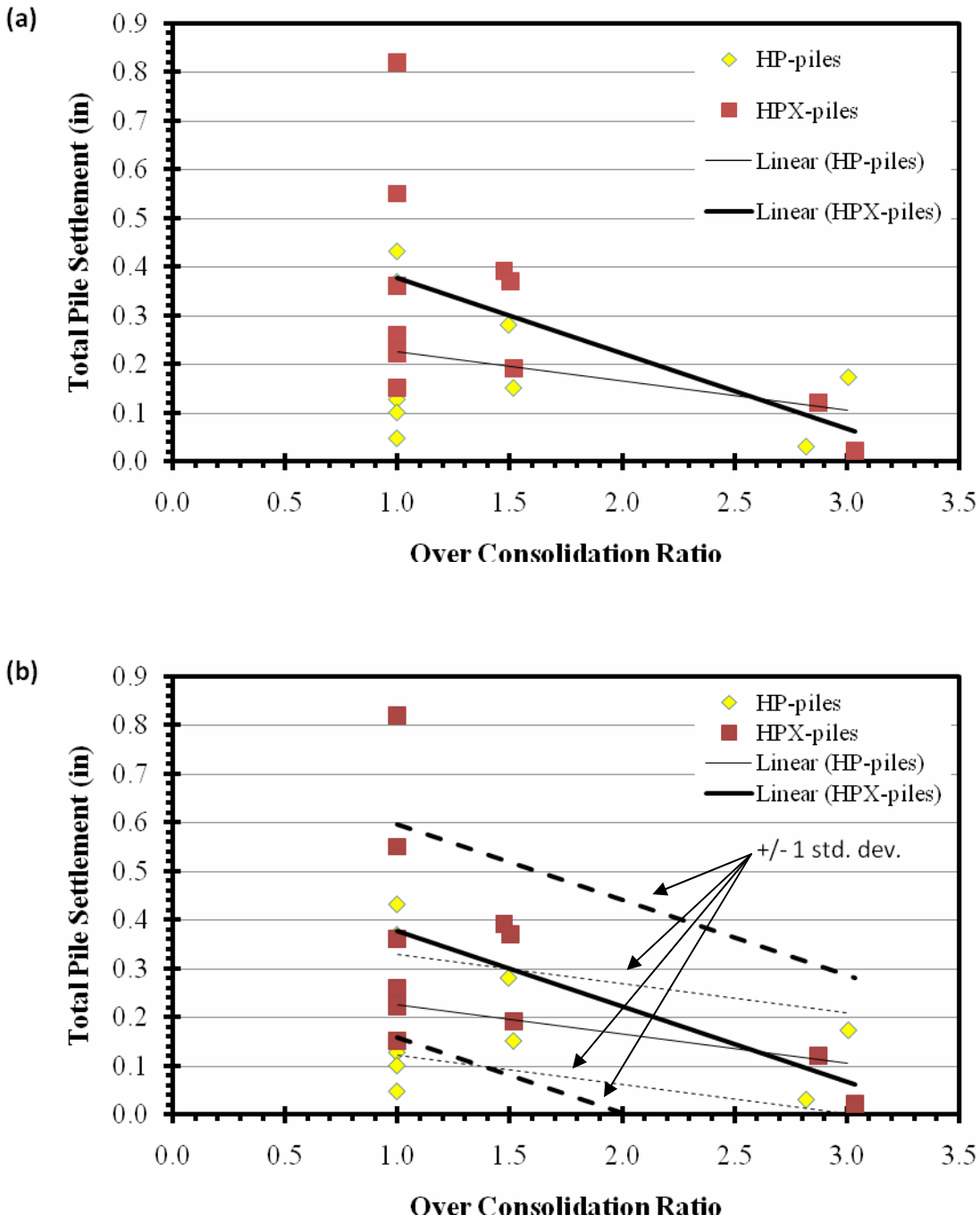

Figure 5.17. Total pile settlement vs over consolidation ratio for tests with flange plugs: (a) linear trends and (b) linear trends conditional standard deviation about the trend determined using the expected range method.

5.3 Discussion

Typical literature β values and the back calculated β values from this research are presented in Table 5.7. The range of β values determined using Bhushan's relation presented in Equation 2.5 was determined for relative densities or 0.35 and 0.55. Back calculated β values presented are for the analyses in which soil plugs were assumed to form in the pile flanges. It should be noted that, while the HP pile produced the highest individual β value, overall the HPX-piles tended to produce higher β values. The increase in β values for HPX-piles relative to HP-piles can be explained by the increased skin friction caused by the texturing of the HPX-piles.

The sand used in this research typically had a relative density of approximately 40 percent. This correlates to a β value of approximately 0.44 using Bhushan's relation. While this value is within the typical range of values found in literature, it is approximately 25 percent higher than the highest back calculated β values. This is most likely because Bhushan relation is for large displacement piles while the HP and HPX piles tested are small displacement piles. β values for small displacement piles are expected to be lower because there is relatively little soil displacement and thus less tendency to densify the surrounding soil and to increase the normal stress on the pile-soil interface.

Table 5.7. Comparison of literature and back calculated β values.

	Literature Values			Laboratory Load Tests	
	Bhushan	Fellenius	API	HP Piles	HPX Piles
β value range	0.40 - 0.54	0.3 - 0.6	0.13 - 0.58	0.18 - 0.35 *	0.2 - 0.33 *†

* - assumes soil plugs formed in pile flanges

† - does not inclued values from tests without flange plugs

The results of laboratory load tests conducted in this research show an increase in capacity for HPX-piles when compared to HP-piles. On average, the HPX-piles showed an increase in capacity of approximately 10 percent over HP-piles for the tests that were conducted with flange plugs, the more reliable tests. Results of several field load tests along with the laboratory load tests are summarized in Table 5.8. The laboratory load tests compare most closely with the field tests conducted at the Berkley, South Carolina and Hickman, Arkansas sites. These two sites also had soil conditions that were relatively similar to the soils used in the laboratory tests. The Berkley site consisted primarily of very loose to loose clayey sand while the Hickman site consisted primarily of medium silty sand and dense sand with silt. It is not surprising that the sites with soil conditions similar to the laboratory testing conditions resulted in similar testing results. The soil conditions at the Crawfordsville, Indiana site were primarily stiff sandy clays. The soil conditions at the other two sites (Armorel, Arkansas and Memphis, Tennessee) are unknown.

Table 5.8. Comparison of the ultimate capacity from field and laboratory load tests of HP and HPX piles.

Site Locaiton	Ultimate Capacity, tons		Percent Gain in Capacity, %
	HP 14x73	HPX 14x73	
Crawfordsville Indiana	325	472	45.2
Berkeley South Carolina	270	291	7.8
Hickman Arkansas	290	358	23.4
Armorel Arkansas	315	285	-9.5
Memphis Tennessee	170	260	52.9
Laboratory Tests *	N/A	N/A	8 to 15

* - Tests with flange plugs only

At a given vertical effective stress, the HPX piles tested without flange plugs consistently resulted in the lowest ultimate capacity, unit side shear, and β values. However, the linear trends of these tests were generally parallel the other the tests. This suggests that there was an issue with these tests. It is the author's opinion that there was likely an issue with the load cell and/or the pressure transducer used for the HPX tests performed without flange plugs. Consistently lower measurements of applied load or higher measurements of bladder pressure, or both, would shift the linear trends of the data similar to what was observed for the tests on the HPX piles that were performed without flange plugs. Another possible explanation is human error during testing. The tests performed without flange plugs were conducted near the start of the research process

when the methodology, procedure, and process were still being formulated. The testing process was not as familiar to the researchers as it was during the tests performed with the flange plugs.

5.4 Summary

This chapter presented the results of collective analyses of the entire data set in terms of the ultimate unit side shear, the side shear parameter β and the settlements observed at failure for all tests. The ultimate load and unit side shear were analyzed as a function of effective stress. The side shear parameter β was back calculated and then analyzed as a function of the vertical effective stress and the over consolidation ratio. The pile settlement at failure was also examined. Simple statistical analyses of the results were also conducted. Linear trends were developed for the HP and HPX piles in each test group, and the standard deviation about those trends was determined.

Comparison between the HP and HPX piles were made and the similarities and differences were noted. The unit side shear and side shear parameter β were analyzed for the two possible failure conditions: assuming the pile flanges plugged and assuming the pile flanges did not plug. The assumed failure condition did not have a large effect on the general trends observed and only affected the magnitude of the values being analyzed. β values were compared with typical literature values and similarities and differences were noted. The change in pile capacity for HP and HPX piles was also compared with field load tests.

CHAPTER 6: Summary, Conclusions, and Recommendations

6.1 Summary

HP-piles are a type of driven pile used as deep foundations. Typically, H-piles are used as end bearing foundation elements, with the pile tip driven to bedrock or other firm strata. Presumably, if the side shear capacity of HP-piles can be increased, their use in applications where end bearing is not necessarily the dominate source of pile capacity will increase. A laboratory testing program was developed to provide experimental data on the effect of texturing on the side shear capacity of HP-piles. Descriptions of the work performed to construct, instrument, and test two types of H-piles, data from the tests, and results of analyses of the data were presented in this thesis.

A review of HP-piles, analytical estimation of pile capacity, static load tests, and interpretation of load test results was presented in Chapter 2. Two effective stress methods for the determination of driven pile capacity in sands were presented. The quick load test method presented in ASTM D-1143 including the basic procedure and instrumentation was summarized. Two methods for the interpretation of static load test results were also presented.

A description of the experimental apparatus is presented in Chapter 3. The apparatus consists of a chamber assembly, a reaction frame, piles, a bladder system to apply the desired vertical effective stresses, and an instrumentation system to measure the applied axial load, pile settlement, bladder pressure, and soil density. Each component was described in detail, along with the characteristics of the sand used in the testing program. The testing procedures from test setup through disassembly of the apparatus were also explained.

In Chapter 4, the testing program was described and the experimental results presented. Two types of HP-piles were used in the testing program: conventional smooth 14x76 HP-piles and textured 14x76 HPX-piles. Eight test series were divided into two groups based on the bladder system used during testing. Each test series consisted of four or five load tests. Tests without flange plugs included one test series for an HP-pile and two test series for an HPX-pile. The tests with flange plugs included two test series for an HP-pile and three test series for two HPX-piles. Results for each test, including written summaries of testing conditions and load settlement curves for each load test were presented in Chapter 4.

The data analysis procedures and data analysis results are presented in Chapter 5. The methods used to determine the ultimate load, unit side shear, and side shear parameter β are explained. The first step of the analysis procedure was to determine the ultimate load for each load test. Because only pile side shear was tested, interpretation methods were not necessary. The ultimate pile capacity was subsequently used to back calculate the unit side shear and side shear parameter β. Statistical analyses were performed to evaluate the significance of any difference between capacities for the two pile types. Analyses of settlement at failure were performed to determine if texturing had any effect on the pile settlement at failure. Back calculated β values were compared to typical literature values, and the change ultimate pile capacities were compared to field load tests.

A brief summary of the work performed is presented in this chapter. Each chapter is summarized and the main points are emphasized. The relevant conclusions that can be drawn from this research are also presented. Specifically, the relative performance of HP

and HPX piles is summarized and appropriate conclusions are drawn. Finally, recommendations for further research are presented.

6.2 Conclusions

Data reported in this thesis lead to several conclusions regarding the research and analysis methods, the performance of the experimental apparatus, and the relative performance of HP and HPX piles. First, the laboratory load testing device (experimental apparatus) and the general technique utilized for the research proved to be an effective means for evaluating side shear capacity of steel H-piles. The apparatus allowed a testing program including thirty nine tests of HP and HPX piles to be performed while reducing several unknowns associated with field load tests. The instrumentation system collected generally thorough and reliable records of all important data for each test with the notable exception of Test Series A1-1.

Results of the tests performed without flange plugs and the tests performed with flange plugs are contradictory and therefore comparison between the two test groups is difficult. The most likely source of the contradictory results is Test Series A1-1. It is the only test series conducted on a HP-pile without using flange plugs and, as such, it has a large effect on the results and conclusions drawn about tests without flange plugs. The validity of Test Series A1-1 is further highlighted by the results and conclusions regarding the load test performed with flange plugs. While it is possible that differences between the load tests performed without flange plugs and with flange plugs are the result of the slightly different testing conditions, it is the author's opinion that the disparity is the result of some inaccuracy in the Test Series A1-1 data. The disparity in the results between the two load test groups will be further addressed in the recommendations.

The following conclusions were drawn from the tests performed with flange plugs because these tests deemed to be more reliable: Note that the general observed trends for the unit side shear and side shear parameter β analyses were the same whether the pile flanges were assumed to plug or not. The only difference being the magnitude of the various values.

- The HPX-piles had about a 1 to 2 ksi higher nominal load than the HP-piles at a given effective stress, and the linear trends of the data were approximately parallel showing increasing nominal load with increasing effective stress.
- The HPX-piles had about a 40 psf higher unit side shear at a given vertical effective stress than the HP-piles and the linear trends of the data were approximately parallel showing increasing nominal load with increasing effective stress.
- Both the unit side shear analyses and nominal capacity analyses resulted in non-zero capacities at zero effective stress. This is likely the result of friction between the pile and the apparatus as well as non-linearity of the "failure envelope" at low vertical effective stresses.
- The side shear parameter β is greater for the HPX-piles ranging from about 0.2 to 0.3 compared to 0.18 to 0.25 for the HP-piles.
    - β values for both the HP and HPX piles decrease with increasing effective stress with approximately parallel linear trends.
    - β values for the HP and HPX piles increase with increasing over consolidation ratio. The linear trends are approximately parallel.

- The general trends of the nominal capacity and side shear analysis were similar because of the close relationship between nominal load and unit side shear. This evident for the side shear parameter β as well, albeit to a lesser extent.
- Qualitatively, the pile settlement at failure tends to decrease with both increasing unit side shear and with increasing over consolidation ratio.
- The HPX-piles tended to experience more settlement then the HP-piles in normally consolidated soils, but the effect lessened with increasing over consolidation ratio.
- Back calculated β values from the load tests conducted with flange plugs fell within typical ranges reported in literature.
- The relative increase in ultimate capacity from HP to HPX piles agreed with field load tests in similar soils.

6.3 Recommendations

Data reported in this thesis also lead to several recommendations for future work to further evaluate the effect of texturing on the side shear capacity of H-piles:

- Additional load tests are needed using the experimental setup and procedures used for the tests without flange plugs. With further testing the results of the tests without flange plugs can be clarified. Specifically, Test Series A1-1 can be validated or disproved.
- Additional load tests are needed in various soil types. The field tests presented in Chapter 2 had only one test performed in clay.

- The results of the load tests performed with flange plugs do show an increase in pile capacity with texturing. However, the significance of the difference in real world applications is debatable. All things being equal there appears to be a benefit to using textured HPX-piles over conventional HP-piles. In real world applications factors such as ease of installation and cost must be accounted for. Ultimately, cost benefit analysis will need to be run on a case by case basis to determine the applicability of textured HPX-piles.

REFERENCES

American Petroleum Institute (1981), API Recommended Practice for Planning, Desinging, and Constructing Fixed Offshore Platforms, API, Production Division, 211 Noth Ervay, Suite 1700, Dallas, Texas 74201

American Society for Testing and Material, ASTM (1994). Annual Book of Standards, ASTM D-1143, Standard Test Method for Piles Under Static Axial Compressive Load.

American Society for Testing and Material, ASTM (2006). Annual Book of Standards, ASTM D-4253, Standard Test Method for Maximum Index Density and Unit Weight of Soils Using a Vibratory Table.

American Society for Testing and Material, ASTM (2006). Annual Book of Standards, ASTM D-4254, Standard Test Method for Minimum Index Density ad Unit Weight of Soils and Calculation of Relative Density.

Beacher, G.B., and J.T. Christian (2003) Reliability and Statistics in Geotechnical Engineering, John Wiley and Sons

Bhushan, Kul (1982), Discussion of "New Desing Correlations for Piles in Sand," Journal of the Geotechnical Engineering Division, Vol. 108, No. GT11, p. 1508-1501, ASCE

Bowders, J.J. (2007) "Bearing Capacity," Class Notes, CE 8410 *Advanced Foundation Engineering*, University of Missouri – Columbia.

Coduto, D.P. (2001) Foundation Design Principles and Practices, 2nd Ed, Prentice Hall, Upper Saddle River, NJ.

Davisson, M.T. (1973), " High Capacity Piles" in Innovatins in Foundatin Construction, proceedings of a lecture series, Illinois Section ASCE, Chicago

Design Manual: Soil Mechanics, Foundation and Earth Structures, NAVDOCKS DM-7, Department of the Navy, Bureau of Yards and Docks, Washingtion D.C., 1962.

Elsayed, A.S. (2004), unpublished report to Nucor-Yamato Steel, Inc. describing load tests performed at Crawfordsville, Indiana.

Elsayed, A.S. (2005a), unpublished report to Nucor-Yamato Steel, Inc. describing load tests performed at Berkeley, South Carolina.

Elsayed, A.S. (2005b), unpublished report to Nucor-Yamato Steel, Inc. describing load tests performed at Hickman, Arkansas.

Elsayed, A.S. (2006), unpublished report to Nucor-Yamato Steel, Inc. describing load tests performed at Armorel, Arkansas.

Elsayed, A.S. (2007a), unpublished report to Nucor-Yamato Steel, Inc. describing load tests performed at Berkeley, South Carolina, Crawfordsville, Indiana, and Hickman, Arkansas.

Elsayed, A.S. (2007b), unpublished report to Nucor-Yamato Steel, Inc. describing load tests performed at Memphis, Tennessee.

Fellenius, B.H. (1990). Guidelines for the Interpretation and Analysis of Static Loading Test. Deep Foundations Institute, Sparta, NJ.

Manjrikan, G. (2006). The Foundation Engineering Handbook, CRC Press

Neely, William J. (1991), "Bearing Capacity of Auger-Cast Piles in Sand," ASCE Journal of Geotechnical Engineering, Vol. 117, No. 2, p. 331-335

Terzaghi, K., and R.B. Peck (9148) Soil Mechanics in Engineering Practive, John Wiley and Sons

Snedecor G. W. and Cochran W. G. (1956), Statistical methods applied to experiments in agriculture and biology. 5th ed. Ames, Iowa: Iowa State University Press, 1956.